2007-05-07

Towards Early State Disease Detection in Microdevices: Fabrication and Testing of Micro Total Analysis Systems for Bioanalytical Applications

Tao Pan
Brigham Young University - Provo

TOWARDS EARLY STAGE DISEASE DETECTION IN MICRODEVICES: FABRICATION AND TESTING OF MICRO TOTAL ANALYSIS SYSTEMS FOR BIOANALYTICAL APPLICATIONS

by

TAO PAN

A dissertation submitted to the faculty of

Brigham Young University

in partial fulfillment of the requirements for the degree of

Doctor of Philosophy

Department of Chemistry and Biochemistry

Brigham Young University

August 2007

BRIGHAM YOUNG UNIVERSITY

GRADUATE COMMITTEE APPROVAL

of a dissertation submitted by

TAO PAN

This dissertation has been read by each member of the following graduate committee and by majority vote has been found to be satisfactory.

_____	_____
Date	Adam T. Woolley, Chair
_____	_____
Date	Steven W. Graves
_____	_____
Date	Steven R. Herron
_____	_____
Date	Milton L. Lee
_____	_____
Date	Gerald D. Watt

BRIGHAM YOUNG UNIVERSITY

As chair of the candidate's graduate committee, I have read the dissertation of Tao Pan in its final form and have found that (1) its format, citations, and bibliographical style are consistent and acceptable and fulfill university and department style requirements; (2) its illustrative materials including figures, and charts are in place; and (3) the final manuscript is satisfactory to the graduate committee and is ready for submission to the university library.

_____ _____

Date

Adam T. Woolley
Chair, Graduate Committee

Accepted for the Department

_____

David V. Dearden
Graduate Coordinator

Accepted for the College

_____

Thomas W. Sederberg
Associate Dean, College of Physical and Mathematical Science

ABSTRACT

TOWARDS EARLY STAGE DISEASE DETECTION IN MICRODEVICES: FABRICATION AND TESTING OF MICRO TOTAL ANALYSIS SYSTEMS FOR BIOANALYTICAL APPLICATIONS

Tao Pan
Department of Chemistry and Biochemistry

Doctor of Philosophy

The past few years have seen a rapid expansion in interest in the characterization of the entire complement of proteins, or proteome. Micro total analysis systems (μTAS) are an emerging promising method, offering rapid, sensitive and low sample consumption separations.

I have demonstrated microchip capillary electrophoresis (CE) devices made of CaF_2. New methods have been developed for micromachining enclosed capillaries in CaF_2. CE analysis of fluorescently labeled amino acids was used to illustrate bioanalytical applications of these microdevices. Initial on-chip infrared spectroscopy results for qualitative analyte identification were achieved in microfluidic CaF_2 channels.

I have also shown the evaluation of poly(methylmethacrylate) (PMMA) and thermoset polyester (TPE) microchips for use in protein profiling. To improve separation efficiency and reduce protein adsorption, dynamic coating and poly(ethylene glycol) (PEG) grafting using atom transfer radical polymerization (ATRP) have been used in PMMA

microdevices. Proteins, peptides and protein digests have been separated electrophoretically in these PMMA microchips. My results demonstrate that PMMA microdevices should be well suited as microfluidic systems for high performance separations of complex biological mixtures.

In-channel ATRP has been developed for the surface modification of TPE microdevices. Characterization indicates that PEG-modified microchannels have much lower and more pH-stable electroosmotic flow, more hydrophilic surfaces and reduced nonspecific protein adsorption. CE of amino acid and peptide mixtures in these PEG-modified TPE microchips had good reproducibility. Phosducin-like protein and phosphorylated phosducin-like protein were also separated to measure the phosphorylation efficiency. My results show that PEG-grafted TPE microchips have broad potential application in biomolecular analysis.

Cancer marker analysis is important for medical research and applications. I report a method that can covalently attach appropriately oriented antibodies of interest on monolith surfaces. To reduce nonspecific adsorption, protein solutions were used to effectively block the monolith surface. Selective preconcentration and elution of human chorionic gonadotropin have been performed in my affinity columns, demonstrating that this type of system should have promising applications in cancer marker detection.

ACKNOWLEDGEMENTS

First of all, I thank my advisor Dr. Adam T. Woolley for his time, patience, thoughtful instructions, and kind mentoring, which helped me pass all the challenges in my Ph.D. study at Brigham Young University. I also thank my graduate committee members, Dr. Graves, Dr. Herron, Dr. Lee and Dr. Watt, for their invaluable suggestions in many areas. In particular, I am grateful to Dr. Lee for his support in both funding and thoughtful direction. Additionally, I thank the Department of Chemistry and Biochemistry at Brigham Young University and NIH for funding my research. Dr. Jikun Liu and Dr. Ryan T. Kelly are specially thanked for their close collaboration in my research. I also thank Dr. Huijun Xin, Xuefei Sun, and Hernan Fuentes for their kind helpfulness in my research. My lab mates in both Dr. Woolley's and Dr. Lee's labs have been helpful which made me really enjoy my study here. I am grateful to the Department of Chemistry and Biochemistry at Brigham Young University, for giving me the opportunity to study here. Finally, I thank my wife, Caihui Song, for her tremendous sacrifice and support during my study at Brigham Young University.

TABLE OF CONTENTS

LIST OF FIGURES

LIST OF TABLES

Chapter 1. Introduction

1.1 Micro Total Analysis Systems for Bioanalytical Applications

1.1.1 Introduction to Micro Total Analysis Systems

Micro total analysis systems (μTAS), or miniaturized analysis platforms, have greatly expanded in recent years. In the 1970s, the first μTAS device, a gas chromatography analyzer, was fabricated on a silicon wafer to separate a simple mixture in seconds [1, 2]. Although this device was remarkable, μTAS did not get much attention until the early 1990s when several articles about miniaturized analysis systems fabricated in inorganic materials were published [3-5]. Since then, μTAS have grown rapidly, and today it is one of the hottest research areas in analytical chemistry. Many types of materials (both inorganic and polymeric) have been evaluated as μTAS device substrates; moreover, various methods have been developed for device production, surface modification and integration. Also, many separation methods have been miniaturized into μTAS.

Compared to conventional analysis systems, μTAS have several advantages. First, the cycle time for μTAS analysis is shorter; second, sample consumption is lower. Third, multiple functions such as sample pretreatment, separation, and detection can be integrated into one μTAS device [6, 7]. Fourth, μTAS can give comparable performance to conventional analysis methods. Last, high-throughput analysis can be achieved by integration of parallel μTAS units on one chip [8].

Nowadays, the most common application for μTAS is microchip capillary electrophoresis (CE), because of two distinct advantages that fit the requirements of miniaturization. The first is that the electroosmotic flow (EOF) in CE can serve as a pumping system. Thus, the

transportation and injection of analytes in CE can be controlled easily by adjusting electrical potentials, so external valves or pumps are not needed. The second advantage is that in CE, band broadening is caused only by longitudinal diffusion, which makes the separation efficiency in microchip CE exclusively dependent on the magnitude of the voltage used. Thus, in a microchip with a very short separation capillary, high efficiency can still be achieved.

1.1.2 Microfluidic Devices Made of Inorganic Materials

1.1.2.1 Inorganic Materials

Due to rapid developments in the semiconductor industry, photolithography and fabrication of glass, quartz and silicon have been investigated intensively. Meanwhile, advances in separation science indicate that miniaturization is an effective way to improve separation performance, and reduce separation time and sample consumption [9]. All these factors make fabrication of inorganic material microfluidic devices both possible and desirable.

Inorganic substrates were the first-generation materials used in making μTAS platforms. The first microfluidic devices were made in silicon [2] and glass [3, 4]. Nowadays, a broad range of inorganic materials are used in μTAS, including glass [3, 4, 10, 11], silicon [2, 12, 13], quartz [14-16] and CaF_2 [17]. Among all these materials, glass is the most widely used, because it has good mechanical, electrical, optical and thermal properties. In addition, the surface chemistry of glass is well developed. The second most commonly used inorganic material is silicon. However, silicon is not transparent to UV or visible light, and its breakdown voltage is relatively low (~500 V) [18]. Thus, only microdevices that can function within these constraints are made completely in silicon. Since silicon has

good mechanical and thermal properties, silicon-glass (or silicon-quartz) hybrid microfluidic devices are found often [19, 20]. Quartz, or fused silica, has superior physical and optical properties to glass or silicon, and is a highly suitable material for microfluidic devices. However, the high cost and difficult fabrication of quartz limit its application to special circumstances (e.g., when UV detection is required). CaF_2 is the inorganic materials, CaF_2 has the best optical properties [17], and it is transparent to a wide range of wavelengths of light (170 – 7800 nm). Thus, CaF_2 microfluidic devices are suitable for various types of optical detection methods, including IR, UV, Raman, fluorescence, etc. However, the fabrication and bonding procedures are a limitation in making microdevices from CaF_2.

1.1.2.2 Fabrication of Glass, Quartz and Silicon Microfluidic Devices

The fabrication of glass, quartz and silicon microfluidic devices is based on photolithography techniques. Photoresist, a light-sensitive material/polymer, is key to this process. In photolithography, photoresist is used to form patterned features on surfaces. The fabrication process includes pretreatment, photolithography, etching and bonding. In a typical fabrication process, a substrate is cleaned by hot, concentrated H_2SO_4/H_2O_2, or NH_4F/HF (Figure 1.1a). Then, an etch mask (e.g., Cr/Au [10, 14], amorphous Si [8] or SiO_2 [21, 22]) is coated on the substrate (Figure 1.1b). The coating protects the inorganic substrate during the etching process. Next, the substrate is attached to a spinner, and several drops of photoresist are put on top of the substrate. Once the assembly is spinning, a thin layer of photoresist will be coated on top of the etch mask (Figure 1.1c) [4, 8, 23]. After soft baking, a photomask, which is a glass plate or a transparent polymer sheet

bearing high-resolution patterns, is positioned on the top of the surface. The substrate is exposed to UV radiation through the photomask for a short period of time, which transfers the pattern on the photomask to the photoresist (Figure 1.1d). During development, some parts of the photoresist will be removed, leaving a pattern on the substrate.

There are two types of photoresist: positive and negative [24]. When positive photoresist is used, only the UV-exposed material will be dissolved during development; the unexposed photoresist will remain on the substrate (Figure 1.1e). Thus, the pattern transferred to the photoresist is identical to the photomask. In contrast, when a negative photoresist is used, the unexposed photoresist will be removed, while the UV-exposed photoresist will stay. Thus, a reversed pattern is generated after development (Figure 1.1i). After photoresist development, patterned inorganic substrates are typically etched to create microstructures (Figure 1.1f, g, j, k). For silicon etching in the liquid phase, concentrated KOH or HNA solution (a mixture of HF, HNO_3 and CH_3COOH) is used commonly [21, 22, 25]. KOH solution is a typical anisotropic etchant for silicon, attacking the <100> plane and resulting in the side wall forming a 54.74º angle with the top surface [24]. HNA solution is an isotropic etchant, which produces rounded sidewalls and corners on silicon surfaces. In the gas phase, reactive ion etching (RIE) has also been applied to silicon and can produce high-aspect-ratio and complex patterns [26]. For glass and quartz, HF-containing etchants can be used, including HF/HNO_3, HF/NH_4F, HF/HCl and concentrated HF [10, 11, 14, 27]. To produce high-aspect-ratio features on glass and quartz surfaces, RIE has also been used [15]. Last, the photoresist and/or etch mask need to be removed to give the final patterned substrate (Figure 1.1h, l).

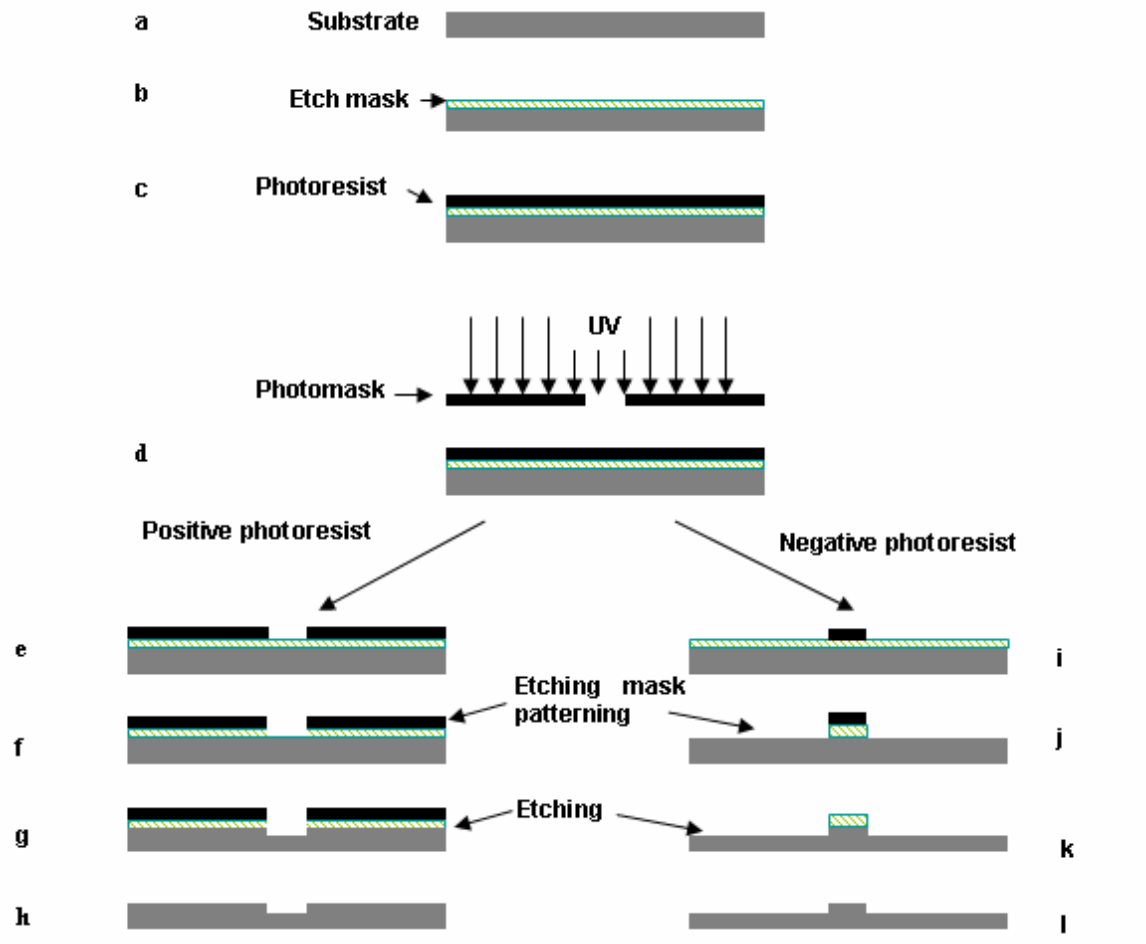

Figure 1.1 Fabrication of inorganic microfluidic systems.

1.1.2.3. Bonding Techniques

Thermal bonding is the dominant method for glass, silicon and quartz microchannel enclosure. Typically, clean glass substrates are treated by hot, concentrated H_2SO_4/H_2O_2, generating reactive silanol groups. Then the glass substrates are clamped together to form a temporary bond. To obtain permanent bonding, the assembly is heated in an oven at a high temperature for a period of time, until siloxane bonds are formed between silanol

groups at the contact surface. Most glass bonding is performed in the temperature range of 500 – 700 ºC [10, 11, 23]. Sometimes, temperature programming is necessary for optimal bonding. For the sealing of quartz substrates, a very high temperature (~1100 ºC) is needed. For the bonding of silicon to silicon or glass, electric-field-assisted thermal bonding (or anodic bonding) is used, with a potential ranging from 200 – 1000 V applied at 180 – 500 ºC to assist the thermal bonding process [13, 28, 29].

Adhesive bonding is an alternative method for enclosing inorganic microfluidic devices [17, 30, 31]. One advantage of adhesive bonding is that it can be applied to almost all kinds of materials. Moreover, the bonding process can be carried out at lower temperatures (even at room temperature). However, a major concern for adhesive bonding is that the adhesive can affect the surface properties of the microchannels, which may influence device performance. In CaF_2 substrate bonding, a patterned photoresist layer is prepared on a cover plate, which is carefully aligned with a patterned CaF_2 substrate to form a bonding assembly. Then, this assembly is heated to 120 ºC for 30 min to achieve bonding [17]. In this approach, the patterned photoresist serves as an adhesive. Since the channel section in the bonded CaF_2 device is free of photoresist, the influence of the adhesive on the channel surface properties can be minimized.

1.1.2.4 Thin–Film Fabrication

Recently, a new approach called thin-film fabrication was reported [32], as shown in Figure 1.2. First, a quartz (or other) substrate is cleaned, a ~500 nm thick layer of aluminum is deposited by thermal evaporation, and a ~3 μm thick layer of photoresist is spin coated afterwards (Figure 1.2a). The aluminum and photoresist form a sacrificial layer for microfabrication. Photolithography techniques are used to pattern the sacrificial

layer, followed by removal of exposed photoresist and aluminum from unpatterned areas (Figure 1.2b). The channel features are thus defined by the sacrificial layer, and a SiO_2 layer is deposited on the substrate to form channels and enclose the sacrificial features (Figure 1.2c). Last, the sacrificial layer is removed to form a hollow tube structure (Figure 1.2d).

Thin-film methods have several advantages over conventional fabrication approaches for microdevices. First, one can build channels and structures on almost any kind of material. Also, by changing the films which are deposited on the substrate, channel patterns can be made out of different materials. Moreover, using this technique, complex (e.g., three-dimensional) structures can be fabricated easily on surfaces, because features are created from bottom to top. Thus, after one layer of thin-film feature is fabricated, a new structure can be added on top. Depending on the structure and geometry of the sacrificial layers, unique fluidic designs can be created easily. Furthermore, because the SiO_2 layer deposited on the substrate is transparent to a wide range of light wavelengths, it is possible to detect in the visible and UV. Finally, this technique enables multiple microdevices to be fabricated on one substrate simultaneously, making parallel analysis possible. However, the major challenge with thin-film methods is removal of the sacrificial layer.

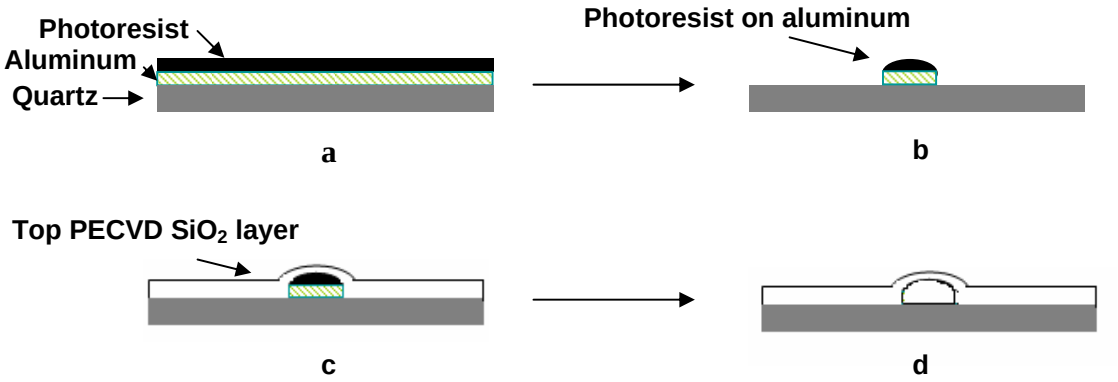

Figure 1.2 Fabrication of microfluidic devices using thin-film methods. (a) A quartz substrate is coated with aluminum and photoresist. (b) The photoresist and aluminum are patterned. (c) Plasma enhanced chemical vapor depostion (PECVD) is used to deposit SiO_2 over the sacrificial layer. (d) Etching of the sacrificial layer forms a hollow tube.

1.1.3 Microfluidics Made in Polymeric Materials

1.1.3.1 Polymer Materials

Although microfluidic devices made using inorganic materials have had great success, the disadvantages of inorganic substrates (such as cost, fragility, and fabrication) have limited their application. Thus, scientists have been investigating the possibility of fabricating microfluidic devices in polymeric materials. Nowadays, many commericial polymers have been used in microfluidic device fabrication. The most commonly used polymers are polydimethylsiloxane (PDMS) [33-35], poly(methyl methacrylate) (PMMA) [21, 22, 36, 37], polystyrene (PS) [38, 39], polycarbonate (PC) [40, 41], polyimide (PI) [42, 43] and cyclic olefin copolymer (COC) [44-46]. Due to the diverse properties of different polymeric materials, various methods have been developed for the fabrication of polymer microfluidic devices.

1.1.3.2 Forming Features in Polymer Surfaces

Imprinting. Imprinting is probably the most widely used method for polymer microdevice fabrication [21, 22, 45, 47]. Polymers that can be imprinted include PMMA, PC, PS, polyethylene terephthalate (PET), COC and many others. To use this method, one needs a hard, patterned template (made of silicon, glass, metal or SU-8 photoresist) and a softened polymer substrate. When the hard template and softened polymer are clamped together, the pattern on the template is transferred to the polymer.

Two methods have been developed for imprinting: hot embossing and solvent imprinting. Typically, hot embossing is accomplished in several steps. First, a polymer substrate is clamped to a template (Figure 1.3a) and placed in an oven at a temperature higher than the glass transition temperature (T_g) of the polymer. After sufficient time, the polymer substrate is softened and pressure is applied to compress the polymer against the template, which embosses the patterns on the template into the polymer surface (Figure 1.3b). Then, the assembly is cooled to room temperature, and the patterned polymer substrate is detached from the template (Figure 1.3c). Trapping of air bubbles and thermally induced stress are the two major concerns for hot embossing [48]. To obtain optimal results, the template and polymer substrates need to be cleaned (e.g., in a cleanroom). Alternatively, hot embossing under vacuum is another choice for good imprinting results [49].

Recently, a new method called solvent imprinting was developed (Fig. 1.3d-f). First, several drops of a solvent (e.g., acetonitrile for PMMA) are deposited on a polymer surface, and then a planar template (with patterned SU-8 photoresist) is compressed against the polymer substrate (Figure 1.3d) until the pattern is transferred from the template to the softened polymer surface (Figure 1.3e). Then, the substrate is detached

from the template, and the imprinted polymer piece is ready to use (Figure 1.3f). Compared to hot embossing, solvent imprinting has several advantages. First, solvent imprinting is done at room temperature; second, the cycle time for solvent imprinting is much shorter than hot embossing; and last, the solvent imprinting method can be coupled directly with solvent bonding.

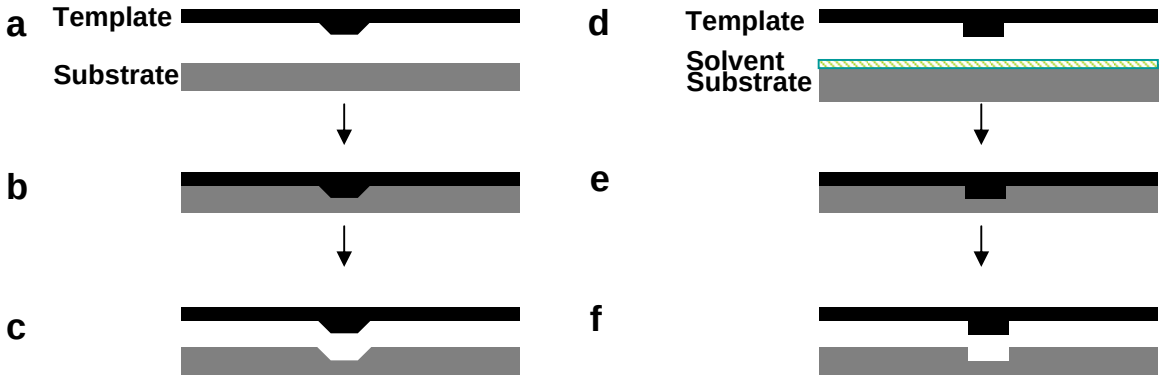

Figure 1.3 Schematics of imprinting methods. (a-c) Hot embossing; (d-f) solvent imprinting.

Silicon and glass templates can be broken during imprinting, due to uneven pressure or thermally induced stress. Thus, metal templates are sometimes utilized to improve imprinting results [50]. However, glass or silicon templates can still be used to imprint 50 to 100 polymeric substrates.

Injection Molding. Injection molding is another method that is used commonly for microfluidic device fabrication [51]. The procedure for injection molding is as follows. First, an assembly with an evacuated cartridge (having templates inside) is prepared. Then, a melted polymer is injected into the cartridge under high pressure to form a replica. After

cooling, the replica can be removed from the cartridge, which is then ready for another run of injection molding.

Compared to imprinting, injection molding is easier for mass production. In addition, the cycle time for injection molding is shorter than for imprinting methods. Moreover, the reproducibility of injection molding is high, as long as the temperature and pressure are controlled appropriately. Lastly, attachments such as optical fibers or metal wires can be integrated easily into the final molded microfluidic devices. The main concern for injection molding is the high cost of the instrumentation, including metal templates [52].

Casting. Casting, or soft lithography, is also a commonly used method for microfluidic device fabrication [53]. Compared to imprinting and injection molding, casting is simpler and easier to control. Thanks to developments in elastomeric polymers, casting can be done on many kinds of materials. Moreover, complex 3D structures (including valves, pumps, etc.) can be fabricated readily using casting [54-57].

PDMS (silicone rubber) is the most widely used elastomer in casting. PDMS monomer is a liquid at room temperature, but it readily solidifies when mixed with a cross-linking agent. For a typical casting process, liquid PDMS is mixed with cross-linking agent and poured into a cartridge with a template on the bottom. Then, the PDMS liquid is cured at room temperature or at high temperature (to reduce curing time), during which the pattern on the template is transferred to the PDMS surface. The casting process is done under mild conditions. Metal, glass, silicon, and softer materials such as SU-8 or even PDMS can serve as templates.

Besides PDMS, many other polymer materials can be used in casting. For example, casting of microdevices from photocurable perfluoropolyethers [58], thermoset polyester [59, 60] and poly(ethylene glycol) (PEG) [61] has been accomplished.

Laser Ablation. Laser ablation or laser micromachining is a direct (template-free) method for microfluidic device fabrication. The features on a polymer surface are produced by laser machining. Typically, in laser ablation the substrate is first positioned on a computer-controlled X-Y motorized stage, and a laser is focused on the surface. The laser will machine material photochemically or by thermal effects. Complex patterns can be fabricated by moving the motorized stage, which is normally controlled by a computer-aided design program.

Two types of laser systems (UV and IR) are used in ablation. UV excimer lasers such as ArF (193 nm) or KrF (248 nm) [62, 63] are operated using pulses of nanosecond duration, machining substrates photochemically without generating much heat. They can make features smaller than 100 μm, and the channel walls are normally straight. CO_2 lasers [36, 64] operate in the IR, so they deform polymer microstructures through photothermal effects. Thus, cross sections of channels made by CO_2 lasers have a Gaussian-like shape, and features are normally larger than 150 μm.

Laser ablation can be applied to many kinds of commercial polymers. One advantage of laser ablation is that it does not need a photomask or template, which makes it very easy to change device design. Moreover, since UV excimer lasers work photochemically, it is possible to carry out surface modification during the laser ablation process.

However, features made by laser ablation are normally rougher than ones made by imprinting, injection molding, or casting. Also, side products produced during laser

ablation may be deposited or trapped on the polymer surfaces, which may affect substrate properties.

Microfluidic Tectonics. Microfluidic tectonics is a novel fabrication approach for microfluidic systems, particularly for complex structures [65, 66]. In a typical microfluidic tectonics process, the first step is to prepare a cartridge with fluidic connections and posts. Then, a monomer solution containing photoinitiators is filled in the cartridge chamber (Figure 1.4a). The size of the cartridge will define the dimensions of the fabricated microdevices. A photomask is positioned on the cartridge, and UV radiation (usually 300 – 400 nm) is used to polymerize the monomer solution (Figure 1.4b) in areas not blocked by the pattern, whereas the monomer solution shadowed by the photomask remains unreacted (Figure 1.4c). Last, the unreacted monomer solution is flushed away to form the final microfluidic structures (Figure 1.4d).

One unique feature of microfluidic tectonics is that it does not need a template or a bonding process. Also, microstructures can be fabricated in parallel in a short period of time. In addition, by using different photomasks, monomers, and multi-step UV polymerization, complex 3D microstructures such as sensors, valves and pumps can be fabricated. Moreover, membranes and metal wires can be integrated into microfluidic devices with this technique [67].

However, microfluidic tectonics cannot be used to fabricate features smaller than ~100 μm, because of side reactions of the UV-initiated polymerization. During patterning, light diffraction at the edge of the photomask may cause partial polymerization in regions close to the pattern edge. Moreover, diffusion of free radicals may also induce polymerization

in undesired locations. To obtain good results using this technique, monomers with low shrinkage and fast reaction should be used.

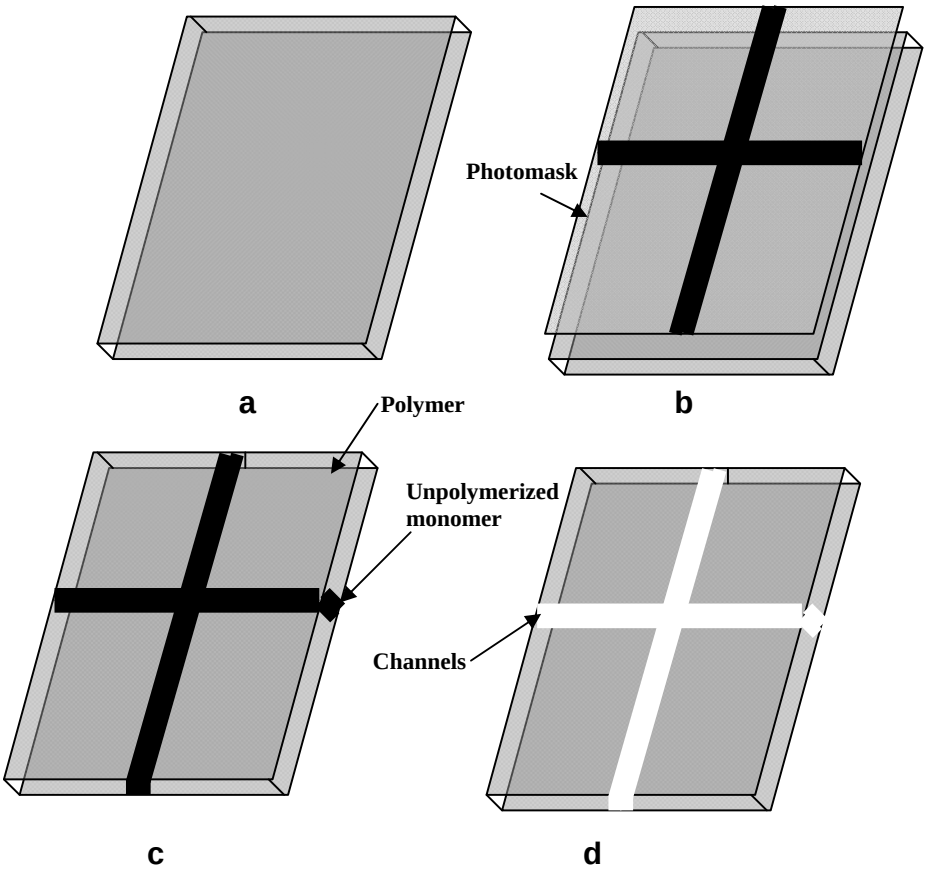

Figure 1.4 Microfluidic tectonics process.

SU-8 Photolithography. Recently, negative SU-8 photoresists have been applied in polymeric microdevice fabrication [68, 69]. Because SU-8 has high thermal stability, chemical resistance, and mechanical strength, it is suitable for microdevice fabrication. The fabrication of SU-8 microdevices is carried out as follows. First, a thin film of SU-8 is spin coated on a glass wafer. This coated SU-8 is exposed to UV radiation through a photomask. Then, a new layer of SU-8 is spin coated on the first SU-8 layer, and is also

exposed to UV radiation through a patterning mask. After exposure, the SU-8 covered by the photomask will be removed in a developer solution, which creates the pattern. The depth of the microstructure is defined by the thickness of the second SU-8 layer. The pattern can then be enclosed by attaching a glass wafer with a SU-8 layer, performing UV exposure and baking at high-temperature to bond the layers together. Because of its good mechanical strength, SU-8 can be used to make features that have a depth of up to 50 μm. In addition, complex 3D structures can be made readily using SU-8, and bonding is straightforward. However, a concern with this technique is that EOF in SU-8 microchannels is highly pH-dependent [68].

1.1.3.3 Bonding Techniques

Thermal Bonding. Thermal bonding is used widely for enclosing polymeric microdevices [21, 70-72]. Typically, a patterned substrate and cover plate are clamped together and heated to near the T_g of the polymer. During this period, intermolecular interaction occurs at the contact surfaces between the two polymer substrates. After an appropriate time, the temperature is lowered, and the bonded microdevice is released from the clamp.

Although thermal bonding is simple and used widely, it still has some disadvantages. The most important problem is that the bonding is not very strong, so delamination often occurs. Also, because the bonding temperature is close to the T_g of the polymer, channel deformation sometimes happens. Thus, to achieve optimal thermal bonding, one needs to adjust carefully the temperature, pressure, and time.

Solvent Bonding. Unlike thermal bonding, solvent bonding has only been applied to polymer microfluidic devices more recently [22, 26, 70]. Two approaches have been used for solvent bonding, as shown in Figure 1.5. In the first method, a thin layer of organic solvent is spin coated on the cover plate (Figure 1.5a) Immediately after this step, a patterned plate is compressed against the coated piece (Figure 1.5b). The pressure is kept for a sufficient time until the organic solvent partially dissolves the two polymer surfaces and strong intermolecular interactions bond them together (Figure 1.5c) [70]. In the second approach, a sacrificial layer (e.g., paraffin wax) is used. In a typical sacrificial layer solvent bonding process, the first step is to cover the patterned polymeric substrate with a PDMS slab to form an enclosed assembly (Figure 1.5d). This assembly is heated above the melting point of the wax, and vacuum is used to fill the channels with melted wax. After all the channels and reservoirs are filled, the assembly is cooled to room temperature and the sacrificial layer is solidified (Figure 1.5e). The PDMS slab is removed carefully from the patterned polymer substrate, and the sacrificial layer protects the channels during the next step. An organic solvent is dispensed on the polymer surface, and a cover plate is compressed against the patterned substrate (Figure 1.5f) until solvent bonding is complete (~2 min). The sacrificial layer can be removed by pipette after heating the bonded microdevice to melt the wax (Figure 1.5g). Finally, hexane is used to dissolve any leftover sacrificial material in the channels [22].

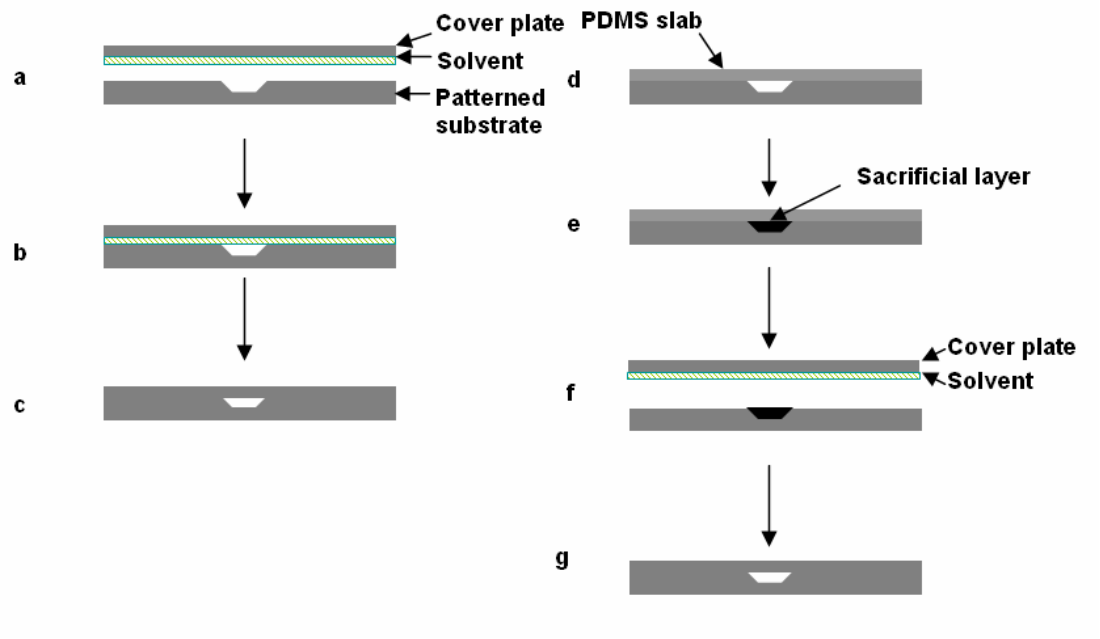

Figure 1.5 Schematic diagram of solvent bonding (a-c) without and (d-g) with a sacrificial layer.

Compared to thermal bonding methods, solvent bonding can be operated at lower temperature, and the bonding strength is much higher. However, the channel surface may be modified by the bonding solvent, which could affect microdevice performance, although this has not been observed in practice [22].

Adhesive Bonding. Adhesive bonding is a method somewhat similar to solvent bonding [34, 73], but the bonding adhesive does not dissolve the surface. Instead, it acts as a glue to secure two polymeric substrates together. To ensure that the surface properties are not changed, an adhesive with similar characteristics to the substrate should be selected, and a very thin layer of adhesive is preferred.

Chemical Bonding. Chemical bonding is also called permanent bonding. In this method, chemical bonds are formed between the contact surfaces of two polymer pieces. Thus, the bonding strength is high and no delamination is expected. Since polymer materials have

different chemical properties, specific methods need to be developed for various polymer types.

Covalent bonding of PDMS to glass, silicon, and PDMS has gained significant interest in recent years. It is well known that PDMS can adhere to materials through intermolecular interactions [74-76]. To bond PDMS covalently, one needs to activate both the PDMS and the other surface by O_2 plasma [35, 53]. During plasma treatment, siloxane bonds on the PDMS surface are activated through cleavage. If the PDMS and blank surface are held together for several minutes, new chemical bonds will form at the contact interface. The reactive broken bonds formed through plasma activation last less than 30 s, such that surfaces must be placed together very quickly [53, 77].

Commercially available PDMS bonding kits employ a different mechanism [57], using two different types of PDMS. One has vinyl groups and a platinum catalyst, while the other has a crosslinker and silicon hydride groups. When these two types of PDMS are brought into contact, the vinyl groups react with silicon hydride to form covalent bonds between the two PDMS surfaces.

TPE is another successful example of chemical bonding enclosure [59, 60]. In the TPE monomer solution, a photoinitiator (2,2-dimethoxy-2-phenylacetophenone, DMPA) and a thermal initiator (methyl ethyl ketone peroxide, MEKP) are used. During the casting process, only DMPA is used to polymerize the TPE. To enclose TPE microchannels, a patterned TPE piece is clamped against the TPE cover plate, and the assembly is subjected to UV radiation. Finally, the assembly is heated, and MEKP initiates the thermally induced polymerization of the unsaturated polyester backbones in the TPE substrates to finish the chemical bonding process.

Resin-Gas Injection Bonding. Resin-gas injection bonding was introduced in 2001 [78, 79]. This method utilizes polymerization of a resin in between two polymer substrates to bond them together as shown in Figure 1.6. Two PMMA pieces (a patterned and cover plate) are clamped together, and a monomer solution containing 2-hydroxyethylmethacrylate (HEMA) and DMPA is flushed through one of the reservoirs (Figure 1.6a). Once the monomer solution fills the channels and gaps between the PMMA pieces, nitrogen gas or vacuum is used to remove the monomer solution from the channels; however, in between the PMMA pieces there is still a thin layer of monomer solution (Figure 1.6b). In the last step, the assembly is exposed to UV light for HEMA polymerization, during which the two PMMA pieces are bonded by poly(HEMA) (Figure 1.6c).

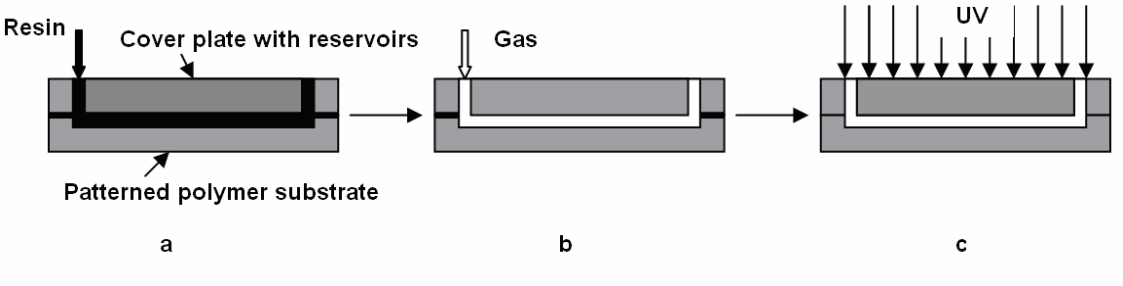

Figure 1.6 Scheme of resin-gas injection bonding

Resin-gas injection bonding can be applied to many kinds of polymer materials. Besides HEMA, other resins, such as epoxy and unsaturated polyester, can also be used to bond polymer substrates [37, 78]. Several methods have been applied to initiate resin curing (polymerization), including light-initiated polymerization, thermal initiation and redox initiation [37, 78, 79].

One unique feature of resin-gas injection is that it can modify the surface during bonding, thus reducing device fabrication time. However, this method may also contaminate the channel surface, which could affect device performance.

1.2 Microchip CE

1.2.1 Introduction

Electrophoresis is one of the most commonly used techniques for biological sample analysis. In electrophoresis, charged analytes migrate under an applied voltage, and they are separated according to differences in both their net charge and size. CE has been used widely for the analysis of peptides [80, 81], proteins [81, 82], nucleic acids [23, 83], saccharides [84], inorganic ions [85] and small organic molecules [86].

CE was used as the separation technique in early μTAS devices [3, 4]. Since then, microchip CE has become very popular, and is probably the dominant separation method in μTAS. The most mature application for microchip CE is DNA analysis [23, 87], but nowadays protein analysis in microchips has gained increased attention [21, 88, 89].

1.2.2 Theory

1.2.2.1 Fundamental Theory

The fundamental theory of modern CE was first described by Jorgenson and Lukacs [90, 91]. CE is a technique that uses an electric field to separate charged analytes. A scheme of microchip CE is shown in Figure 1.7.

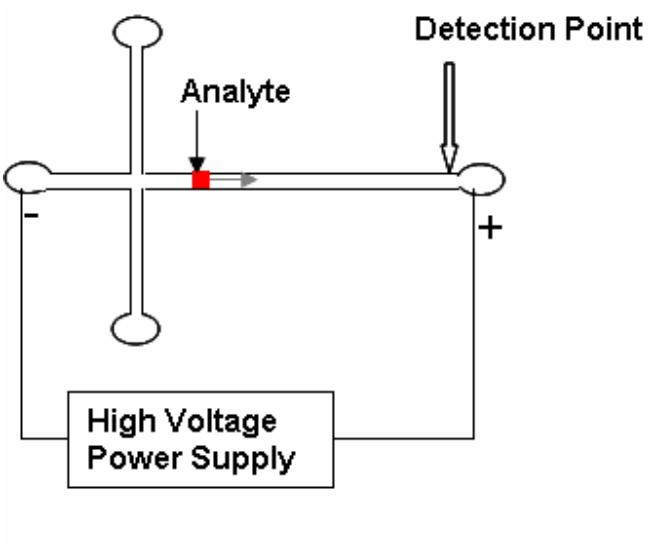

Figure 1.7 Scheme of a microchip CE instrument.

When an electric field is applied through the separation channel, the charged analytes will move toward the electrode of opposite polarity. Different analytes will have different migration velocities (u_p), which are dependent on the electrophoretic mobility of each analyte (μ_p) and the applied electric field (E). The migration velocity can be expressed according to Equation 1.1.

$$u_p = \mu_p E \tag{1.1}$$

In CE, a constant electric field is applied, so two analytes must have a different μ_p to be separated. The electrophoretic mobility of an analyte at a given pH is given by Equation 1.2.

$$\mu_p = \frac{z}{6\pi\eta r} \tag{1.2}$$

In this equation, η is the viscosity of the buffer solution, z is the charge and r is the Stokes radius of the analyte. Equation 1.2 shows that the electrophoretic mobility of an analyte is proportional to its net charge, and is inversely proportional to its radius. The Stokes radius is given by Equation 1.3

$$r = \frac{k_B T}{6\pi\eta D} \tag{1.3}$$

where k_B is the Boltzmann constant, T is the temperature, and D is the diffusion coefficient.

The above discussion gives the theoretical explanation for electrophoretic mobility. However, it is not easy to calculate electrophoretic mobility directly from theory. In practice, the electrophoretic mobility is determined experimentally from the migration time of an analyte, the applied potential and the column length, as shown in Equation 1.4.

$$\mu_p = \left(\frac{L}{t_r}\right)\left(\frac{L_t}{V}\right) \tag{1.4}$$

Here, L is the migration distance of an analyte from injection to the detection point, t_r is the migration time of the analyte, V is the applied voltage, and L_t is the total length of the capillary. Since only charged species are affected by the electric field, neutral analytes are not separated by CE.

1.2.2.2 Electroosmotic Flow (EOF)

In Section 1.2.2.1, the fundamental theory of CE is given, based on the assumption that the electric field and friction are the only forces that exist during CE. In most cases, due to the surface properties of columns, EOF also occurs during CE. Thus, the effects of EOF must be included in CE theory. EOF is the movement of an electrolyte solution inside a capillary induced by an applied electric field. EOF is caused by charged groups on the column surface. For example, in silica–based (glass, fused silica, silicon, etc.) CE columns, silanol (Si-OH) groups are present on the surface. When the solution in the capillary has a pH value >3, these silanol groups are ionized to form silanoate ($Si\text{-}O^-$) groups. The negatively charged capillary surface will attract positively charged counter ions from the buffer solution to form two ionic layers (the electrical double layer or diffuse double layer), as shown in Figure 1.8. The first layer of cations is attracted to the capillary surface tightly, and is called the fixed layer. The second (or mobile) layer of cations is further from the capillary surface, and is free to move toward the cathode when an electric field is applied. This motion of the mobile layer causes the bulk migration of solution in a capillary. Besides silica-based columns, polymer microdevices can also have EOF. The rate of EOF is dependent on the electric field and the charge density on the capillary wall, which can vary with the pH of the buffer solution. In silica-based columns, EOF will increase with pH until the capillary wall is fully ionized.

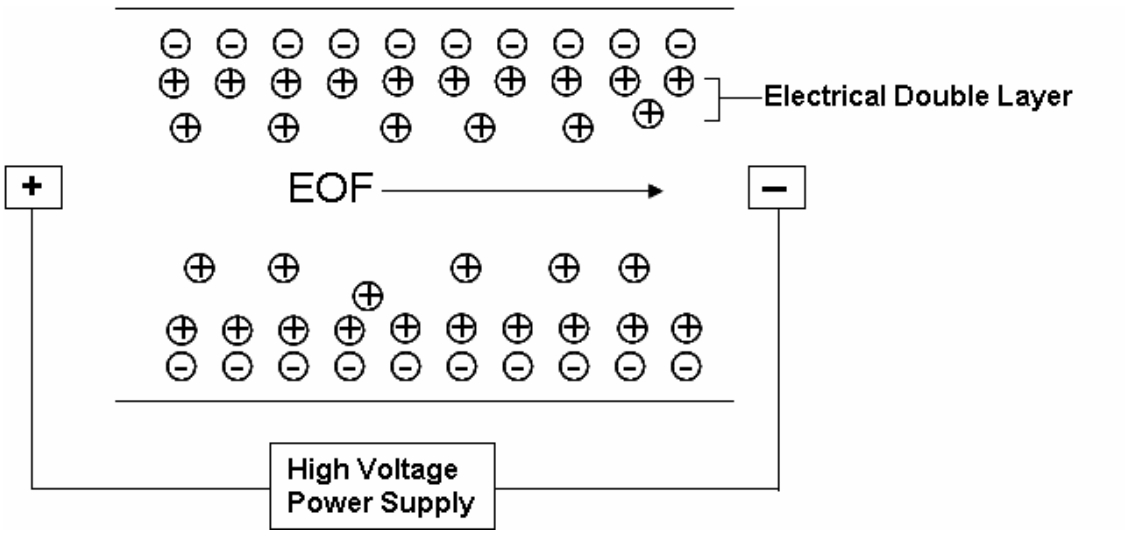

Figure 1.8 Schematic diagram of EOF in a fused silica capillary.

Since EOF is induced by an applied electric field, the electroosmotic velocity (u_o) can be written as

$$u_o = \mu_o E \tag{1.5}$$

where μ_o is the apparent electroosmotic mobility, which can be determined by experiment. In theory, μ_o is given by Equation 1.6

$$\mu_o = \frac{\varepsilon\zeta}{\eta} \tag{1.6}$$

where ζ is the zeta potential of the column and ε is the relative permittivity of the solution. The zeta potential is dependent on channel surface properties and the pH of the solution in the column.

Two methods are commonly used to determine EOF. The first is to measure the retention time of a neutral analyte during CE [92]; current monitoring [21, 59, 93] is the other method to measure EOF.

The above discussion indicates that the migration of an analyte in CE is dependent upon both the rate of EOF and the electrophoretic velocity. Thus, Equation 1.7 defines the net velocity (u) of an analyte in an electric field.

$$u = u_p + u_o = (\mu_p + \mu_o)E \tag{1.7}$$

In a typical CE system, the EOF is directed toward the cathode. Since analytes in CE migrate toward the electrode of opposite polarity, negatively charged species migrate opposite to the EOF direction, while positively charged analytes migrate with the EOF. Thus, negatively charged analytes are retained longer than positively charged ones.

1.2.2.3 Efficiency and Resolution in CE

In chromatography, theoretical plate counts are used to evaluate the separation performance. The number of theoretical plates (N) in CE is given by Equation 1.8

$$N = \frac{\mu V}{2D} \tag{1.8}$$

where μ is the apparent mobility (electrophoretic plus electroosmotic mobility) in the separation medium. Thus, the separation efficiency in CE is dependent only on the applied voltage and analyte diffusion; band broadening in CE is theoretically caused only

by longitudinal diffusion. This indicates that high performance can be achieved even with very short separation lengths, provided that heat dissipation is sufficient.

The resolution (R_s) in CE can be written as Equation 1.9.

$$R_s = \frac{1}{4}\left(\frac{\Delta\mu_p\sqrt{N}}{\mu_p + \mu_o}\right) \tag{1.9}$$

Equation 1.9 indicates that in order to achieve maximum resolution, the electrophoretic and electroosmotic mobilities should be similar in magnitude, but opposite in sign. In addition, higher resolution in CE can be achieved with lower net velocity.

1.2.3 Injection

In microchip CE, reproducible injection is critical to separation performance. Because of the small separation distance and channel dimensions, only a very short plug of sample should be injected into the separation channel for CE analysis. Otherwise, a large sample volume will lead to broad bands and decrease the separation efficiency. Currently, most injection methods for microchip CE are based on electrokinetic effects. Due to the influence of buffers, pH, ionic strength and EOF, different injection modes are used to adjust performance and compensate for these variables.

1.2.3.1 Cross Injection

Cross injection was the first method that was introduced in microchip CE [3], and the mechanism is shown in Figure 1.9. During the sample loading process, an electric field is applied between reservoirs 1 and 2, which drives sample through the intersection region.

Once the sample stream is formed, the electric field between reservoirs 1 and 2 is canceled, and a potential is simultaneously applied between reservoirs 0 and 3. This electric field will drive the sample in the channel intersection downstream and separate it. This technique is valuable because repeatable injections are feasible, but cross injection cannot control sample size reproducibly.

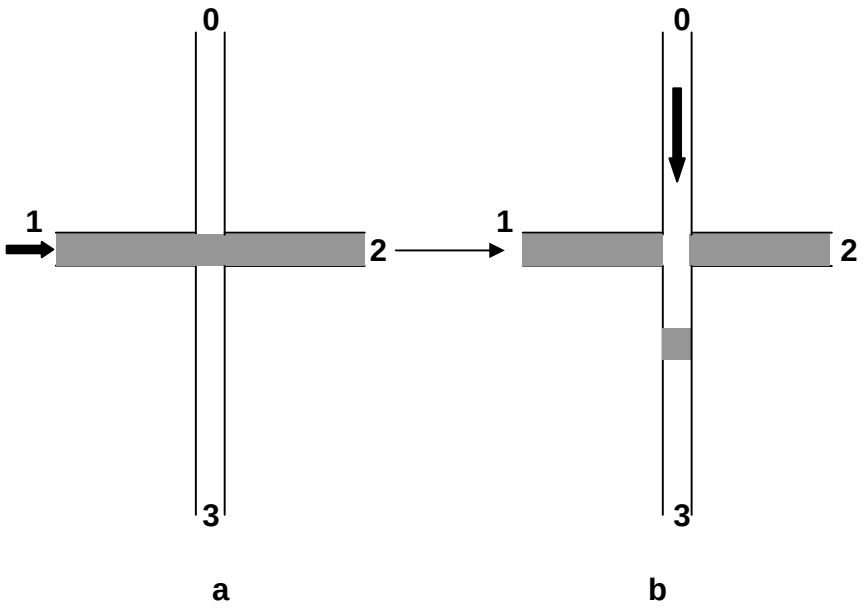

Figure 1.9 Cross injection. Sample (a) loading and (b) injection.

1.2.3.2 Double-T Injection

Double-T injection was introduced in 1993 [5]. In the sample loading step, a voltage is applied between reservoirs 1 and 2, while reservoirs 0 and 3 are floated. This voltage will drive the sample from 1 to 2 (Figure 1.10a). Once the analyte stream has passed the intersection, reservoirs 1 and 2 are floated, and a separation voltage is applied between

reservoirs 0 and 3. Thus, the sample plug is loaded into the separation channel for analysis (Figure 1.10b).

One advantage of double-T injection is that it can control injection plug size more accurately than cross injection. However, double-T injection has a serious problem of sample leaking from the injection channel into the separation channel [10]. This issue is mostly due to convection and diffusion, and it may cause the background signal to fluctuate and affect resolution.

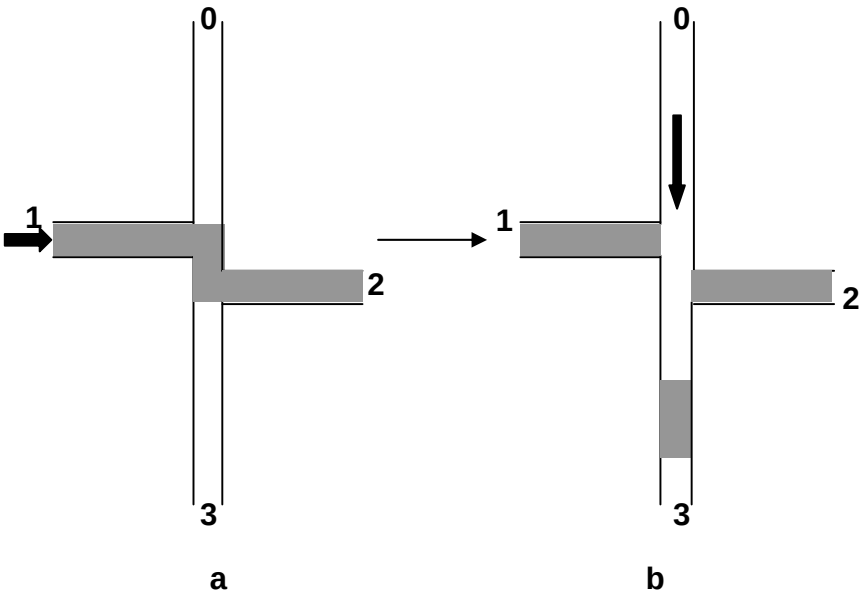

Figure 1.10 Double-T injection. Sample (a) loading and (b) injection.

1.2.3.3 Pinched Injection

Pinched injection was first reported by Jacobson *et al.* in 1994 [11] to address sample leakage problems of other methods. The scheme of pinched injection is shown in Figure 1.11. During loading, reservoir 2 is grounded, while potentials are applied to reservoirs 0, 1 and 3. For separation, voltage is applied on reservoir 0, while reservoirs 1-3 are

grounded. In this case, only a well-defined and reproducible sample plug at the channel intersection will be loaded on the column and separated. Pinched injection can not only avoid sample leakage, but also provide reproducible sample loading.

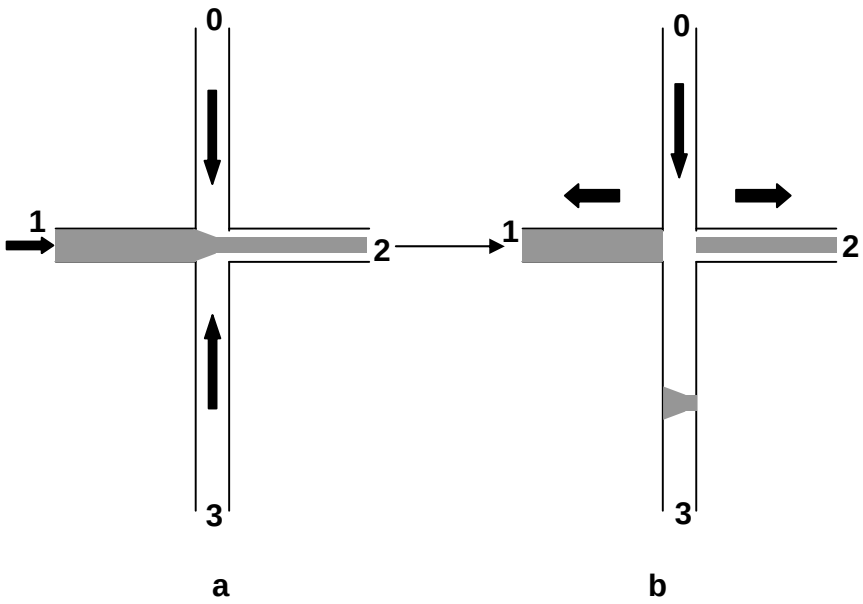

Figure 1.11 Pinched injection. Sample (a) loading and (b) injection.

1.2.3.4 Single-T injection

Single-T injection was among the first generation of injection modes introduced for microchip CE [4]. The scheme of single-T injection is shown in Figure 1.12. In the loading step, the sample is driven from reservoir 1 toward reservoir 2 by applying a potential. Once the sample stream reaches the separation channel, the voltage is reconfigured and applied between reservoirs 0 and 2 to drive the sample plug into the channel for CE separation. This scheme is simple, and is still in use today; however, injection bias for higher-mobility analytes can be introduced.

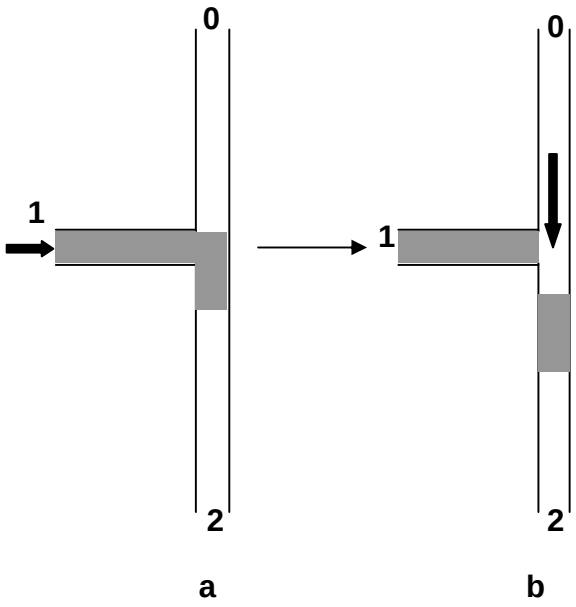

Figure 1.12 Single-T injection. Sample (a) loading and (b) injection.

1.2.3.5 Gated Injection

As a continuous sampling method, gated injection was introduced in 1994 [11]. This method includes three steps, as shown in Figure 1.13. In the first step, two voltages are applied, one from reservoirs 0 to 2, and the other from 1 to 3. These applied potentials prevent sample leakage into the separation channel. Next, the voltage from reservoirs 1 to 3 is canceled for a brief (<2 s) time, and a small amount of sample enters the separation channel due to diffusion. Then, the voltage between reservoirs 1 and 3 is resumed, and the small sample plug is separated. One advantage of this technique is that it can control the injection time and amount by careful voltage adjustment.

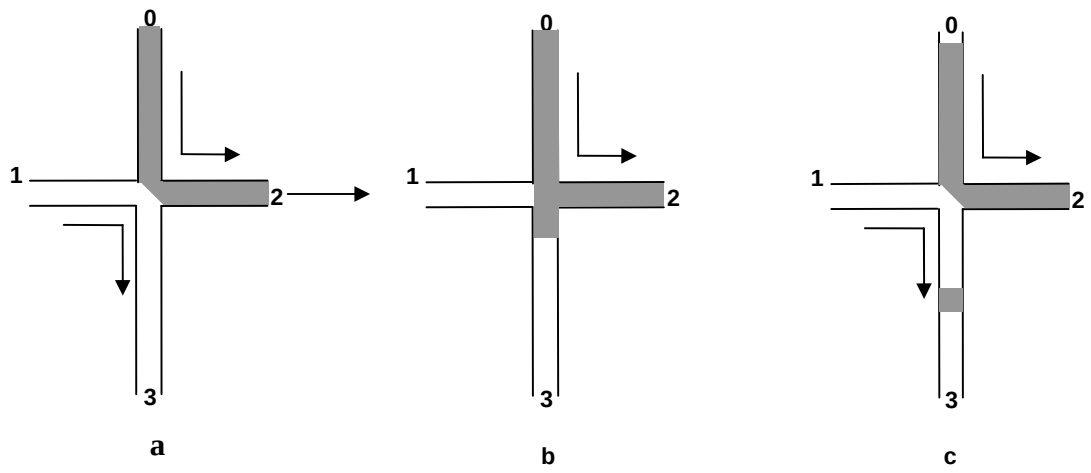

Figure 1.13 Gated injection. Sample (a) loading, (b) injection and (c) separation.

1.2.3.6 Optically Gated Injection

Optically gated injection is an advanced method that can produce tiny and reproducible sample plugs for CE [94] and microchip CE [95]. This technique uses a laser beam to bleach the sample stream, such that sample plugs are only produced when the laser is blocked. Optically gated injection can produce picoliter loaded volumes and provide <3% relative standard deviation in injection reproducibility.

1.2.3.7 Double-L injection

Double-L or low-leakage injection, has been studied by Fu *et al.* [96, 97]. This method uses "L"-shaped voltage paths to control the movement of analytes, as shown in Figure 1.14. At first, an "L"-shaped voltage is applied from reservoir 1 to 0 to form the sample stream (Figure 1.14a). Next, this voltage is canceled, and a new voltage is applied from reservoirs 2 to 3, driving the sample plug into the separation channel for CE analysis

(Figure 1.14b). Double-L injection is claimed to be very suitable for biochemical analysis to gain high resolution, high throughput and precision.

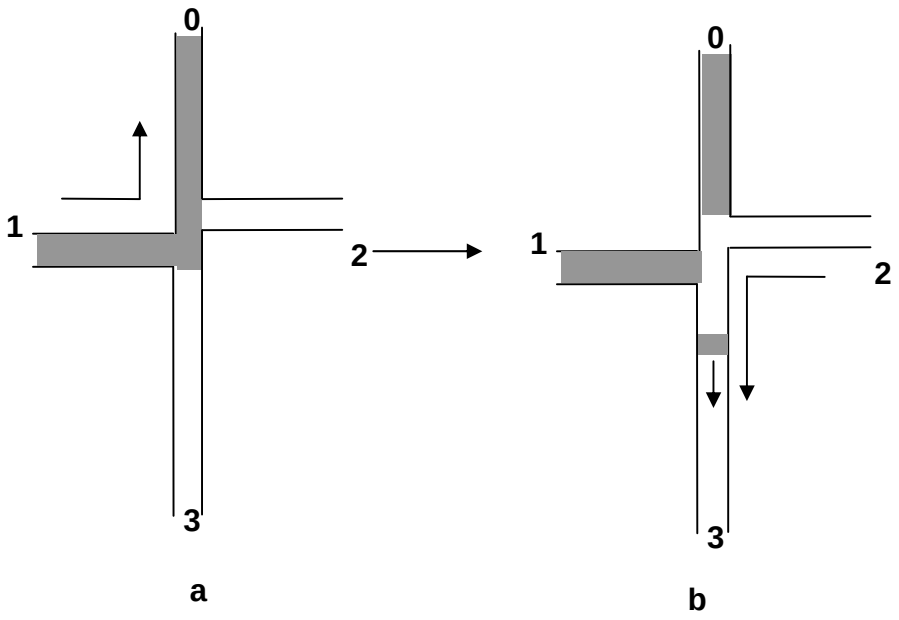

Figure 1.14 Double-L injection. Sample (a) loading and (b) injection.

1.2.4 Detection Approaches in Microchip CE

1.2.4.1 Optical Detection

UV-absorbance detection is the most commonly used optical detection method for conventional CE and HPLC. Importantly, native samples can be detected by UV absorbance. UV detection is also used occasionally for inorganic CE microdevices (e.g., glass) [98-100]; but to date little UV absorbance detection has been done in polymeric CE microchips. Now, things are changing with the development of UV-transparent PMMA (OP-1) and Topas COC polymers, such that in the future UV absorbance should also find application in polymer microchip CE systems.

Laser induced fluorescence (LIF) is the most widely used optical detection method for microchip CE [4, 5, 10, 17, 21, 22, 35, 53, 101] because most microchip CE materials are transparent to visible wavelengths of light. Another advantage of LIF is that it has very low limits of detection. However, most analytes such as proteins and peptides do not have intrinsic fluorescence at visible excitation wavelengths (e.g., 488 or 532 nm). Thus, labeling with fluorescent dyes is needed for microchip CE with LIF detection [17, 21, 22]. Several methods have been developed for protein and peptide tagging, including widely used FITC labeling.

Two-photon excited fluorescence (TPEF) detection has also been introduced for CE [102, 103] and microchip CE [104] to detect the native fluorescence of proteins, peptides and other analytes. In single-photon florescence, the fluorophore only absorbs one photon in jumping to an excited electronic state; during relaxation to the ground state, fluorescence is emitted. In some circumstances a molecule can absorb two photons to transition to an excited state. In a typical TPEF process, a tightly focused laser beam provides a high density of photons. If the fluorophore absorbs two photons sequentially within ~1 fs, it will transition to the excited state. When the fluorophore relaxes to the ground state, fluorescence is emitted. If two photons are not absorbed sequentially within ~1 fs, no fluorescence is emitted. TPEF has two advantages when compared to UV and LIF detection. First, excitation in TPEF is in the visible range. Second, since TPEF is not in the same wavelength region as the excitation light (in most situations it is at a shorter wavelength than the source), it is easier to discriminate fluorescence from the excitation source and background [105].

IR and Raman detection have not been reported in microchip CE; however, papers have shown the application of IR [17] and Raman [106] methods in microfluidic devices.

1.2.4.2 Electrochemical Detection

Compared to optical methods, electrochemical detection can be simpler and less expensive. Moreover, electrochemical detection can be integrated readily into microfluidic devices. Furthermore, electrochemical methods have low detection limits (~0.75 pM) [107] and fast response times (300 ms) [108]. Application of electrochemical detection in a μTAS system was first reported in 1998 [23] in the amperometric mode. Since then, conductometry [109, 110] and voltammetry [111] have also been used in microchip detection.

1.2.4.3 Mass Spectrometry

Mass spectrometry (MS) is a very powerful tool in analytical chemistry, and offers small sample consumption, high sensitivity and fast analysis time. Moreover, MS can elucidate the structure of analytes, which is extremely useful in biological applications. Microchip CE devices have been coupled to MS through electrospray ionization interfaces [112-115].

1.2.5 Surface Modification

1.2.5.1 Dynamic Coating

Dynamic coating is a simple and fast surface modification method. In a typical dynamic coating process, a surface modifier is added to the separation buffer and flushed through the channel at a constant speed for a period of time. During this process, the surface modifier is physically adsorbed onto the channel surface. Adsorbed surface modifier can reduce EOF and protein adsorption, thus improving CE performance. Species used in

dynamic coating include charged compounds, neutral polymers, surfactants and nanoparticles.

Several kinds of charged compounds have been applied in dynamic coating, including polybrene, dextran, polystyrene sulfonate, poly(allylamine hydrochloride) and low-molecular weight charged compounds (e.g., mono-, di-, and triethylamines) [39, 116-118]. The molecular weight of the surface modifier is important to the coating performance. For large polymers, hydrophobic interactions of analytes with the coating may induce peak tailing [39]. However, low-molecular-weight charged compounds cannot effectively cover all the channel surface, which means that biomolecule adsorption on surfaces may not be eliminated [118].

Neutral hydrophilic polymers are used in CE to reduce biomolecule adsorption to the column surface [87, 119]. To reduce nucleotide adsorption, mixtures containing hydroxypropyl methylcellulose (HPMC), mannitol, glucose, glycerol and poly(ethylene glycol)-poly(propylene glycol)-poly(ethylene glycol) copolymer have been used [87, 119]. To reduce protein and/or peptide adsorption, poly(ethylene glycol) (PEG), hydroxyethylcellulose, HPMC, poly(N,N'-dimethylacrylamide) and methylcellulose have been used [88, 118].

Other commonly used compounds for dynamic coating include surfactants, which are used to dynamically coat hydrophobic surfaces. Because surfactants have both hydrophobic and hydrophilic ends, they can be adsorbed on surfaces through hydrophobic interactions. Once surfactants are aligned on a surface, their hydrophilic ends extend outward and change channel surface properties. Reported surfactants used for dynamic

coating include Brij35, Brij76, Brij78, cetyltrimethylammonium, dodecyltrimethylammonium, dodecyl sulfate and tetrabutylammonium [89, 118-121]. Recently, gold nanoparticles (GNP) have been used with polymers for dynamic coating. [122, 123]. GNPs increase the viscosity and stability of the coating, thus improving CE performance.

1.2.5.2 Permanent Surface Modification

Although dynamic coating is the simplest method for surface modification, its effects do not last long. Compared to dynamic coating, permanent surface modification is complex and lab intensive, but it is more effective. Two methods have been used for permanent surface modification. One is conducted by specific chemical reactions to modify the surface chemistry, while the other method uses a high energy source to activate or alter the chemical structure of the surface.

Surface Modification of Inorganic Microdevices. Since most inorganic materials used for microdevices are silica-based (glass, quartz, etc.), they can be derivatized using silane chemistry [124-126]. The surface modification of inorganic microdevices is not closely related to my research, so further details will not be given here.

Oxygen Plasma Treatment. Oxygen plasma treatment is a simple and rapid method for polymer surface modification. This method utilizes a high energy plasma to form hydrophilic structures on polymer surfaces, such as on PDMS [53] or TPE [59]. However, the hydrophilic effect induced by the plasma does not last long, so in most cases, oxygen plasma treatment is used to activate the polymer surface for the immobilization of other functional groups. For example, alkyltrichlorosilanes [127], 2-

[methoxy(polyethyleneoxy)propyl] trimethoxysilane and poly(ethylene glycol) di(triethoxy)silane [128] have been immobilized on plasma-activated PDMS surfaces to reduce protein adsorption.

UV Radiation Treatment. UV radiation is another high-energy source for surface modification of polymer materials. UV radiation can generate high-energy, short-lived free radicals on polymer surfaces. If a monomer solution is present on the surface, these free radicals can initiate polymerization [129-131]. However, one-step UV-activated grafting requires a high dose of UV radiation, and polymerization is not easily controllable, which often leads to channel clogging. Thus, "surface-directed" graft polymerization was developed [131, 132] in which PDMS is first immersed in an organic solution that contains free radical initiators (photoinitiator or thermal initiator) to adsorb them into the PDMS. Then, the PDMS is taken out of solution, dried and transferred into an aqueous solution of a hydrophilic monomer. After this step, heat or UV radiation is used to activate the graft polymerization of monomer on PDMS. Using this method, a uniform layer of a hydrophilic polymer can be grafted on the PDMS surface. Peptide separations were shown in PDMS devices coated by this method, indicating its effectiveness in permanent surface modification [130].

Atom Transfer Radical Polymerization. Atom-transfer radical polymerization (ATRP) [133-135] has been used for chemical modification of PDMS [33, 136] and PMMA [21] microchannels. ATRP modification of plastics involves activation of the surface via plasma oxidation, immobilization of the initiator, and subsequent grafting of the chosen polymer to the surface (see Section 3.2.3 and Figure 3.3). In ATRP, the length of polymer attached to the surface can be controlled readily. ATRP has been used in surface

attachment of various polymers, including polyacrylamide [137], hydroxypropyl cellulose [138], methacrylate [139], PEG [21], and peptidoglycans [140]. Typically, neutral polymers are used to eliminate electrostatic interactions with analytes. PEG-modified PMMA devices have shown improved separation performance relative to unmodified ones [21].

1.3 Affinity CE for Cancer Marker Protein Analysis

1.3.1 Cancer Marker Proteins

1.3.1.1 Introduction

Cancer markers are species, such as proteins, hormones, small molecules, etc., which are produced by cancer cells or by the body in response to cancer [141-143]. These moieties are called "markers" because they are associated with cancers, or at least their identification and measurement can be used to evaluate the existence and potentially the stage of cancers. Cancer markers can be found in blood, urine and body tissues, and their concentrations are several orders of magnitude lower than abundant proteins (such as IgG, hemoglobin and albumin) [142, 144].

Cancer markers can be used for the following purposes: 1) to monitor people or high risk populations for cancers, 2) to diagnose the existence of cancers, 3) to determine the stage of an existing cancer, and 4) to monitor cancer recurrence during or after treatment [142, 143]. An ideal cancer marker should meet all of the above four purposes, and any assay should be 100% sensitive, without false negatives. However, none of the currently known cancer markers can do this. Most cancer markers are neither sensitive nor specific enough to diagnose cancer without the support of other clinical tools. It is also possible for a

cancer patient to have similar marker levels to a healthy person. Importantly, cancer markers do have the potential to help doctors diagnose cancer.

Several commonly known cancer markers include human chorionic gonadotropin (hCG), a marker for testicular cancer; carcinoembryonic antigen, a marker for colorectal cancer; prostate-specific antigen, a marker for prostate cancer; alpha-fetoprotein, a marker for hepatic and testicular cancers; cancer antigen 125, a marker for ovarian cancer; and cancer antigens 15-3 and 27.29, markers for breast cancer.

1.3.1.2 Human Choronic Gonadotropins and Their Analysis

Human chorionic gonadotropin is well known as the analyte that is probed in pregnancy tests [145]. It is a peptide hormone produced by human females and is overexpressed in pregnancy. The hCG protein is composed of 244 amino acids (heterodimeric with 2 subunits) with a molecular mass of 36.7 kDa [146]. The α subunit has 92 amino acids and is identical to that of the luteinizing hormone, follicle-stimulating hormone, and thyroid-stimulating hormone. The β subunit is unique to hCG but shares some common amino acid sequences with the α subunit [144, 145]. In biological fluids, hCG appears as intact hCG, free α subunit, free β subunit, and various fragments such as nicked hCG and nicked free βhCG.

In pregnancy, hCG is overexpressed, and its level can increase over 10,000 fold during pregnancy [145]. For example, non-pregnant females have hCG levels lower than 5.0 mIU/mL in blood, a woman in her first two months of pregnancy will have an hCG level as high as 5000-200,000 mIU/mL, and a female in her 3rd trimester will have hCG levels

between 1000-50,000 mIU/mL [147]. Thus, hCG levels provide an excellent diagnostic marker for pregnancy.

The β subunit of hCG is also overexpressed in some cancers including teratomas, choriocarcinomas (often found in the testes and ovaries) and islet cell tumors (e.g., in the brain as dysgerminoma) [145, 148]. Thus, both hCG and free βhCG should be detected in individuals with these cancers, and an elevated level of total hCG should occur. However, for females, elevated hCG levels are not always linked to cancer occurrence. Also, women with low hCG levels are not totally excluded from cancer risk. Since males don't normally produce βhCG, any detectable βhCG level indicates a high risk of cancer. Moreover, once cancer is diagnosed, hCG levels are useful for doctors to ascertain the effects of cancer treatments. After a successful treatment, the patient's hCG level is expected to drop [142, 145, 149].

Currently, detection of hCG involves immunological means, such as enzyme-linked immunosorbent assay (ELISA), radioimmunoassay (RIA) and western blotting, which normally gives a "true" or "false" result [145]. This is sufficient to diagnose pregnancy, but for cancer, a "true" or "false" result is not enough, because the level of hCG in a patient correlates with the existence, stage, or recurrence of cancer. In cancer diagnosis, two different hCG antibodies (anti-α- and anti-βhCG) should be used. The anti-βhCG antibody will give the total hCG amount, while the anti-αhCG antibodies give only the level of intact hCG in the sample. The difference between these two results yields the amount of βhCG in the sample, which is very useful for cancer diagnosis. Unfortunately, this dual antibody method is expensive, labor intensive, and time consuming, such that a

new approach should be developed for detection of both hCG and βhCG. In Chapter 5, I further discuss the potential of one such approach.

1.3.2 Affinity Methods for Cancer Marker Detection

1.3.2.1 Protein Analysis

Biological samples such as blood, urine, and body fluids are very complex, and may contain hundreds or even thousands of different proteins [150, 151]. For example, ~500 distinct proteins have been identified in serum using on-line reversed-phase micro capillary liquid chromatography coupled with ion trap MS [152]. In samples like blood, protein concentrations range widely from 50 mg/mL for albumin [153] to several ng/mL for some cancer markers [154, 155]. When cells/tissues are damaged (as in some cancers), cellular proteins can also escape into the blood or intravascular fluids.

Currently, the most prevalent method in proteomics is two-dimensional (2D) gel electrophoresis [156, 157], which can isolate more than one thousand protein bands in a sample. However, this technique is expensive, labor intensive, time consuming, and not reproducible. Also, 2D gel electrophoresis cannot resolve both large and small proteins, and analyte recovery from the gels is limited, due to the low mass loading (<300 μg). Moreover, numerous treatments need to be done before and after the sample is separated by 2D gel electrophoresis, because this method cannot automatically select the target proteins in a complex sample. Thus, although 2D gel electrophoresis is effective for protein analysis, it is still a bottleneck in proteomic studies. Besides 2D gel electrophoresis, other approaches such as 2D liquid-phase separation [158] and 2D liquid chromatography [159] have been developed to improve performance in protein analysis, but more work still needs to be done.

1.3.2.2 Applications of Affinity Techniques in Cancer Marker Analysis

In Section 1.3.2.1, I discussed the current methods for protein analysis and concluded that no approach is ideal. Also, in many situations it is not necessary to identify all the proteins in a sample when one only needs to know the concentrations of certain target proteins. For this reason, affinity techniques have become popular in many assays involving cancer markers.

Affinity methods are based on the strong and selective interaction between antibody and antigen. For cancer diagnosis, normally one only needs to quantify several marker proteins in a mixture that may have numerous types of other proteins; thus, it is not necessary to separate and isolate every protein in the sample. Affinity techniques can be used to extract and concentrate proteins of interest from a sample mixture. These advantages of affinity methods explain why so far, most approaches for cancer diagnosis are based on immunological techniques, such as RIA [160], ELISA [161] and western blotting [162].

1.3.2.3 Monolithic Columns

The use of a monolith was first demonstrated by Hjerten in 1989 [163]. The monolith was originally called a continuous bed or continuous polymer bed. Monolithic columns contain continuous rods with micrometer-dimension canal-like through pores and nanometer-size pores within the bed structure. These structures are formed in a column by polymerization/sol-gel reaction, so compared with conventional packing, monolithic materials require lower pumping pressures (lower back pressure), and no frit is needed [164-167].

There are two types of monoliths. Those based on a silica backbone are synthesized using a sol-gel reaction in a mold [168-170]. This type of monolith is typically hydrophobic after surface derivatization and is only suitable for the separation of small molecules. Thus, I will not discuss these in detail here. The second type of monolith includes polymer monoliths, which are typically prepared *in situ* using UV or thermal polymerization of solutions composed of a monomer, crosslinker, porogen, and initiator [164-167, 171]. Polymerization can be initiated using a redox system (e.g., tetramethylethylenediamine and ammonium persulfate) or a free radical initiator (DMPA). The detailed mechanism of monolith formation is not completely known, but it is believed that the porogen aids in the formation of the monolith structure and pores.

One advantage of a monolithic material is that it has high chemical resistivity, which makes it suitable for use under extreme conditions. Also, because monoliths can be polymerized inside columns and covalently attached to the surface, no frit or fitting is needed. The large canal-like through pores ensure high mass transfer rates and low flow resistance; while nanometer-size pores create faster diffusion between the mobile and stationary phases. Consequently, rapid and high-quality separations can be achieved in monolith columns, and polymeric monoliths have been proposed as phases for antibody attachment [137, 165, 172].

In Chapter 5, I discuss a monolith based on glycidyl methacrylate (GMA), which has a hydrophilic surface. Both basic and acidic model proteins have been separated successfully in such columns [165, 171]. Importantly, the reactive epoxy groups on the GMA monolith surface make it a perfect candidate for antibody attachment.

1.3.3 Immobilization of Antibodies on GMA Polymer Monoliths

Since GMA epoxy groups in monoliths are reactive, considerable effort has been placed on attachment of proteins of interest to these surfaces. Currently, there are four methods that can perform antibody attachment successfully on GMA monoliths.

1.3.3.1 Direct Attachment

The active epoxy groups present on GMA monoliths can react directly with an amino group of a protein to form a covalent linkage [164]. Armenta *et al*. successfully attached protein G to a GMA monolith using this method [165, 171]. Protein was first dissolved in pH 9.2 carbonate buffer and flushed through the GMA monolith. Then both ends of the column were sealed and the monolith was heated for 20 h at 34 ºC. However, this attachment needed a high concentration of protein sample (>1 mg/mL), long reaction time and somewhat elevated temperature. Moreover, because most proteins have both terminal and side chain amino groups, direct amine reaction cannot control the orientation of a protein attached to a monolith. The orientation of antibodies on the surface is critical to function and activity.

1.3.3.2 Acid Hydrolysis Followed by Oxidation

An alternative to direct attachment is acid hydrolysis followed by oxidation (Figure 1.15) [137, 173]. Typically, the surface GMA groups are first hydrolyzed, followed by oxidation using periodate. Then the activated aldehyde groups can react with protein amine functionalities to form an imine (–C=N-) group. Because the imine group is not very stable, it needs to be reduced to –C-NH- to increase attachment robustness. Compared to direct attachment, this method is more effective, particularly with respect to

reaction time and efficiency. However, this technique cannot control the orientation of proteins attached to the surface.

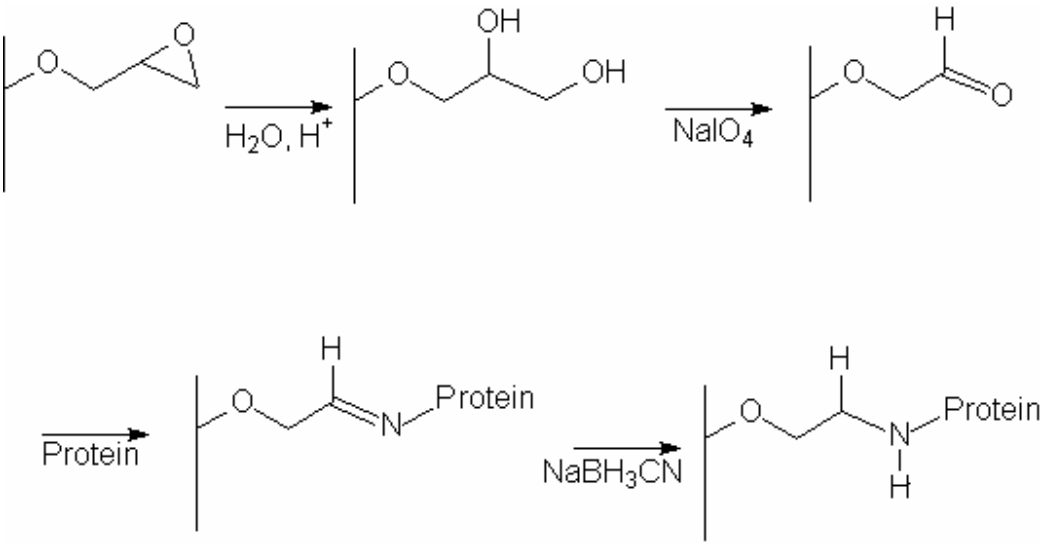

Figure 1.15 Attachment of protein to a GMA monolith by acid hydrolysis/oxidation.

1.3.3.3 Aminolysis Followed by Dialdehyde Activation.

Another method to immobilize proteins on GMA monoliths uses aminolysis followed by dialdehyde reaction (Figure 1.16) [174-176]. In this method, the epoxy groups are first reacted with a diamine, followed by activation with a dialdehyde to extend the length of the anchoring chain. The terminal aldehyde groups on the anchoring chain can then react with protein amine groups to attach them to the monolith. Finally, the imine groups are reduced, as in Section 1.3.3.2. One advantage of this approach is that the anchoring chain is extended so the attached protein has greater orientational flexibility. Moreover, this method is well-developed. However, this technique cannot control the orientation of attached proteins.

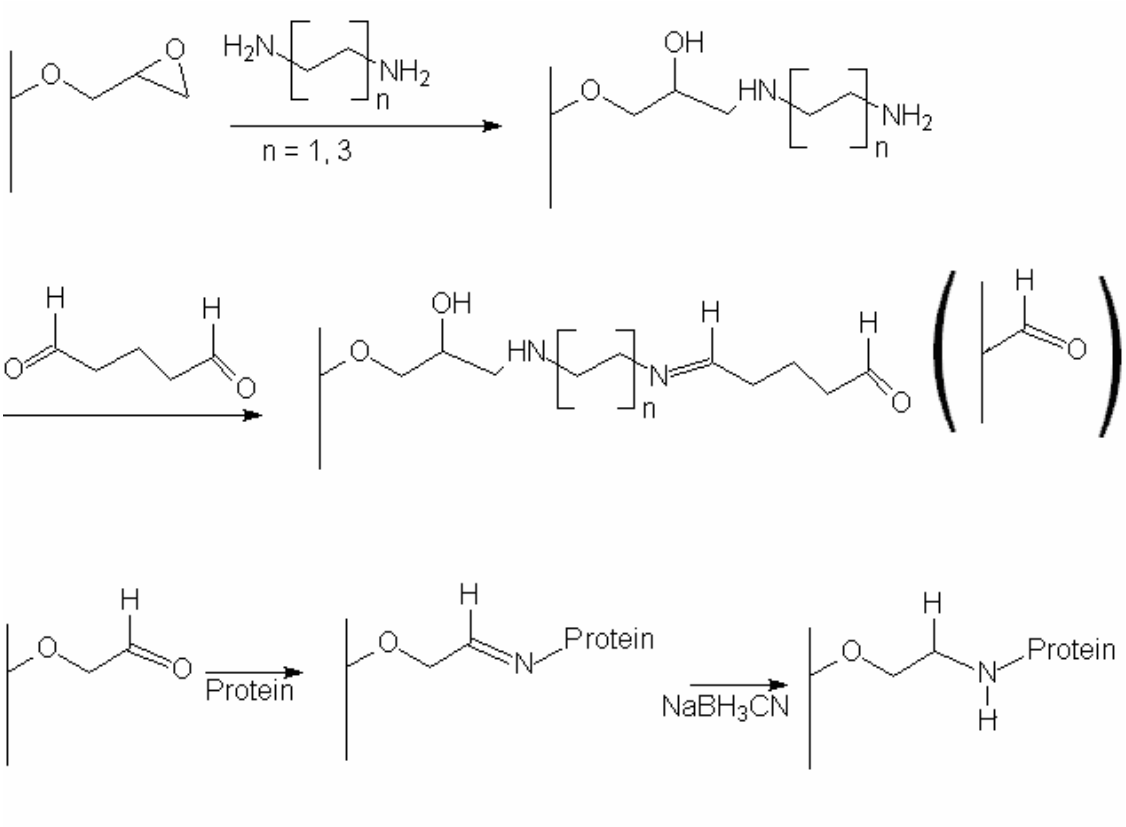

Figure 1.16 Attachment of protein to a GMA monolith by aminolysis and dialdehyde activation.

1.3.3.4 Hydrolysis Followed by Carbonyldiimidazole Activation

Hearn *et al.* [177] first proposed this attachment approach; in 2004, this method was used to attach trypsin on GMA [178]. The mechanism of attachment is shown in Figure 1.17. After acid hydrolysis, the GMA surface is reacted with carbonyldiimidazole (CID), which has high reactivity toward amine groups, and can be used to link proteins to the monolith. Unreacted CID groups on the GMA monolith can be quenched by Tris buffer or aspartic acid solution. One advantage of this method is that the reaction between CID and protein is very fast; furthermore, a literature report indicates that this method can provide better column performance than direct attachment [178]. However, the orientation of the

attached proteins is not controlled in this approach.

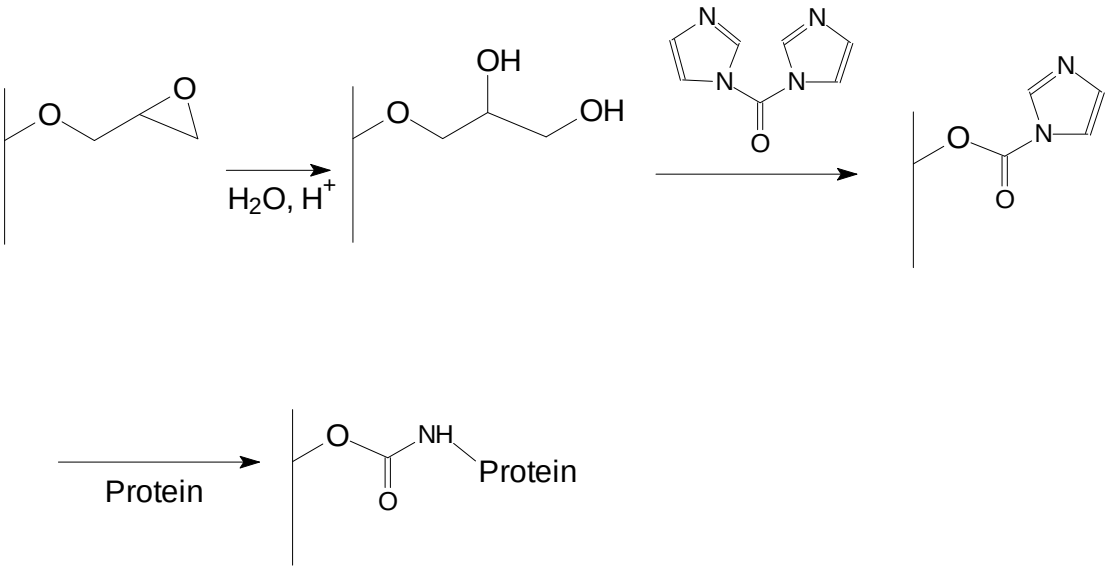

Figure 1.17 Attachment of protein to a GMA monolith by hydrolysis and CID activation.

1.3.3.5 Attachment of Antibodies to Surfaces Using the Pierce Method

Pierce (Rockford, IL) has a standard method for oriented antibody attachment to glass surfaces [179]. Briefly, a glass surface is first treated with 3-aminopropyltriethoxysilane, which will create amine groups. Then, a crosslinker which can react with both amine and thiol groups is attached to the amine-modified surface. Next, the antibody is partially reduced to create free thiol groups, and this protein reacts with the surface. This method has the unique feature of controlling orientations of attached antibodies to retain activity. The disadvantages of this method are that it requires multiple steps and is complicated. My antibody attachment procedure has a similar mechanism, and details will be discussed in Chapter 5.

1.4 Electric Field Gradient Focusing (EFGF)

1.4.1 Principle of EFGF

Field-gradient methods were first defined by Giddings [180] as techniques that can isolate and focus analytes at certain points under different gradients/forces. EFGF is an equilibrium-gradient method for charged analytes in which a constant flow is created in one direction while a gradient in electric field is applied in the opposite direction. As shown in Figure 1.18, when a charged analyte is introduced into an EFGF device, it will be driven by the constant flow in one direction, countered by electrophoretic migration in an electric field gradient in the opposite direction. Since the electric field varies along the column, a given protein will have a different electrophoretic velocity, depending on its position in the channel. When the electrophoretic and flow velocities of a protein are opposite in direction and equal in magnitude, the protein will be focused at that point in the EFGF channel. Since proteins normally have different electrophoretic mobilities, they will focus at distinct positions in an EFGF device.

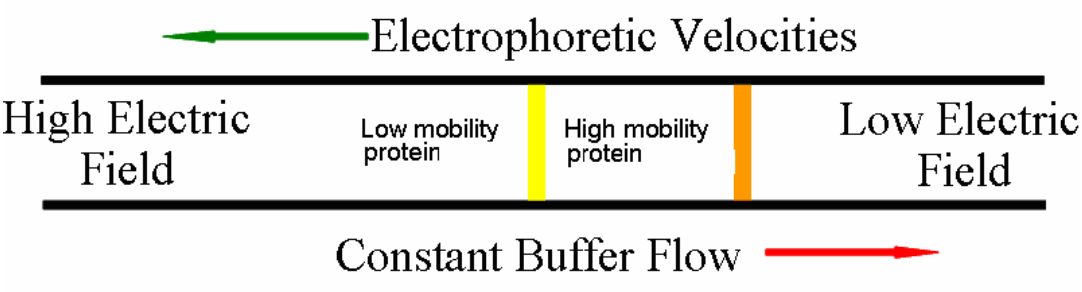

Figure 1.18 Scheme of EFGF; proteins are focused based on the equilibrium between electrophoretic velocity and constant flow.

Compared to other protein separation techniques, EFGF has several advantages. First, EFGF has the potential to provide high resolution and peak capacity [72, 181, 182]. Theoretical studies have shown that EFGF should be able to separate two proteins with a pI difference of less than 0.001 [183]. Moreover, EFGF parameters can be adjusted easily; by simply changing the applied potential or flow rate, one can control the movement and focusing position of analytes. In addition, EFGF can be used to trap selected proteins of interest in a column. Other proteins, which have either too high or too low electrophoretic mobilities, will not be kept inside the EFGF channel. Last, EFGF can concentrate analytes while they are being separated. Since most cancer markers are many orders of magnitude lower in concentration than major serum proteins (such as IgG and albumin), the last two advantages are very important in cancer marker analysis.

Two types of EFGF devices have been developed in our laboratories. One is capillary based [72], as shown in Figure 1.19. The other is microchip based, and uses either a sacrificial layer [184] or a weir structure [185] instead of a wire to define the EFGF channel.

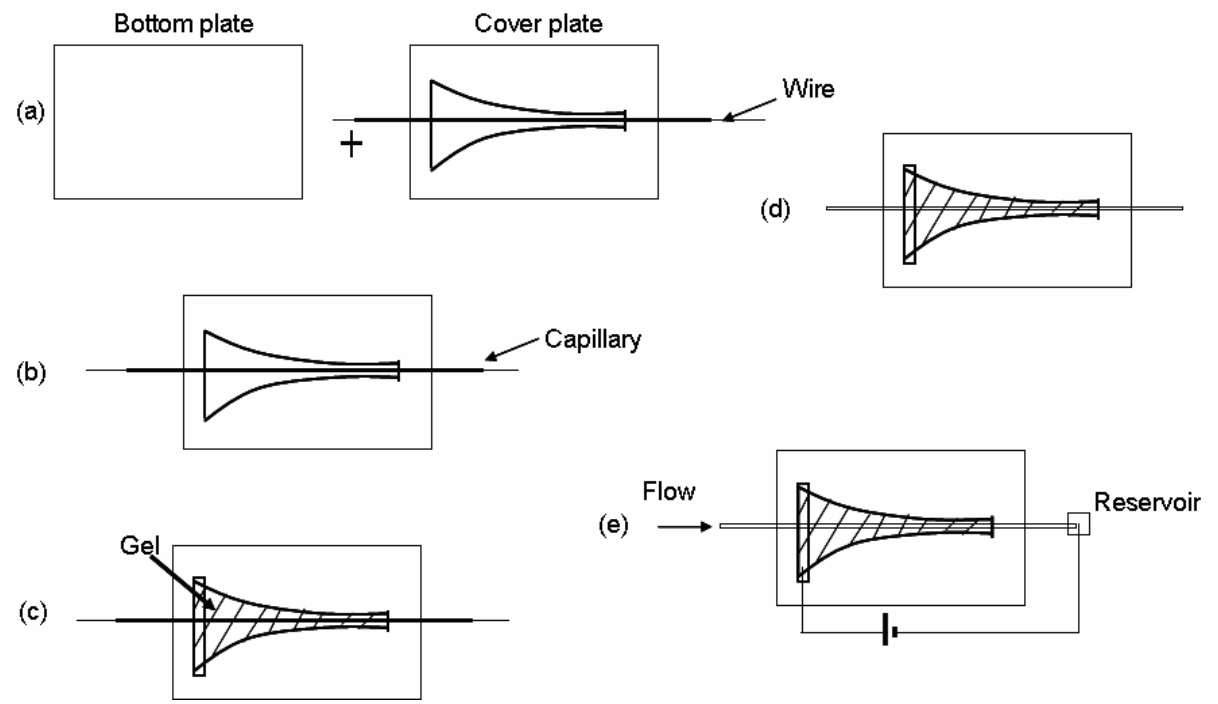

Figure 1.19 Fabrication and operation of a capillary-based EFGF device. (a) Two PMMA plates and two capillaries with a suspended wire are needed to prepare a device. (b) The assembly is formed by thermal bonding. (c) The conductive gel is polymerized. (d) The wire is removed to make the final EFGF device. (e) Operation of an EFGF device: a syringe pump is connected to the left capillary to provide flow. Sample can be injected from the reservoir by the applied electric field, or from the syringe pump.

A protein mixture containing green fluorescent protein (GFP) and R-phycoerythrin (R-PE) can be separated successfully using such EFGF devices (Figure 1.20). Microchip-based EFGF systems have better resolution than the capillary-based setup, because of the smaller channel dimensions and lower laminar flow dispersion compared to capillary-based EFGF devices.

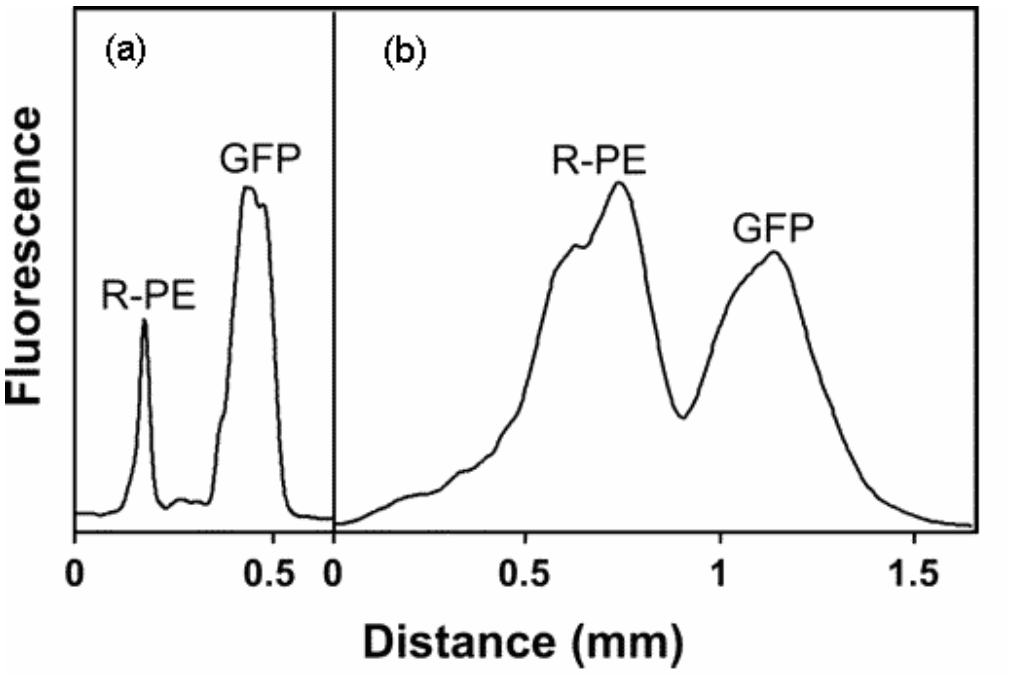

Figure 1.20 EFGF focusing of two proteins, GFP and R-PE in (a) microchip-based, and (b) capillary-based EFGF devices. Reprinted with permission from [184] (copyright 2006 American Chemical Society).

1.4.2 Advantages of Affinity-Coupled EFGF

As discussed in Section 1.3.2.1, current methods for cancer marker analysis have some disadvantages, and new techniques should be developed. Affinity-coupled EFGF is a potentially advantageous candidate for high-performance cancer marker analysis, compared to conventional methods. First, this technique should be simpler and less hazardous because it does not need either radioactive materials or addition of secondary antibodies, as in RIA, ELISA or western blotting. Moreover, EFGF patterns can be adjusted readily by changing the flow rate or applied potential. Affinity-coupled EFGF should also allow selection and concentration of target proteins from a complex biological

sample without interference from other analytes. I believe affinity-coupled EFGF has broad potential in protein analysis.

1.5 Dissertation Overview

My dissertation work focused on three general areas of miniaturized analysis. The first project involved the development of new microdevices made of CaF_2 as described in Chapter 2. A method was devised for machining enclosed CaF_2 microchannels, and amino acid separations were carried out in these microdevices. Moreover, on-chip IR detection was performed for the first time on these microchips. My second area of emphasis was the surface modification of polymer microdevices to improve their CE performance in bioanalytical applications. Two different polymers, PMMA and TPE, were derivatized covalently using ATRP. Microchip CE of proteins, peptides and amino acids was used to test the performance of surface-modified PMMA and TPE microdevices. Derivatization and characterization of surface-functionalized PMMA and TPE microchips are presented in Chapters 3 and 4, respectively. Chapter 5 describes the development of an affinity column−CE system for the selective enrichment and CE separation of hCG, which could be used for cancer marker analysis. I developed a new method to attach oriented antibodies on monoliths such that activity was retained. Finally, conclusions and future directions are discussed in Chapter 6.

1.6 References

[1] Terry, S. C., Ph.D Dissertation, Stanford University 1975.

[2] Terry, S. C., Jerman, J. H., Angell, J. B., *IEEE Trans. Electron Devices* 1979, *ED26*, 1880-1886.

[3] Manz, A., Harrison, D. J., Verpoorte, E. M. J., Fettinger, J. C.*, et al.*, *J. Chromatogr.* 1992, *593*, 253-258.

[4] Harrison, D. J., Manz, A., Fan, Z., Luedi, H., Widmer, H. M., *Anal. Chem.* 1992, *64*, 1926-1932.

[5] Effenhauser, C. S., Manz, A., Widmer, H. M., *Anal. Chem.* 1993, *65*, 2637-2642.

[6] Tang, T., Badal, M. Y., Ocvirk, G., Lee, W. E.*, et al.*, *Anal. Chem.* 2002, *74*, 725-733.

[7] Broyles, B. S., Jacobson, S. C., Ramsey, J. M., *Anal. Chem.* 2003, *75*, 2761-2767.

[8] Shi, Y., Simpson, P. C., Scherer, J. R., Wexler, D.*, et al.*, *Anal. Chem.* 1999, *71*, 5354-5361.

[9] Reyes, D. R., Iossifidis, D., Auroux, P. A., Manz, A., *Anal. Chem.* 2002, *74*, 2623-2636.

[10] Fan, Z. H., Harrison, J. D., *Anal. Chem.* 1994, *66*, 177-184.

[11] Jacobson, S. C., Hergenroder, R., Koutny, L. B., Warmack, R. J., Ramsey, J. M., *Anal. Chem.* 1994, *66*, 1107-1113.

[12] Lambertus, G. R., Fix, C. S., Reidy, S. M., Miller, R. A.*, et al.*, *Anal. Chem.* 2005, *77*, 7563-7571.

[13] Kamholz, A. E., Weigl, B. H., Finlayson, B. A., Yager, P., *Anal. Chem.* 1999, *71*, 5340-5347.

[14] Jacobson, S. C., Moore, A. W., Ramsey, J. M., *Anal. Chem.* 1995, *67*, 2059-2063.

[15] He, B., Tait, N., Regnier, F., *Anal. Chem.* 1998, *70*, 3790-3797.

[16] Tokeshi, M., Minagawa, T., Kitamori, T., *Anal. Chem.* 2000, *72*, 1711-1714.

[17] Pan, T., Kelly, R. T., Asplund, M. C., Woolley, A. T., *J. Chromatogr. A* 2004, *1027*, 231-235.

[18] Borrello, L., Bernardini, J., Dell'Orso, R., Dutta, S*., et al.*, *IEEE Trans. Nucl. Sci.* 2002, *49*, 1035-1039.

[19] Lee, T. M.-H., Carles, M. C., Hsing, I. M., *Lab Chip* 2003, *3*, 100-105.

[20] Bergkvist, J., Ekström, S., Wallman, L., Löfgren, M*., et al.*, *Proteomics* 2002, *2*, 422-429.

[21] Liu, J., Pan, T., Woolley, A. T., Lee, M. L., *Anal. Chem.* 2004, *76*, 6948-6955.

[22] Kelly, R. T., Pan, T., Woolley, A. T., *Anal. Chem.* 2005, *77*, 3536-3541.

[23] Woolley, A. T., Lao, K., Glazer, A. N., Mathies, R. A., *Anal. Chem.* 1998, *70*, 684-688.

[24] Madou, M. J., *Fundamentals of Microfabrication-The science of miniaturization*, CRC Press, New York 2002.

[25] Fiorini, G. S., Jeffries, G. D. M., Lim, D. S. W., Kuyper, C. L., Chiu, D. T., *Lab Chip* 2003, *3*, 158-163.

[26] Griebel, A., Rund, S., Schonfeld, F., Dorner, W*., et al.*, *Electrophoresis* 2004, *4*, 18-23.

[27] Haab, B. B., Mathies, R. A., *Anal. Chem.* 1999, *71*, 5137-5145.

[28] Fonslow, B. R., Bowser, M. T., *Anal. Chem.* 2005, *77*, 5706-5710.

[29] Petersson, F., Nilsson, A., Jonsson, H., Laurell, T., *Anal. Chem.* 2005, *77*, 1216-1221.

[30] Wang, H. Y., Foote, R. S., Jacobson, S. C., Schneibel, J. H., Ramsey, J. M., *Sens. Actuators B* 1997, *45*, 199-207.

[31] Huang, Z., Sanders, J. C., Dunsmor, C., Ahmadzadeh, H., Landers, J. P., *Electrophoresis* 2001, *22*, 3924-3929.

[32] Peeni, B. A., Conkey, D. B., Barber, J. P., Kelly, R. T.*, et al.*, *Lab Chip* 2005, *5*, 501-505.

[33] Xiao, D., Zhang, H., Wirth, M., *Langmuir* 2002, *18*, 9971-9976.

[34] Wu, H., Huang, B., Zare, R. N., *Lab Chip* 2005, *5*, 1393-1398.

[35] McDonald, J. C., Duffy, D. C., Anderson, J. R., Chiu, D. T.*, et al.*, *Electrophoresis* 2000, *21*, 27-40.

[36] Klank, H., Kutter, J. P., Geschke, O., *Lab Chip* 2002, *2*, 242-246.

[37] Lai, S., Cao, X., Lee, L. J., *Anal. Chem.* 2004, *75*, 1175-1183.

[38] Barker, S. L. R., Ross, D., Tarlov, M. J., Gaitan, M., Locascio, L. E., *Anal. Chem.* 2000, *72*, 5925-5929.

[39] Barker, S. L. R., Tarlov, M. J., Canavan, H., Hickman, J. J., Locascio, L. E., *Anal. Chem.* 2000, *72*, 4899-4903.

[40] Liu, Y., Ganser, D., Schneider, A., Liu, R.*, et al.*, *Anal. Chem.* 2001, *73*, 4196-4201.

[41] Vreeland, W. N., Locascio, L. E., *Anal. Chem.* 2003, *75*, 6906-6911.

[42] Gobry, V., van Oostrum, J., Martinelli, M., Rohner, T. C.*, et al.*, *Proteomics* 2002, *2*, 405-412.

[43] Yin, H., Killeen, K., Brennen, R., Sobek, D.*, et al.*, *Anal. Chem.* 2005, *77*, 527-533.

[44] Stachowiak, T. B., Rohr, T., Hilder, E. F., Peterson, D. S.*, et al.*, *Electrophoresis* 2003, *24*, 3689-3693.

[45] Castaño-Álvarez, M., Fernández-Abedul, M. T., Costa-García, A., *Electrophoresis* 2005, *26*, 3160-3168.

[46] Yang, Y., Li, C., Lee, K. H., Craighead, H. G., *Electrophoresis* 2005, *26*, 3622-3630.

[47] Kelly, R. T., Woolley, A. T., *Anal. Chem.* 2003, *75*, 1941-1945.

[48] Becker, H., Gartner, C., *Electrophoresis* 2000, *21*, 12-16.

[49] Nils, R., Matthias, W., Thomas, G., Hella-Christin, S., in: Roxann, L. E. (Ed.), *Proceedings of SPIE -- Volume 5037*, SPIE 2003, pp. 211-218.

[50] Chen, Z., Gao, Y., Lin, J., Su, R., Xie, Y., *J. Chromatogr. A* 2004, *1038*, 239-245.

[51] McCormick, R. M., Nelson, R. J., Alonso-Amigo, M. G., Benvegnu, D. J., Hooper, H. H., *Anal. Chem.* 1997, *69*, 2626-2630.

[52] Olmsted, B. A., Davis, M. E., *Practical Injection Molding*, Marcel Dekker Inc, New York 2001.

[53] Duffy, D. C., McDonald, J. C., Schueller, O. J. A., Whitesides, G. M., *Anal. Chem.* 1998, *70*, 4974-4984.

[54] Anderson, J. R., Chiu, D. T., Jackman, R. J., Cherniavskaya, O*., et al.*, *Anal. Chem.* 2000, *72*, 3158-3164.

[55] Unger, M. A., Chou, H.-P., Thorsen, T., Scherer, A., Quake, S. R., *Science* 2000, *288*, 113-116.

[56] Fu, A. Y., Chou, H. P., Spence, C., Arnold, F. H., Quake, S. R., *Anal. Chem.* 2002, *74*, 2451-2457.

[57] Thorsen, T., Maerkl, S. J., Quake, S. R., *Science* 2002, *298*, 580-584.

[58] Rolland, J. P., VanDam, R. M., Schorzman, D. A., Quake, S. R., DeSimone, J. M., *J. Am. Chem. Soc.* 2004, *126*, 2322-2323.

[59] Fiorini, G. S., Lorenz, R. M., Kuo, J. S., Chiu, D. T., *Anal. Chem.* 2004, *76*, 4697-4704.

[60] Fiorini, G. S., Chiu, D.T., *BioTechniques* 2005, *38*, 429-446.

[61] Liu, J., Sun, X., Lee, M. L., *Anal. Chem.* 2007, *79*, 1926-1931.

[62] Roberts, M. A., Rossier, J. S., Bercier, P., Girault, H., *Anal. Chem.* 1997, *69*, 2035-2042.

[63] Bianchi, F., Chevolot, Y., Mathieu, H. J., Girault, H. H., *Anal. Chem.* 2001, *73*, 3845-3853.

[64] Bowden, M., Geschke, O., Kutter, J. P., Diamond, D., *Lab Chip* 2003, *3*, 221-223.

[65] Beebe, D. J., Moore, J. S., Bauer, J., Yu, Q*., et al.*, *Nature* 2000, *404*, 588-590.

[66] Beebe, D. J., Moore, J. S., Yu, Q., Liu, R. H*., et al.*, *Proc. Natl. Acad. Sci. USA* 2000, *97*, 13488-13493.

[67] Kenis, P. J. A., Ismagilov, R. F., Whitesides, G. M., *Science* 1999, *285*, 83-85.

[68] Sikanen, T., Tuomikoski, S., Ketola, R. A., Kostiainen, R*., et al.*, *Lab Chip* 2005, *5*, 888-896.

[69] Tuomikoski, S., Franssila, S., *Sens. Actuators A* 2005, *120*, 408-415.

[70] Wang, J., Pumera, M., Chatrathi, M. P., Escarpa, A*., et al.*, *Electrophoresis* 2002, *23*, 596-601.

[71] Doherty, E. A. S., Meagher, R. J., Albarghouthi, M. N., Barron, A. E., *Electrophoresis* 2003, *24*, 34-54.

[72] Humble, P. H., Kelly, R. T., Woolley, A. T., Tolley, H. D., Lee, M. L., *Anal. Chem.* 2004, *76*, 5641-5648.

[73] Meng, Z., Qi, S., Soper, S. A., Limbach, P. A., *Anal. Chem.* 2001, *73*, 1286-1291.

[74] Xia, Y.-M., Hua, Z.-S., Srivannavit, O., Ozel, A. B., Gulari, E., *J. Chem. Tech. & Biotech.* 2007, *82*, 33-38.

[75] Yamamoto, T., Fujii, T., Nojima, T., *Lab Chip* 2002, *2*, 197-202.

[76] Liu, C., Cui, D., Cai, H., Chen, X., Geng, Z., *Electrophoresis* 2006, *27*, 2917-2923.

[77] Ren, X., Bachman, M., Sims, C., Li, G. P., Allbritton, N., *J. Chromatogr. B* 2001, *762*, 117-125.

[78] Lai, S., Hudiono, Y., Lee, L. J., Daunert, S., Madou, M., *Proceedings of SPIE Vol 4557: SPIE- Micromachining and Microfabrication Process Technology VII*, San Francisco 2001, pp. 280-287.

[79] Madou, M. J., Lee, L. J., Daunert, S., Lai, S., Shih, C. H., *Biomedical Microdevices* 2001, *3*, 245-254.

[80] Cobb, K. A., Novotny, M. V., *Anal. Chem.* 1992, *64*, 879-886.

[81] Mazzeo, J. R., Krull, I. S., *Anal. Chem.* 1991, *63*, 2852-2857.

[82] Wiktorowicz, J. E., Colburn, J. C., *Electrophoresis* 1990, *11*, 769-773.

[83] Heiger, D. N., Cohen, A. S., Karger, B. L., *J. Chromatog.* 1990, *516*, 33-48.

[84] Liu, J., Shirota, O., Novotny, M., *Anal. Chem.* 1991, *63*, 413-417.

[85] Kaneta, T., Tanaka, S., Taga, M., Yoshida, H., *Anal. Chem.* 1992, *64*, 798-801.

[86] Camilleri, P., *Capillary Electrophoresis: Theory and Practice*, CRC Press, Boca Raton, FL 1993.

[87] Xu, F., Jabasini, M., Baba, Y., *Electrophoresis* 2002, *23*, 3608-3614.

[88] Tabuchi, M., Kuramitsu, Y., Nakamura, K., Baba, Y., *Anal. Chem.* 2003, *75*, 3799-3805.

[89] Youssouf, B. M., Wong, M., Chiem, N., Salimi-Moosavi, H., Harrison, D. J., *J. Chromatogr. A* 2002, *947*, 277-286.

[90] Jorgenson, J. W., Lukacs, K. D., *Anal. Chem.* 1981, *53*, 1298-1302.

[91] Jorgenson, J. W., Lukacs, K. D., *Science* 1983, *222*, 266-272.

[92] Culbertson, C. T., Ramsey, R. S., Ramsey, J. M., *Anal. Chem.* 2000, *72*, 2285-2291.

[93] Huang, X., Gordon, M. J., Zare, R. N., *Anal. Chem.* 1988, *60*, 1837-1838.

[94] Monnig, C. A., Jorgensen, J. W., *Anal. Chem.* 1991, *63*, 802-807.

[95] Pittmann, J. L., Trekhov, A. I., Suljak, S. W., Gilman, S. D., *Anal. Chim. Acta.* 2003, *496*, 195-204.

[96] Fu, L. M., Lin, C. H., *Anal. Chem.* 2003, *75*, 5790-5796.

[97] Fu, L. M., Yang, R. J., Lee, G. B., *Anal. Chem.* 2003, *75*, 1905-1910.

[98] Lu, H., Schmidt, M. A., Jensen, K. F., *Lab Chip* 2001, *1*, 22-28.

[99] Mao, Q., Pawlisyn, J., *Analyst* 1999, *124*, 637-641.

[100] Nishimoto, T., Fujiyama, Y., Abe, H., Kanai, M*., et al.*, *Proceedings of Micro Total Analysis Systems 2000*, Kluwer Academic Publishers, Dordrecht 2000, pp. 395-398.

[101] Jacobson, S. C., Hergenroder, R., Moore, A. W., Ramsey, J. M., *Anal. Chem.* 1994, *66*, 4127-4132.

[102] Shear, J. B., *Anal. Chem.* 1999, *71*, 598A-605A.

[103] Okerberg, E., Shear, J. B., *Anal. Chem.* 2001, *73*, 1610-1613.

[104] Zugel, S. A., Burke, B. J., Regnier, F. E., Lytle, F. E., *Anal. Chem.* 2000, *72*, 5731-5735.

[105] Xu, C., Shear, J. B., Webb, W. W., *Anal. Chem.* 1997, *69*, 1285-1287.

[106] Lee, M., Lee, J.-P., Rhee, H., Choo, J.*, et al.*, *J. Raman Spectrosc.* 2003, *34*, 737-742.

[107] Fritsch, I., Aguilar, Z. P., *Anal. Bioanal. Chem.* 2007, *387*, 159-163.

[108] Tierney, M. J., Kim, H. O. L., *Anal. Chem.* 1993, *65*, 3435-3440.

[109] Galloway, M., Stryjewski, W., Henry, A., Ford, S. M.*, et al.*, *Anal. Chem.* 2002, *74*, 2407-2415.

[110] Wang, J., Tian, B., Sahlin, E., *Anal. Chem.* 1999, *71*, 5436-5440.

[111] Hebert, N. E., Kuhr, W. G., Brazill, S. A., *Anal. Chem.* 2003, *75*, 3301-3307.

[112] Ramsey, R. S., Ramsey, J. M., *Anal. Chem.* 1997, *69*, 1174-1178.

[113] Li, J., Thibault, P., Bings, N. H., Skinner, C. D.*, et al.*, *Anal. Chem.* 1999, *71*, 3036-3045.

[114] Wachs, T., Henion, J., *Anal. Chem.* 2001, *73*, 632-638.

[115] Zhang, B., Foret, F., Karger, B. L., *Anal. Chem.* 2000, *72*, 1015-1022.

[116] Liu, Y., Fanguy, J. C., Bledsoe, J. M., Henry, C. S., *Anal. Chem.* 2000, *72*, 5939-5944.

[117] Ro, K. W., Chang, W.-J., Kim, H., Koo, Y.-M., Hahn, J. H., *Electrophoresis* 2003, *24*, 3253-3259.

[118] Dang, F., Zhang, L., Hagiwara, H., Mishina, Y., Baba, Y., *Anal. Chem.* 2003, *24*, 714-721.

[119] Song, L., Fang, D., Kobos, R. K., Pace, S. J., Chu, B., *Electrophoresis* 1999, *20*, 2847-2855.

[120] Ocvirk, G., Munroe, M., Tang, T., Oleschuk, R.*, et al.*, *Electrophoresis* 2000, *21*, 107-115.

[121] Wang, S. C., Perso, C. E., Morris, M. D., *Anal. Chem.* 2000, *72*, 1704-1706.

[122] Lin, Y.-W., Chang, H.-T., *J. Chromatogr. A* 2005, *1073*, 191-199.

[123] Pumera, M., Wang, J., Grushka, E., Polsky, R., *Anal. Chem.* 2001, *73*, 5625-5628.

[124] Prakash, S., Long, T. M., Selby, J. C., Moore, J. S., Shannon, M. A., *Anal. Chem.* 2007, *79*, 1661-1667.

[125] Breisch, S., de Heij, B., Lohr, M., Stelzle, M., *J. Micromech. Microeng.* 2004, *14*, 497-505.

[126] Pesek, J. J., Matyska, M. T., *J. Chromatogr. A* 1996, *736*, 255-264.

[127] Ferguson, G. S., Chaudhury, M. K., Biebuyck, H. A., Whitesides, G. M., *Macromolecules* 1993, *26*, 5870-5875.

[128] Papra, A., Bernard, A., Juncker, D., Larsen, N. B*., et al.*, *Anal. Chem.* 2001, *17*, 4090-4095.

[129] Hu, S., Ren, X., Bachman, M., Sims, C. E*., et al.*, *Langmuir* 2004, *20*, 5569-5574.

[130] Hu, S., Ren, X., Bachman, M., Sims, C. E*., et al.*, *Anal. Chem.* 2002, *74*, 4117-4123.

[131] Hu, S., Ren, X., Bachman, M., Sims, C. E*., et al.*, *Anal. Chem.* 2004, *76*, 1865-1870.

[132] Hu, S., Brittain, W. J., *Macromolecules* 2005, *38*, 6592-6597.

[133] Kamigaito, M., Ando, T., Sawamoto, M., *Chem. Rev.* 2001, *101*, 3689-3745.

[134] Wang, J.-S., Matyjaszewski, K., *J. Am. Chem. Soc.* 1995, *117*, 5614-5615.

[135] Kato, M., Kamigaito, M., Sawamoto, M., Higashimura, T., *Macromolecules* 1995, *28*, 1721-1723.

[136] Xiao, D., Le, T. V., Wirth, M. J., *Anal. Chem.* 2004, *76*, 2055-2061.

[137] Hermanson, G. T., Mallia, A. K., Smith, P. K., *Immobilized affinity ligand techniques*, Academic Press, New York 1992.

[138] Shen, D., Yu, H., Huang, Y., *Celluose* 2006, *13*, 235-244.

[139] Zhai, G., Shi, Z. L., Kang, E. T., Neoh, K. G., *Macromol. Biosci.* 2005, *5*, 974-982.

[140] Velter, I., Ferla, B. L., Nicotra, F., *J. Carbohydrate Chem.* 2005, *25*, 97-138.

[141] Lindblom, A., Liljegren, A., *British Med. J.* 2000, *320*, 424-427.

[142] Bronchud, M. H., Foote, M., Giaccone, G., Olopade, O., Workman, P., *Principles of molecular oncology*, Humana Press, Totowa NJ 2004.

[143] Chatterjee, S. K., Zetter, B. R., *Future Oncol.* 2005, *1*, 37-50.

[144] Abeloff, M., Armitage, J., Niederhuber, J., Kastan, M., McKenna, G., *Clinical Oncology*, Elsevier, Philadelphia 2004.

[145] Acevedo, H. F., *J. Experimental Therapeutics & Oncol.* 2002, *2*, 133.

[146] Wu, H., Lustbader, J. W., Liu, Y., Canfield, R. E., Hendrickson, W. A., *Structure* 1994, *2*, 545-558.

[147] Curtis, G. B., Fischer, D., *Your Pregnancy After 30 (Your Pregnancy Series)*, Perseus Books Group, New York 1996.

[148] Konishia, I., Kurodab, H., Mandai, M., *Oncology* 1999, *57*, 45-48.

[149] Perkins, G. L., Slater, E. D., Sanders, G. K., Prichard, J. G., *Am. Fam. Physician* 2003, *68*, 1075-1082.

[150] Kawakami, T., Hoshida, Y., Kanai, F., Tanaka, Y*., et al.*, *Proteomics* 2005, *5*, 4287-4295.

[151] Pieper, R., Gatlin, C. L., Makusky, A. J., Russo, P. S*., et al.*, *Proteomics* 2003, *3*, 1345-1364.

[152] Adkins, J. N., Varnum, S. M., Auberry, K. J., Moore, R. J*., et al.*, *Mol. Cell. Proteomics* 2002, *1*, 947-955.

[153] Hoefs, J. C., *J. Lab Clin. Med.* 1983, *102*, 260-273.

[154] Soltani, K., *J. Investig. Dermatol.* 1979, *72*, 211-213.

[155] Makarov, D. V., Carter, H. B., *J. Urol.* 2006, *176*, 2383-2385.

[156] O'Farrell, P. H., *J. Biol. Chem.* 1975, *250*, 4007-4021.

[157] Klose, J., *Electrophoresis* 1999, *20*, 643-652.

[158] Wall, D. B., Kachmann, M. M., Song, S., Misek, D.*, et al.*, *Anal. Chem.* 2000, *72*, 1099-1111.

[159] Link, A. J., Eng, J., Schieltz, D. M., Carmack, E.*, et al.*, *Nat. Biotech.* 1999, *17*, 676-682.

[160] Robertson, D. M., Cahir, N., Burger, H. G., Mamers, P.*, et al.*, *Clin. Chem.* 1999, *45*, 651-658.

[161] Scholler, N., Crawford, M., Sato, A., Drescher, C. W.*, et al.*, *Clin. Cancer Res.* 2006, *12*, 2117-2124.

[162] Cheng, Z.-Z., Corey, M. J., Parepalo, M., Majno, S.*, et al.*, *Clin. Chem.* 2005, *51*, 856-863.

[163] Hjerten, S., Liao, J. L., Zhang, R., *J. Chromatogr.* 1989, *473*, 273-275.

[164] Mallik, R., Hage, D. S., *J. Sep. Sci.* 2006, *29*, 1686-1704.

[165] Armenta, J. M., Gu, B., Humble, P. H., Thulin, C. D., Lee, M. L., *J. Chromatogr. A* 2005, *1097*, 171-178.

[166] Tsujioka, N., Hira, N., Aoki, S., Tanaka, N., Hosoya, K., *Macromolecules* 2005, *38*, 9901-9903.

[167] Peters, E. C., Svec, F., Frechet, J. M. J., Viklund, C., Irgum, K., *Macromolecules* 1999, *32*, 6377-6379.

[168] Naik, S. P., Fan, W., Yokoi, T., Okubo, T., *Langmuir* 2006, *22*, 8614-8614.

[169] Huesing, N., Raab, C., Torma, V., Roig, A., Peterlik, H., *Chem. Mater.* 2003, *15*, 2690-2692.

[170] Kikuta, K., Ohta, K., Takagi, K., *Chem. Mater.* 2002, *14*, 3123-3127.

[171] Gu, B., Armenta, J. M., Lee, M. L., *J. Chromatogr. A* 2005, 382-391.

[172] Svec, F., *Electrophoresis* 2006, *27*, 947-961.

[173] Luo, Q. Z., Mao, X. Q., Huang, X., Zou, H. F., *J. Chromatogr. B* 2002, *776*, 139-147.

[174] Svec, F., Hrudkova, H., Horak, D., Kalal, J., *Angew. Macromol. Chem.* 1977, *63*, 37-45.

[175] Petro, M., Svec, F., Frechet, J. M., *J. Biotech. Bioeng.* 1996, *49*, 355-263.

[176] Zhou, D. M., Zou, H. F., Ni, J. Y., Yang, L.*, et al.*, *Anal. Chem.* 1999, *71*, 115-118.

[177] Hearn, W., Bethek, G. S., Ayers, J. S., Hancock, W. S., *J. Chromatogr.* 1979, *185*, 463-470.

[178] Bencina, K., Podgornik, A., Atrancar, A., Bencina, M., *J. Sep. Sci.* 2004, *27*, 811-818.

[179] http://www.piercenet.com, 2006.

[180] Giddings, J. C., Dahlgren, K., *Sep Sci* 1971, *6*, 345-356.

[181] Kelly, R. T., Woolley, A. T., *J. Sep. Sci.* 2005, *28*, 1985-1993.

[182] Tolley, H. D., Wang, Q., LeFebre, D. A., Lee, M. L., *Anal. Chem.* 2002, *74*, 4456-4463.

[183] Ivory, C. F., *Sep. Sci. Tech.* 2000, *35*, 1777-1793.

[184] Kelly, R. T., Li, Y., Woolley, A. T., *Anal. Chem.* 2006, *78*, 2565-2570.

[185] Liu, J., Sun, X., Farnsworth, P. B., Lee, M. L., *Anal. Chem.* 2006, *78*, 4654-4662.

Chapter 2. Fabrication of CaF_2 Capillary Electrophoresis Microdevices for Online IR Detection*

2.1. Introduction

Miniaturization of tools for chemical analysis offers significant advantages [1] in terms of speed, throughput, and reagent consumption. The benefits of decreased size in separation methods are illustrated best by the significant advances in microchip capillary electrophoresis (CE) technology during the past decade [2]. Laser-induced fluorescence (LIF) detection at visible wavelengths was used in the initial demonstration of the microchip CE concept [1], and this detection scheme continues to enjoy broad use at present [3]. LIF detection at ultraviolet (UV) wavelengths [4] or in the near infrared (IR) [5] is less commonly utilized, although detection in these regions of the spectrum offer distinct advantages in terms of chromophore availability for UV wavelengths and reduced background for the near IR region.

Many different substrates have been used for construction of microfluidic electrophoresis systems, including glass [6-9], quartz [4], silicon [10] and polymeric materials [11-13]. Borosilicate glass is transparent from 350 to 2000 nm [14], but detection with devices composed of this material is not possible beyond the near IR or in the UV region of the

spectrum. The use of quartz substrates for microchip CE enables UV detection [4], but useful IR, as well as the shorter UV wavelengths still remain inaccessible. Maximum versatility in optical detection methods for laboratory-on-a-chip systems would be achieved with substrate materials having the broadest wavelength transmission ranges. Microdevices composed of such materials would allow not only quantitative analysis by probing samples in one region of the spectrum (e.g. UV or visible), but also qualitative analyte identification by IR spectroscopy. CaF_2 is an ideal candidate material for such experiments because it has a transmission range of 170–7800 nm [15]. Indeed, a recent report demonstrated the successful coupling of an IR-transparent CaF_2 flow cell with a conventional fused silica capillary for end-column Fourier-transform (FT) IR detection in CE [16]. However, the post-column coupling of a CaF_2 cell with a capillary column increases instrumental complexity and can contribute to band broadening. Ideally, IR detection should be performed on column, but this approach requires the construction of a separation system with suitable optical properties.

Here, I present the fabrication and use of microfluidic CE devices made from CaF_2 substrates. The application of these devices to chemical analysis was demonstrated by the separation of fluorescently labeled amino acids. Also, on-chip IR detection in microfluidic channels was accomplished for the first time, demonstrating the potential for separating, quantifying, and spectroscopically identifying analytes in a microfluidic platform.

2.2 Experimental Section

2.2.1. Microfabrication

Fabrication of CaF_2 CE microdevices is depicted schematically in Figure 2.1. Briefly, the microchips were made by photolithographic patterning, followed by chemical etching of CaF_2 substrates in a saturated aqueous $Fe(NH_4)(SO_4)_2$ solution. Each etched CaF_2 piece containing the channel design was then bonded to a second, photoresist-patterned CaF_2 substrate to form microcapillary structures.

Conventional photolithographic procedures were used to pattern the microchannel and cover plate following previously reported work [17]. The microchip CE device pattern consisted of 100 μm wide channels with a simple cross-injector [6, 9]. The injection channel was 1.5 cm long, while the separation channel was 2.0 cm long, and the injection channel intersected the separation channel 0.5 cm from reservoir 2 (Figure 2.1f). CaF_2 substrates of 1.0 in. diameter and 0.12 in. thickness (Casix, Chatsworth, CA, USA) were spin coated with 1.1 μm of S1813 photoresist (Shipley, Marlborough, MA, USA; Figure 2.1a; 1 in. = 2.54 cm). Next, the microfluidic design was transferred to the photoresist, as illustrated in Figure 2.1.b, and the unpatterned side of each substrate was coated with acrylic fingernail polish to prevent backside etching. The exposed channel areas were etched in a saturated aqueous $Fe(NH_4)(SO_4)_2$ solution for 24 h at room temperature (Figure 2.1c); the etchant solution was stirred using a Teflon-coated spin bar rotating at

100–120 rpm. After etching, the residual photoresist and fingernail polish were removed using acetone.

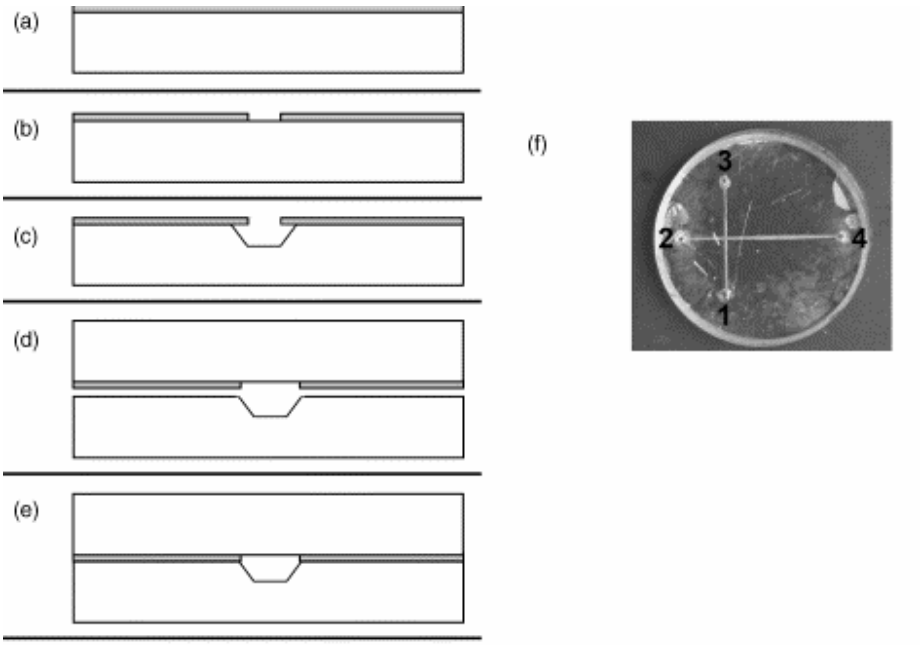

Figure 2.1. Fabrication of CaF_2 microdevices for CE. (a) The CaF_2 substrate (white) is spin-coated with photoresist (gray). (b) Exposure and development of the photoresist provides the surface pattern on the CaF_2. (c) The substrate is etched in unmasked areas. (d) The etched CaF_2 piece is aligned with the patterned photoresist on another CaF_2 substrate, and the two pieces are brought into contact. (e) The aligned CaF_2 plates are clamped and heated to cause the photoresist to bond the substrates together. (f) Photograph of a bonded CaF_2 microchip. The substrate diameter is 1 in. Reservoirs are (1) injection, (2) buffer, (3) injection waste and (4) high voltage. The injection channel runs between reservoirs 1 and 3, while the separation channel connects reservoirs 2 and 4.

Access holes were drilled using a 0.021 in. carbide drill bit (Federal-Mogul, Chicago, IL, USA) to form each of the four buffer reservoirs in the etched CaF_2 substrate. A second CaF_2 piece was spin coated with Shipley S1813 photoresist and patterned like the first, but with a channel width of 200 μm, rather than 100 μm, as shown in the top half of Figure 2.1d. This created an optically transparent window over the entire etched microchannel structure. The photoresist served as an adhesive to bond the two substrates together [16] once they were aligned under a microscope, clamped together, and placed in an oven at 135 °C for 30 min (Figure 2.1e). Elevated temperature treatment was necessary to develop the full mechanical strength and chemical resistance of the Shipley S1813 photoresist. An Alpha-step 200 stylus profilometer (Tencor, Mountain View, CA, USA) scanned with 2 μm lateral resolution was used to measure the dimensions of the etched CaF_2 patterns.

2.2.2 Separation and detection of amino acids

Glycine, arginine, and phenylalanine were purchased from Sigma (St. Louis, MO, USA) and diluted in the run buffer, 30 mM borate, pH 9.0. The borate buffer was filtered using a 0.2 μm pore diameter filter (Pall, East Hills, NY, USA) prior to use. Each amino acid was labeled fluorescently by conjugating fluorescein 5-isothiocyanate (FITC, Sigma) to the amine group [9, 17]. All FITC-tagged amino acids had a concentration of 300 μM in borate buffer after labeling.

Channels were filled by micropipetting 20 µl of run buffer on top of reservoirs 1, 2, and 3 and applying vacuum to reservoir 4 (see Figure 2.1f for reservoir layout), after which reservoir 4 was covered with 20 µL of run buffer. One microliter of sample was transferred into the bottom of reservoir 1 using a 25 µL syringe, and platinum electrodes were inserted into all buffer reservoirs to provide electrical contact. "Pinched" injection [7] for 10 s was used to load sample on the column prior to separation, and the injection volume was ~400 pL. During injection, reservoirs 1, 2, and 4 were grounded and reservoir 3 was maintained at +0.6 kV; for separation, reservoirs 1 and 3 were held at +0.6 kV, reservoir 2 was grounded, and reservoir 4 was maintained at +1.0 kV. The LIF detection system and the setup for data acquisition have been described elsewhere [17]. The sampling rate for data collection in the software was chosen to be 5 Hz.

2.2.3. FT-IR spectrometer

An FT-IR microscope comprised of a Nexus 670 FT-IR spectrometer (Nicolet, Madison, WI, USA) and an IR-Plan IR Microscope Accessory (Spectra Tech, Stamford, CT, USA) was used for on-column IR detection. The CaF_2 microdevice channels were filled with toluene (Fisher, Pittsburgh, PA, USA). To enable the IR beam to be focused correctly, the CaF_2 microdevice was placed in an external optical focusing unit, constructed in the laboratory, in a Perspex unit purged with dry air. The IR beam from an external optical port of the spectrometer was focused on the injection intersection region of the CaF_2 microdevice by means of an off-axis parabolic mirror, prior to impinging on a mercury

cadmium telluride detector. Sixty-four scans were co-added for each spectrum, and the spectral resolution was 4 cm^{-1}. Reference measurements on toluene were obtained using 1 in. diameter CaF_2 windows with 100 μm spacing between the plates.

2.3. Results and Discussion

2.3.1 Fabrication

I have fabricated CaF_2 microdevices for rapid biochemical analysis and flexible optical detection. To generate microfluidic structures in CaF_2, it was necessary to develop methods for etching this material. Although CaF_2 can be etched by laser-induced heating [18] or accelerated ion beams [19], these approaches require costly and sophisticated instrumentation. Thus, I explored methods for the wet etching of CaF_2 and found saturated aqueous $Fe(NH_4)(SO_4)_2$ to be a suitable choice. I also determined that the etch rate of the CaF_2 is dependent on the stirring of the etchant solution. In an unstirred solution, the etch rate is ~8 μm per day, while in a stirred solution the etch rate can be increased to as much as 18 μm per day. These etch rates are sufficient for fabricating microfluidic arrays in CaF_2. I believe the etching mechanism involves the reaction of Fe^{3+} ions in solution with F^- ions in CaF_2 to form the coordination complex $[FeF_6]^{3-}$. Stirring the etchant solution also helped to prevent the precipitation of byproducts on the channel surface, which hindered the etching process.

The channel width designed in the photomask was 100 μm; however, I observed some undercutting of the photoresist protecting layer such that the width of the etched channels typically exceeded the photomask linewidth. I also observed that etchant stirring speeds of 100–120 rpm produced the narrowest channel features, typically having ~200 μm top widths. Profilometry measurements indicated that the channels in the CaF_2 microdevices used for separation experiments had depths of ~10 μm, top widths of ~200 μm, and bottom widths of ~100 μm.

Developing a reliable procedure for bonding two CaF_2 substrates together to form enclosed microcapillaries proved to be somewhat difficult, because of the crystallinity and high melting temperature of CaF_2. I tried to bond CaF_2 wafers using water, acid, ferric ammonium sulfate solution, or aqueous EDTA under a range of temperatures from 25 to 1100 °C. However, none of these methods produced adequate, water-stable bonding. Thus, I opted to use a 1.1 μm layer of Shipley S1813 photoresist to adhere the CaF_2 substrates together [16]. I found that this bonding approach provided sufficient mechanical strength, chemical resistance to aqueous buffer solutions, and stability in the presence of elevated voltages to be compatible with CE experiments. Another advantage of this method is that the bonding photoresist can be photolithographically patterned to leave an optically transparent window along the length of the etched channels. Finally, the thin photoresist layer appears to cause minimal band broadening in these devices,

even though different materials defining a channel cross-section can create inhomogeneities in ζ-potential [20, 21].

2.3.2 Amino Acid Separations

To demonstrate the utility of CaF_2 microchips for biological analysis, I performed CE separations on a mixture of fluorescently labeled amino acids. Separation and detection were performed as described in Section 2.2.2. Figure 2.2a depicts electropherograms of individual amino acids (glycine, arginine and phenylalanine) injected and detected in a CaF_2 microdevice. The electropherograms show that each amino acid eluted within 25 s, and the peaks were symmetrical to some extent, while they were somewhat broad. This is possibly due to two reasons. First, the photoresist used for device bonding might cause analyte adsorption on the channel surfaces. Second, the length of separation channel (1.5 cm) was not long enough to give a high separation performance. However, these results indicate the suitability of CaF_2 as substrate for rapid electrophoretic analysis of biological samples. Figure 2.2b shows a ~30 s separation of a mixture of the same three FITC-labeled amino acids. Peak fitting was used to deconvolute the partially overlapping analyte bands in this separation, and Figure 2.2c displays the results of peak fitting. Three individual components, corresponding to glycine, arginine, and phenylalanine are observed, based on comparison with migration times in Figure 2a. Importantly, the sum of the component peaks closely approximates the experimental data in Figure 2b.

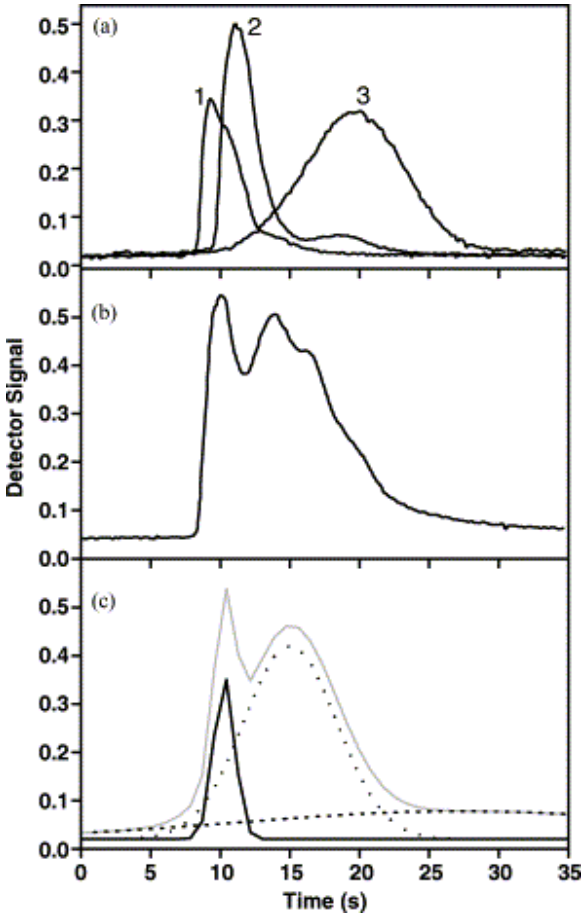

Figure 2.2 Electropherograms of FITC-labeled amino acids separated using a CaF_2 microdevice. (a) Injection and detection of individual FITC-tagged amino acids: (1) Gly, (2) Arg and (3) Phe. (b) Separation and detection of a mixture of FITC-labeled Gly, Arg, and Phe. (c) Peak fitting of the electropherogram in (b) shows three distinct components (solid, dotted and dashed black lines) with migration times similar to those in the individual runs in (a). The sum of the fit to the data is indicated by the gray line in (c). Potentials for injection and separation in all runs are described in Section 2.2.2.

2.3.3 FT-IR Experiment

FT-IR microscopy was used to test the possibility of using IR spectroscopy for on-chip analyte identification in CaF_2 microdevices. I filled the channels with toluene, water, and acetonitrile, respectively, in separate experiments, and obtained IR absorbance spectra. Figure 2.3a depicts the FT-IR absorbance spectrum of toluene in the injection area of a microchannel in a CaF_2 microdevice, while Figure 2.3b shows an IR absorbance spectrum of toluene using standard CaF_2 windows. Comparison of the spectra in Figure 2.3 confirms that toluene within the microchannels can be detected and identified readily, even though the absorbance in Figure 2.3a is lower than in Figure 2.3b because the optical path length was ~10× shorter. Similar agreement between absorbance spectra in microchannels and the sample cell was observed for water and acetonitrile (data not shown). Moreover, the IR spectrum in Figure 2.3a agrees well with the toluene reference IR spectrum in the NIST online database [22], indicating that CaF_2 microdevices are suitable for on-chip IR detection and analyte identification. In these experiments I set the resolution to 4 cm^{-1} to obtain high-resolution IR spectra. However, for real time detection in CE or other separation methods, lower spectral resolution should provide sufficient detail for qualitative analysis, and the decreased optical measurement time should enable higher temporal resolution.

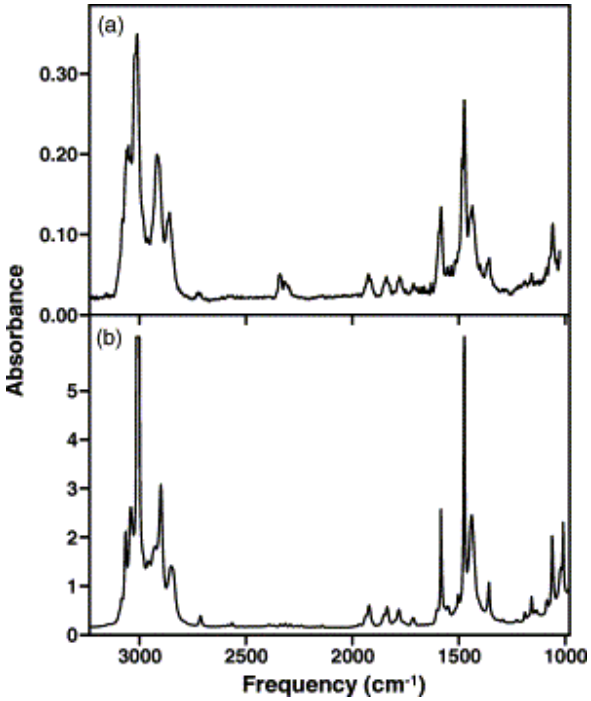

Figure 2.3 FT-IR detection in CaF_2 microchannels. (a) FT-IR spectrum of toluene in the injection region of a microchannel in a CaF_2 microdevice. (b) FT-IR spectrum of toluene in a standard CaF_2 IR cell.

2.4 Conclusion

I have successfully developed methods for the design and fabrication of CaF_2 microfluidic devices for maximum flexibility in optical detection. CE of FITC-labeled amino acids has been performed, and the results indicate that CaF_2 provides a suitable platform for rapid biochemical separations. Moreover, FT-IR tests indicate that CaF_2 microfluidic devices are suitable for real time, on-column FT-IR identification of analytes

in microchannels. These CaF_2 microchips should enable both quantitative and qualitative optical analyses in laboratory-on-a-chip systems.

2.5 References

[1] Manz, A., Harrison, D. J., Verpoorte, E. M. J., Fettinger, J. C., *et al.*, *J. Chromatogr. A* 1992, *593*, 253-258.

[2] Reyes, D. R., Iossifidis, D., Auroux, P. A., Manz, A., *Anal. Chem.* 2002, *74*, 2623-2636.

[3] Auroux, P. A., Iossifidis, D., Reyes, D., Manz, A., *Anal. Chem.* 2002, *74*, 2637-2652.

[4] Jacobson, S. C., Moore, A. W., Ramsey, J. M., *Anal. Chem.* 1995, *67*, 2059-2063.

[5] Wabuyele, M. B., Ford, S. M., Stryjewski, W., Barrow, J., Soper, S. A., *Electrophoresis* 2001, *22*, 3939-3948.

[6] Harrison, D. J., Manz, A., Fan, Z., Luedi, H., Widmer, H. M., *Anal. Chem.* 1992, *64*, 1926-1932.

[7] Jacobson, S. C., Hergenroder, R., Koutny, L. B., Warmack, R. J., Ramsey, J. M., *Anal. Chem.* 1994, *66*, 1107-1113.

[8] Woolley, A. T., Mathies, R. A., *Proc. Natl. Acad. Sci. U.S.A.* 1994, *91*, 11348-11352.

[9] Monnig, C. A., Jorgensen, J. W., *Anal. Chem.* 1991, *63*, 802-807.

[10] Harrison, D. J., Glavina, P. G., Manz, A., *Sens. Actuators B* 1993, *10*, 107-116.

[11] Becker, H., Locascio, L. E., *Talanta* 2002, *56*, 267-287.

[12] Boone, T. D., Hugh, Z. H., Hooper, H. H., Ricco, A. J., *et al.*, *Anal. Chem.* 2002, *74*, 78A-86A.

[13] McCormick, R. M., Nelson, R. J., Alonso-Amigo, M. G., Benvegnu, D. J., Hooper, H. H., *Anal. Chem.* 1997, *69*, 2626-2630.

[14] http://www.technicalglass.co.uk/glassprops.html, 2002.

[15] http://www.casix.com/optics/windows.htm, 2002.

[16] Kolhed, M., Hinsmann, P., Svasek, P., Frank, J., *et al.*, *Anal. Chem.* 2002, *74*, 3843-3848.

[17] Kelly, R. T., Woolley, A. T., *Anal. Chem.* 2003, *75*, 1941-1945.

[18] Wang, J., Niino, H., Yabe, A., *Appl. Surf. Sci.* 2000, *154-155*, 571-576.

[19] Batzill, M., Bardou, F., Snowdon, K. J., *J. Vac. Sci. Technol. A* 2001, *19*, 1829-1834.

[20] Bianchi, F., Wagner, F., Hoffmann, P., Girault, H. H., *Anal. Chem.* 2001, *73*, 829-836.

[21] Liu, Y., Fanguy, J. C., Bledsoe, J. M., Henry, C. S., *Anal. Chem.* 2000, *72*, 5939-5944.

[22] http://webbook.nist.gov/cgi/cbook.cgi?Name=toluene&Units=SI&cIR=on, 2002.

Chapter 3. Microchip Protein and Peptide Separations in Polymeric Devices

3.1 Introduction

Interest in the characterization of proteomes has expanded greatly in recent years. The proteome is the entire complement of expressed proteins in a cell or tissue [1]. Proteome characterization is valuable in gaining a fundamental understanding of complex biological processes, such as cell death, cell differentiation, cell development, signal transduction, etc. Proteomes can vary considerably among different cells or tissue types, and many factors can affect the protein patterns in a cell or tissue (diseases, chemicals, stress, malfunctions, misfunctions, etc.) [2-4]. Thus, protein analysis (i.e., separation, identification and quantification of proteomes) is very important.

Currently, the most effective method for protein analysis is two-dimensional (2D) gel electrophoresis [5, 6], which can isolate more than one thousand protein bands in a sample. However, this technique is expensive, labor intensive, time consuming, and not reproducible. Moreover, numerous treatments need to be done before and after the sample is separated by 2D gel electrophoresis because this method cannot automatically pick the target proteins out from a complex sample. Thus, although 2D gel electrophoresis is somewhat effective for protein analysis, it is still a bottleneck in proteomic studies.

Since the fundamental theory of modern capillary electrophoresis (CE) was first described by Jorgenson and Lukacs [7, 8], CE has become a powerful tool for protein analysis [9-13]. Compared to other protein analysis methods, CE has several advantages, including high sensitivity, good resolving power, low sample consumption and ease of automation. With the rapid development of micro total analysis systems (μTAS), miniaturized CE platforms have received more and more attention. This is because CE has two distinct advantages in terms of miniaturization. The first is that the electroosmotic flow (EOF) in CE can serve as a pumping system. Injection and transportation of analytes in CE can be controlled easily by adjusting electrical potentials, which makes external valves or pumps unnecessary. The second advantage is that in CE, band broadening is caused only by longitudinal diffusion. This makes CE separation efficiency dependent on the magnitude of voltage applied; thus, in a very short capillary, high efficiency can still be achieved.

However, for polymeric microchip CE devices, protein adsorption and unstable EOF are two major barriers that limit the application of polymer devices in protein analysis. As discussed in Section 1.2.5, dynamic coating and permanent surface modification are two effective methods that are used to improve CE performance in polymeric microdevices for protein analysis. Dynamic coating is simple and fast, but its effects do not last long (i.e., it is a temporary surface modification method); permanent surface modification is often complex and labor intensive, but it is more effective. Here I report my protein analysis research using both untreated and surface-modified poly(methyl methacrylate) (PMMA) microdevices. These results indicate that poly(ethylene glycol) (PEG) grafting

for surface modification is an effective method to improve the performance of polymeric microdevices in protein analysis.

3.2 Experimental Section

3.2.1 Materials

Hydroxypropyl cellulose (HPC), 2-bromoisobutyryl bromide (98%), poly(ethylene glycol) methyl ether methacrylate (PEGMEMA, MW ~475), 2,2'-dipyridyl (99+%), copper(I) chloride (98+%), and copper(II) bromide (99%) were purchased from Aldrich (Milwaukee, WI). Heptane, tetrahydrofuran, absolute methanol, urea and pyridine (all reagent grade), trypsin (molecular biology grade) and dithiothreitol (molecular biology grade) were obtained from Fisher Scientific (Fair Lawn, NJ). Fluorescein isothiocyanate (FITC), bovine serum albumin (BSA), trypsinogen, FITC-labeled BSA (FITC-BSA) and FITC-labeled insulin (FITC-insulin) were purchased from Sigma (St. Louis, MO). R-phycoerythrin (PE) and recombinant, enhanced green fluorescent protein (GFP) were purchased from Polysciences (Warrington, PA) and Clontech (Palo Alto, CA), respectively. Phosphorylated phosducin-like protein (p-PhLP) was a gift from Dr. Craig Thulin in the Department of Chemistry and Biochemistry at Brigham Young University. Deionized water was from an EasyPURE UV/UF purification system (Barnstead, Dubuque, IA), and the buffer solution used for CE experiments was 10 mM Trizma hydrochloride (Tris) at pH 8.7, which was filtered using 0.2-μm syringe filters (Pall Gelman Laboratory, Ann Arbor, MI).

3.2.2 Microfluidic Device Fabrication

The fabrication of PMMA (Plaskolite, Columbus, OH) microchips was adapted from protocols described previously [14]. First, an 800 nm thick silicon dioxide layer was grown on 4-inch silicon wafers (Encompass Distribution Services, Pleasanton, CA) at 1100 ºC using a tube furnace with oxygen and water purging (Figure 3.1a). Then, 1 μm thick Shipley 812 positive photoresist (Shipley, Marlborough, MA) was spin coated on an oxidized silicon wafer at 3500 rpm for 120 s, followed by soft baking at 90 ºC for 2 min to increase adhesion and photoresist stability (Figure 3.1b). Photoresist-coated silicon wafers were covered with a photomask and exposed to UV radiation for 40 s using a PLA-501F (Canon, Tokyo, Japan) contact mask aligner. The photomask was designed using Clewin (WieWeb Software) and transferred to a chrome/glass wafer using a pattern generator. After UV exposure, photoresist was developed with Microposit 351 developer (20% aqueous solution, Shipley) for 30 s, followed by hard baking in an oven for 30 min at 150 ºC (Figure 3.1c). Next, the silicon template was immersed into buffered oxide etchant for 15 min to remove silicon dioxide which was not covered by photoresist patterns (Figure 3.1d). Then, the silicon wafer was etched to give the final template using 40% aqueous KOH solution for 40 min at 80 ºC, which gave ~30 μm tall protruding features (Figure 3.1e). A hot embossing method was used to transfer channel features from the etched silicon template to 1.5-mm-thick PMMA substrates in an oven at 120 ºC (Figure 3.1f-g) [14]. Thermal bonding at 95 ºC was used to seal the patterned PMMA substrates to a blank PMMA cover plate (Figure 3.1h-i). For PEG-grafted PMMA microdevices, thermal bonding was conducted after PEG surface modification had been performed.

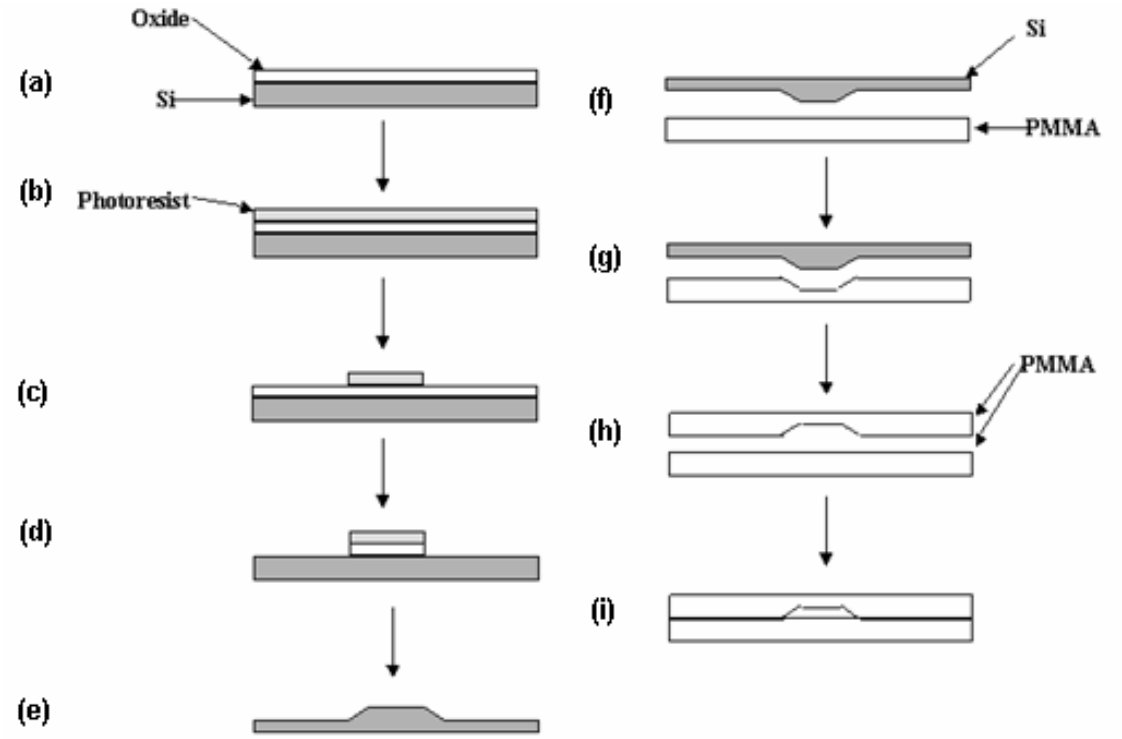

Figure 3.1 Fabrication of PMMA microdevices. Additional details are given in the text.

The dimensions of the PMMA microdevices are shown in Figure 3.2. After imprinting, the microchannels in PMMA are trapezoidal, and have a top width of 115 μm and a bottom width of 49 μm. The depth of the channels is 32 μm. Each short arm of a T section is 0.5 cm long, and the whole length of the separation channel (including one arm of a T section) is 4 cm (Figure 3.2b) [15]. The access holes in the PMMA cover plate were cut using a C-200 CO_2 laser engraving system (Universal Laser Systems, Scottsdale, AZ).

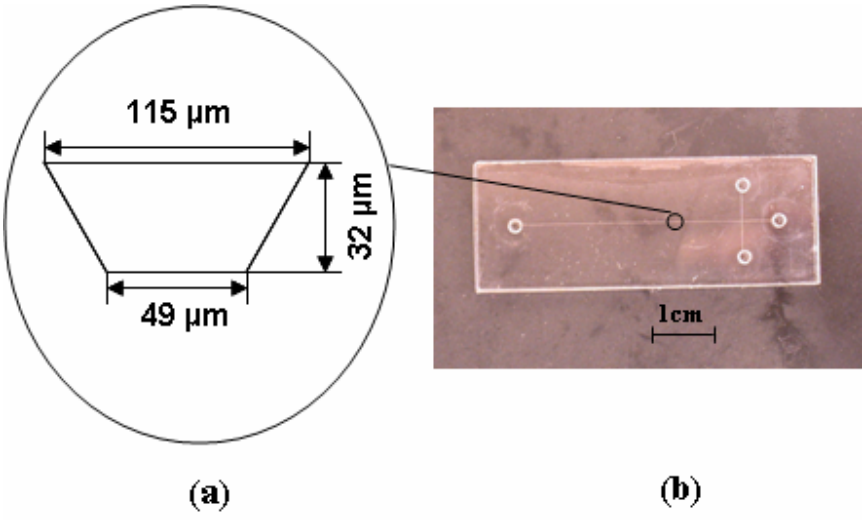

Figure 3.2 (a) Channel profile and (b) picture of a PMMA microdevice.

3.2.3 Surface Modification of PMMA Microchips

The surface modification of PMMA microdevices was mostly done by Dr. Jikun Liu in the Department of Chemistry and Biochemistry at Brigham Young Univeristy [15]. The scheme for surface modification is shown in Figure 3.3. Briefly, the PMMA surface was first activated (oxidized) to give hydroxyl groups using an oxygen plasma generated by a DEM-451 reactive ion etcher (Anelva, Tokyo, Japan). Then, a typical ATRP initiator, 2-bromoisobutyryl bromide, was immobilized on the PMMA channel surface under a water-free environment. Finally, PEG grafting solution containing CuCl, $CuBr_2$, 2,2'-dipyridyl, PEGMEMA, and DI water was used to graft a thin film of poly(PEGMEMA) on the PMMA surface.

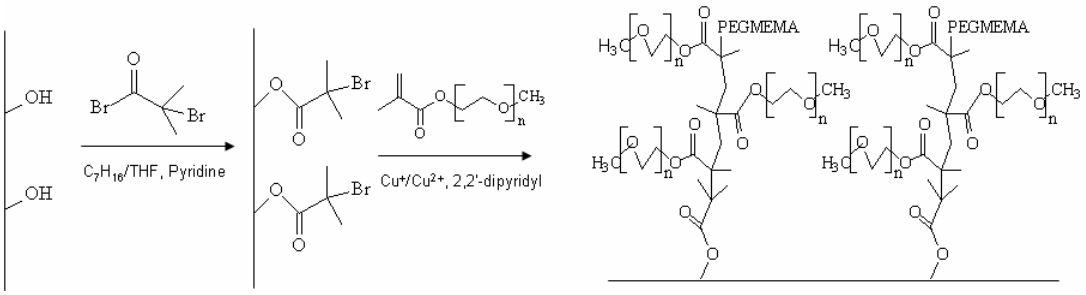

Figure 3.3 PEG grafting on a PMMA surface using ATRP.

3.2.4 Trypsin Digestion of Proteins

The tryptic digestion of BSA was performed following a protocol described in the literature [13]. First, 1 mg of BSA was dissolved in 300 μL of 20 mM Tris buffer (pH 8.7, with 6 M urea). Next, the BSA sample was reduced by dithiothreitol for 1 h, followed by iodoacetamide alkylation for 1 h. Then, trypsin was added to the pretreated BSA sample at the mass ratio of 1:50 (trypsin/BSA). The resulting solution was put in a water bath at 37 ºC and then allowed to react overnight. After the trypsin digestion was done, the BSA digest was desalted using a cellulose ester dialysis membrane with a MWCO of 100 for 24 h. FITC (6 mM) in acetone (10:1 FITC/BSA molar ratio) was used to label the BSA tryptic digest fluorescently. The reaction was run for at least 24 h in the dark at room temperature; longer reaction times (up to 5 days) led to more complete labeling.

The decomposed trypsinogen sample I used in microchip CE was prepared by auto-degradation of a trypsinogen sample. Briefly, trypsinogen was dissolved in Tris buffer (pH 8.7) to make a 2 mg/mL solution. Then an appropriate volume of 6 mM FITC solution was added to the protein solution to make a 5:1 molar ratio of FITC to protein. The labeling and auto-degradation reactions were performed in the dark for 2 weeks,

which finished the degradation reaction and hydrolyzed unreacted FITC. The auto-degradation reaction could happen because no trypsin/trypsinogen inhibitor was added to the mixture.

3.2.5 FITC Labeling of Proteins

The protocols for tagging of proteins with FITC were adapted from previous work [14-16]. Briefly, proteins were dissolved in Tris buffer (pH 8.7) to make a 2 mg/mL solution. An appropriate volume of 6 mM FITC solution was added to the protein solution to make a 5:2 molar ratio of FITC to protein. The reaction time was the same as for FITC labeling of tryptic digests.

3.2.6 Protein Adsorption Tests

To study the protein adsorption in both untreated and PEG-grafted PMMA channels, I flushed FITC-labeled BSA through PMMA microdevices at 2 μL/min [15]. After 30 min, 20 mM Tris buffer was used to wash out unbound protein for 1 h at 10 μL/min. Then, the microchip was placed on a microscope stage, and a ~400 μm diameter region of the device was illuminated with 488 nm laser light. Fluorescence images were recorded with a Nikon Coolpix digital camera [17].

3.2.7 Separation and Detection of Peptides and Proteins

My microchip CE and laser-induced fluorescence detection methods have been described previously [14, 15]. For these experiments, the injection voltage was 0.8 kV, the separation voltage was 2.0 kV, and the data sampling frequency was 100 Hz. For untreated and PEG-grafted PMMA microchips, Tris buffer (pH 8.7) was used. To

perform CE in dynamically coated PMMA microchips, HPC was dissolved in Tris buffer (pH 8.7) to make a 0.5% w/v solution.

3.3 Results and Discussion

3.3.1 Methods to Improve Protein Separation Performance

Polymers represent the second generation of materials to be employed in microdevice fabrication. Compared to inorganic materials, polymer microdevices are easy to fabricate and relatively cheap. However, when applying polymeric microdevices in bioanalytical separations, unstable EOF and nonspecific adsorption are two major barriers. To solve these problems, dynamic coating and permanent surface modification are two possible solutions. I used both dynamic coating with HPC in untreated PMMA microdevices and grafting of a thin film of PEG on the PMMA channel surface using ATRP to improve microchip performance. Protein and peptide separations were compared in these modified and untreated PMMA microdevices to evaluate their efficiency.

3.3.2 Protein Adsorption Studies

When applying polymer microdevices in protein analysis, adsorption is a big concern; indeed, native PMMA has some nonspecific adsorption. Dynamic coating (e.g., with HPC) can reduce protein adsorption temporarily, but this reduction is not reproducible and the effect is reversible. To permanently eliminate nonspecific adsorption, ATRP surface modification is a superior choice. I carried out BSA adsorption experiments, as shown in Figure 3.4. I noticed much greater BSA adsorption (green area) on untreated

PMMA channel surfaces, compared to PEG-grafted PMMA, indicating that the ATRP process significantly reduced surface protein adsorption.

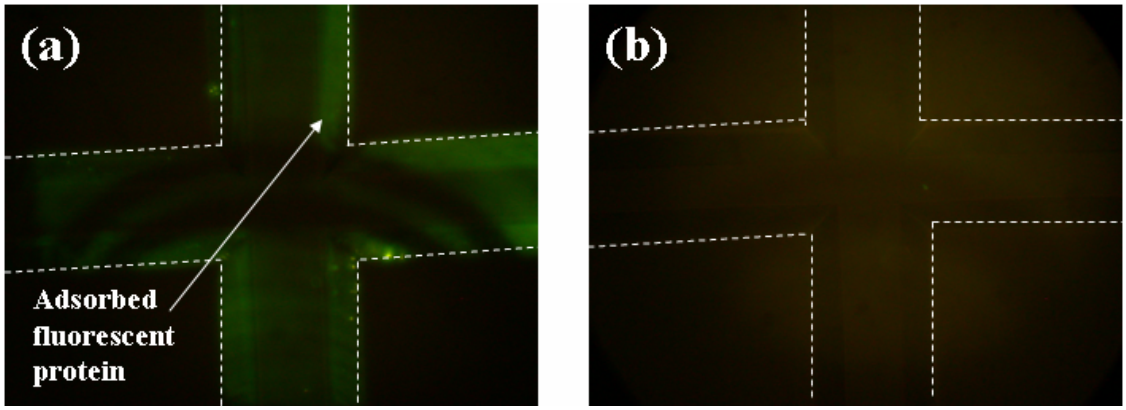

Figure 3.4 Fluorescence micrographs of adsorbed FITC-BSA in (a) native and (b) PEG-grafted devices.

3.3.3 Electrophoresis of Proteins in PMMA Microdevices

Figure 3.5 shows different protein separations in untreated PMMA microchips. GFP and PE eluted as sharp peaks in PMMA microdevices dynamically coated with HPC (Figure 3.5a-b). These results indicate that untreated PMMA microdevices can be used in protein analysis. As shown in Figure 3.5a, three GFP variants were found in CE of the GFP sample, while only one GFP peak was observed in uncoated PMMA microdevices (Figure 3.5c). This indicates that dynamically coated PMMA microdevices had better resolving power than no-HPC-added, untreated PMMA microchips. I used HPC dynamic coating to improve protein separation reproducibility in untreated PMMA microdevices. The number of theoretical plates for the GFP peak in Figure 3.5c is 5.1×10^3 over a 3.5 cm long separation channel. Importantly, the separations of protein mixtures in untreated or

HPC-treated PMMA microdevices (e.g., Figure 3.5) were not very reproducible. I believe this is due to unstable EOF and analyte adsorption on the channel walls.

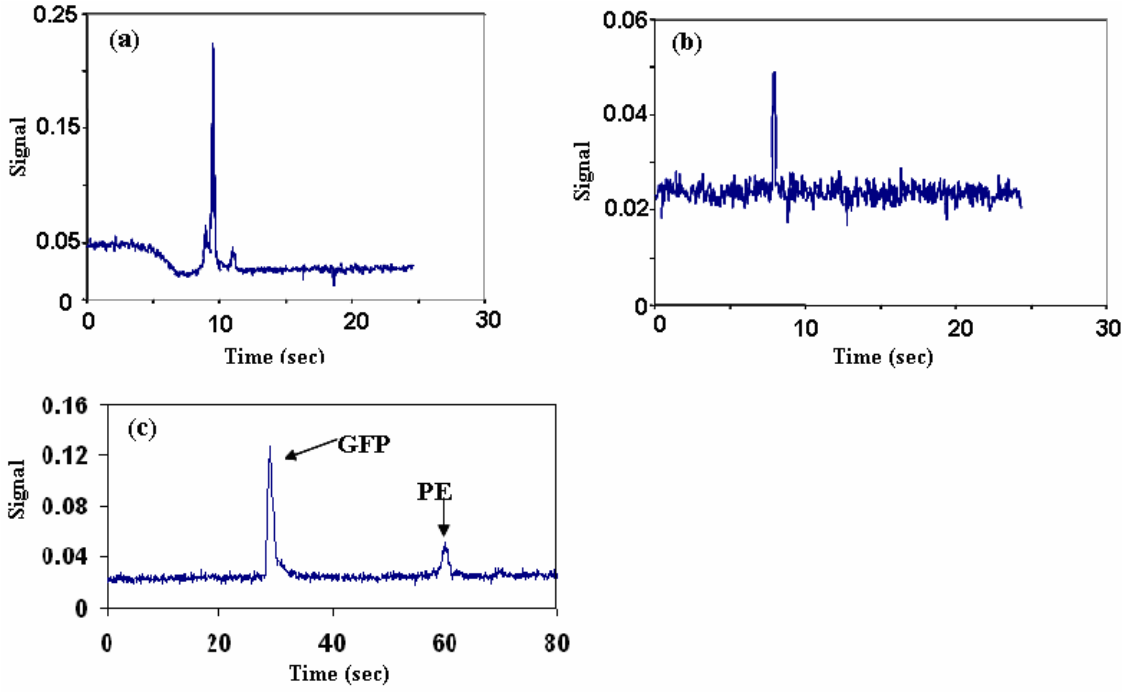

Figure 3.5 Microchip CE of GFP and PE in (a-b) HPC-treated and (c) untreated PMMA microchips. Microchip CE of (a) GFP, (b) PE and (c) GFP and PE. Results were obtained from different PMMA microdevices.

Although HPC dynamic coating improves protein analysis reproducibility in PMMA microdevices, allowing simple protein mixture separations, unmodified PMMA microdevices are not suitable for profiling all proteins. As shown in Figure 3.6a, FITC-BSA could not be separated efficiently in untreated PMMA microdevices. The poor CE performance for FITC-BSA in untreated PMMA microdevices was probably due to unstable EOF and nonspecific adsorption (e.g., interaction between BSA and PMMA).

The number of theoretical plates for the highest peak in Figure 3.6a is 2.7×10^3 over a 3.5 cm separation channel. In contrast, analysis of FITC-BSA in a PEG-grafted PMMA microchip (Figure 3.6b) showed much sharper peaks (2.2×10^4 plates) and shorter separation time, as the PEG coating stabilized EOF and decreased analyte adsorption.

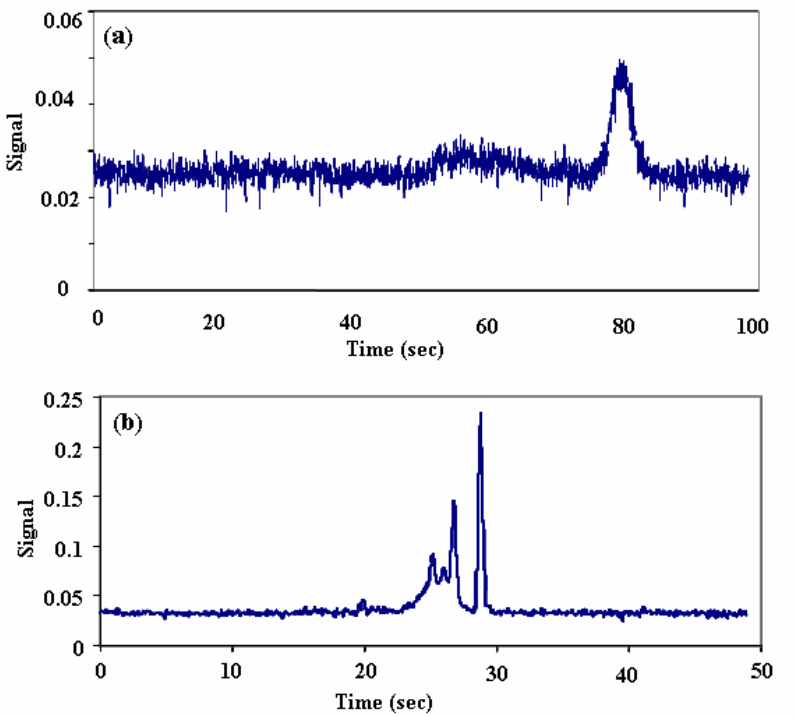

Figure 3.6 Microchip CE of FITC-BSA in (a) untreated and (b) PEG-grafted PMMA microdevices.

Figure 3.7 shows the reproducibility of FITC-BSA CE separations in a PEG-grafted PMMA microdevice. Compared to FITC-BSA separations in untreated PMMA microchips, PEG-grafted PMMA microdevices have much better reproducibility. The relative standard deviation for the largest BSA peak in Figure 3.7 is 1.3% over 10 runs, and more than 20 sequential BSA separations could be achieved reproducibly in PEG-

grafted PMMA microdevices. In addition, the lifetime for good CE separations in PEG-grafted PMMA micrchips was >200 runs, which indicates that the grafted PEG layer is very robust.

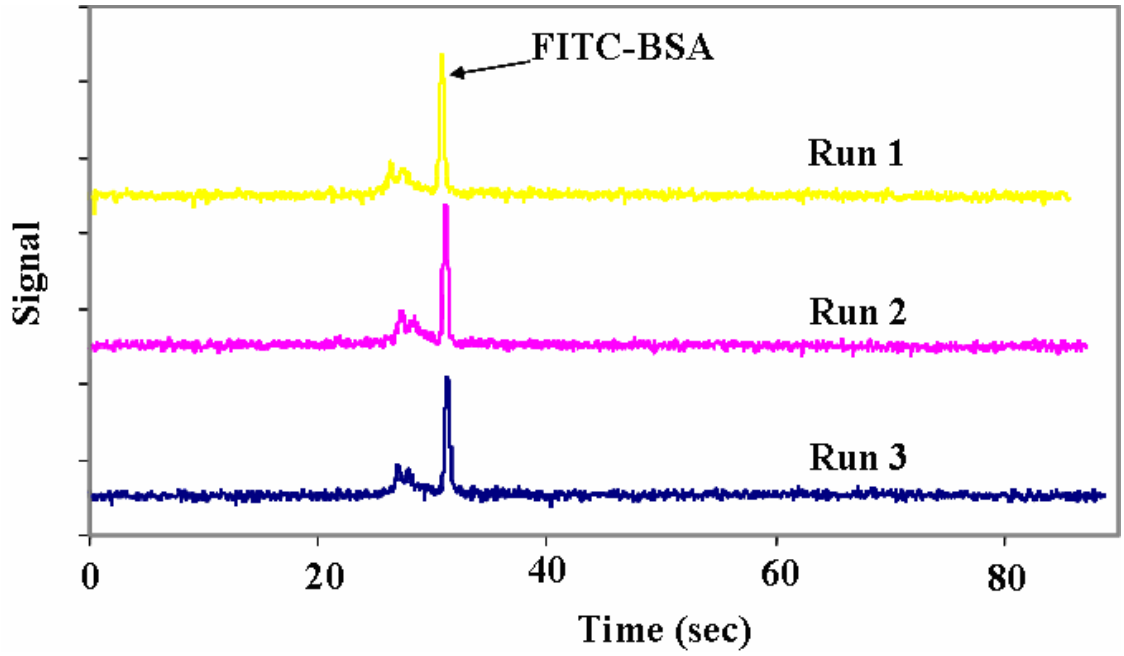

Figure 3.7 Reproducibility of microchip CE of FITC-BSA in a PEG-grafted PMMA microdevice.

I also performed protein mixture separations in PEG-grafted PMMA microdevices. As shown in Figure 3.8, a protein mixture containing BSA, PE and GFP was well resolved in a PEG-grafted PMMA microdevice. At least 6 peaks (1 from PE; 2 from GFP and 3 from BSA) were resolved. The relative standard deviation of the migration time for the last GFP peak was 0.81% over 4 runs, which indicates that PEG-grafted PMMA microdevices are capable of separating protein samples reproducibly.

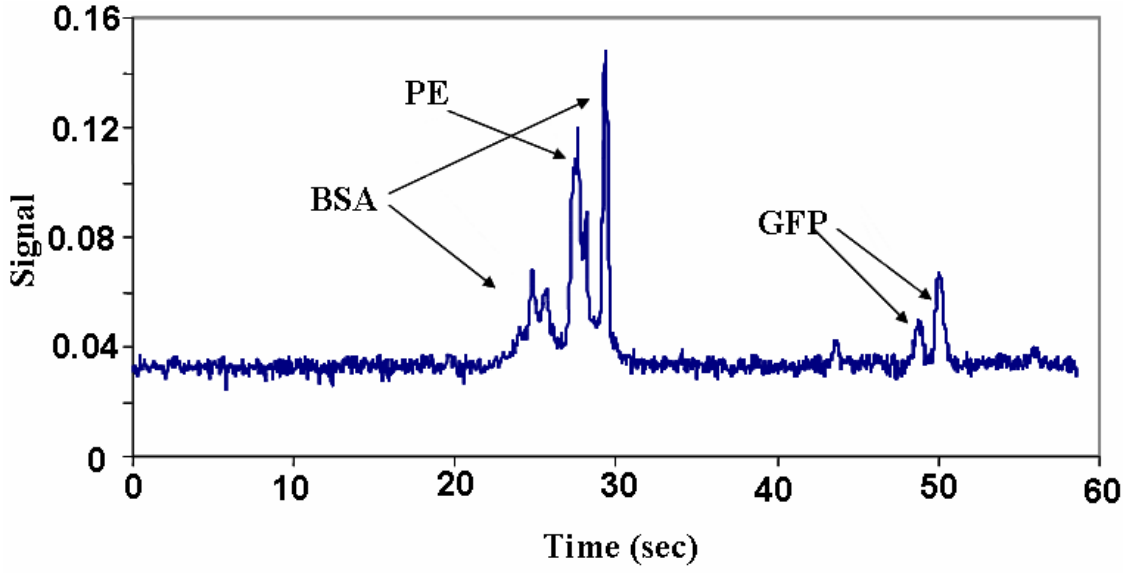

Figure 3.8 Microchip CE of a protein mixture.

3.3.4 Peptide Separations in PMMA Microchips

Peptide separation is another important application of microchip CE. Figure 3.9 shows CE of FITC-insulin in a PEG-grafted microdevice. Seven peaks were identified in the separation, while conventional CE only gave one peak (data not shown). Tricine peptide gel electrophoresis indicated that this FITC-insulin sample had multiple components (data not shown). As many as 2.8×10^4 theoretical plates were obtained for the largest peak in Figure 3.9 with a 3.5 cm long separation channel. The relative standard deviation for this peak's migration time was 0.6% over 5 runs. These results indicate that PEG-grafted PMMA microdevices have high performance in peptide separation.

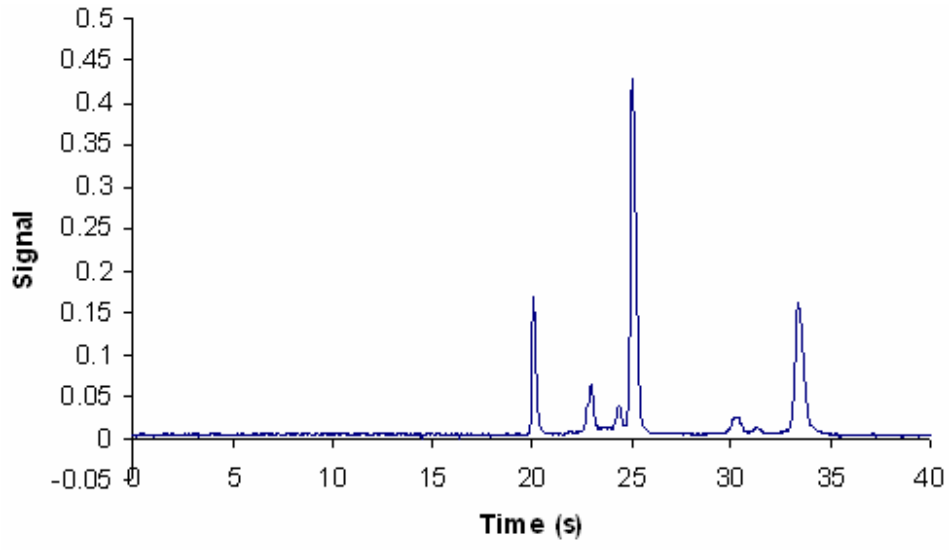

Figure 3.9 Microchip CE of impure FITC-insulin in a PEG-grafted microdevice.

Phosphorylation of proteins is important to their function. To determine the phosphorylation site of a protein, the current protocol includes two steps. The first step is to digest the protein with trypsin (or another enzyme); the second step is to identify the resulting peptide fragments using liquid chromatography (LC) and mass spectrometry [18]. In this protocol, effective separation of the tryptic digest is key. Besides LC, microchip CE is another possible candidate to fractionate tryptic digests, because of rapid analysis and low sample consumption. Figure 3.10 shows microchip CE of a decomposed trypsinogen sample in a dynamically coated PMMA microdevice. At least 15 peptide fragments could be identified in the electropherogram. This result indicates that PMMA microchips have potential to be employed in tryptic digest separations.

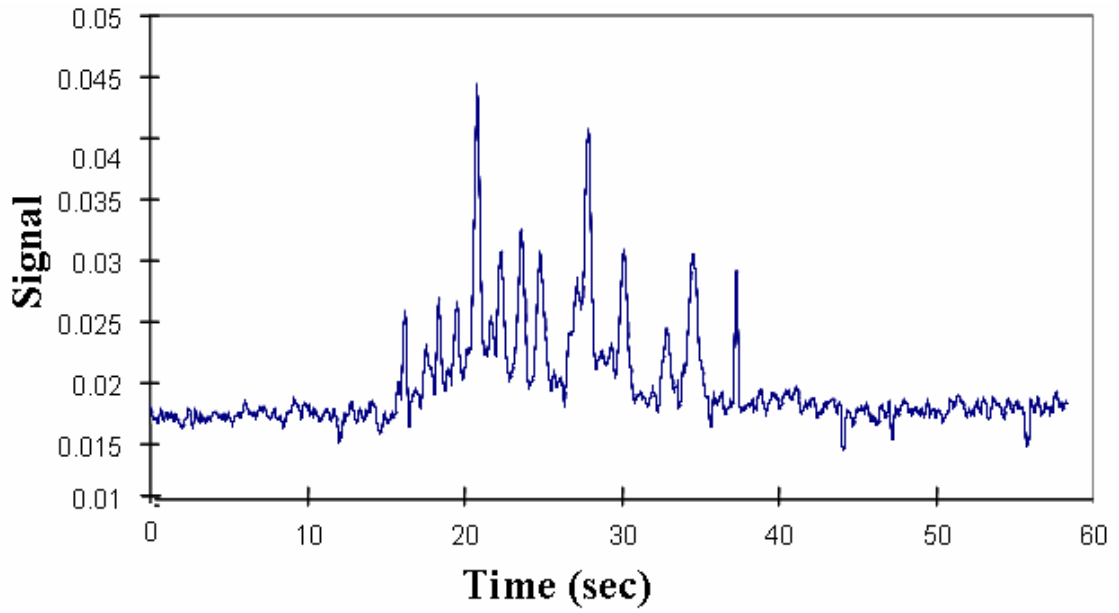

Figure 3.10 Separation of a decomposed trypsinogen sample in an HPC-coated PMMA device.

However, the reproducibility of the tryptic digest separation in untreated PMMA was less than desired. As discussed in the Section 3.3.3, analytes adsorption and unstable EOF are two major reasons. Thus, I also tried microchip CE of a BSA tryptic digest in a PEG-grafted PMMA microdevice (Figure 3.11). The tryptic digest was successfully resolved, and the separations were reproducible with a migration time relative standard deviation of 0.56% over 4 runs for the last peak.

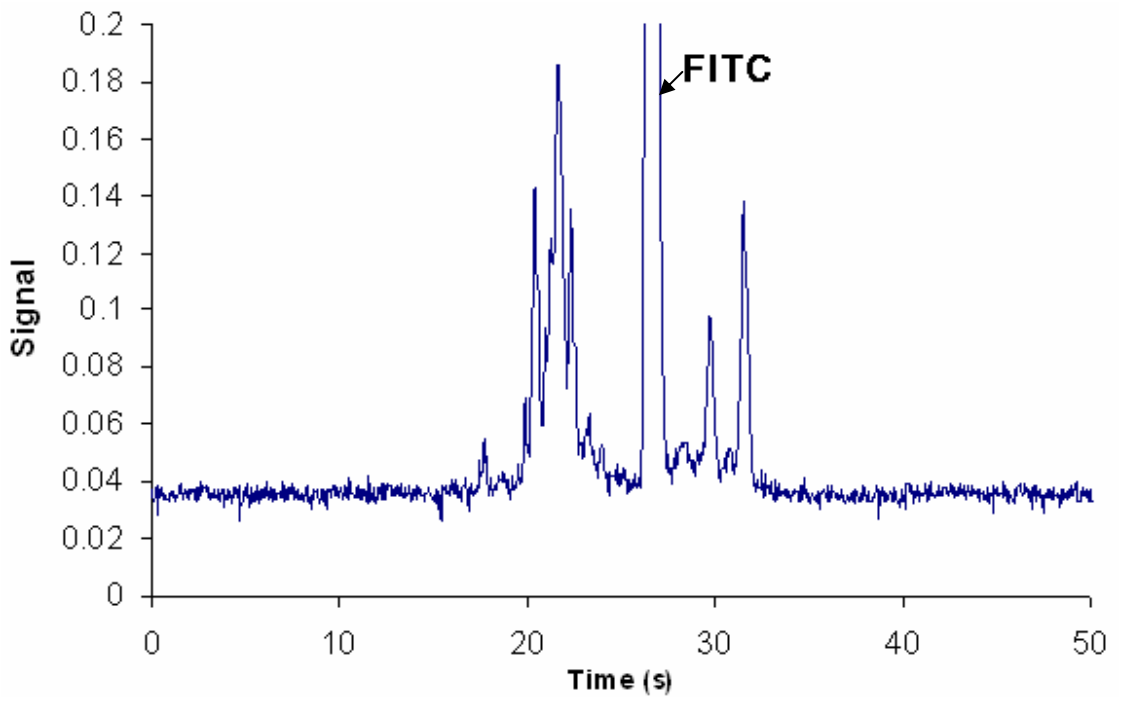

Figure 3.11 Microchip CE of a BSA tryptic digest.

To test a biological application of PEG-grafted PMMA microdevices, I evaluated the CE separation performance of a tryptic digest of phosphorylated PhLP. PhLP is a homologue of phosducin, a known major regulator of Gβγ signaling in the retina and pineal gland; however, as yet, the function of the PhLP remains unclear [19]. One important function of PhLP is that it binds directly to Gβγ in vitro, and phosphorylation of PhLP (to form p-PhLP) is important to its function. However, the mechanism of phosphorylation is not yet known. I used microchip CE to separate a tryptic digest of p-PhLP in a PEG-grafted PMMA microdevice, and the result is shown in Figure 3.12a. Theoretically there should be more than 30 peptide fragments produced when p-PhLP is digested using trypsin; but limitations in the FITC chemistry make it such that not all peptide fragments are well labeled. In microchip CE of p-PhLP, at least 6 peptide fragments were identified, which

was also corroborated by a tricine peptide gel (Figure 3.12b). Importantly, this result indicates that PEG-grafted PMMA microdevices are suitable for real biological sample analysis.

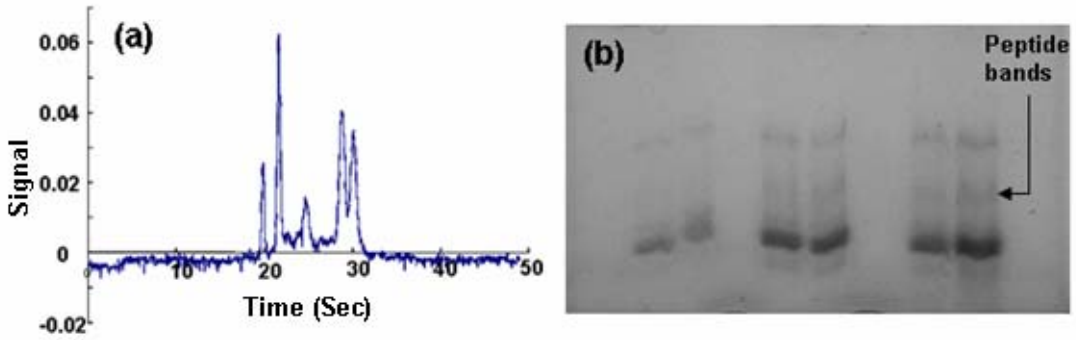

Figure 3.12 Comparison of p-PhLP digest separation in (a) microchip CE and (b) tricine peptide gel.

3.4 Conclusion

Microchip CE of proteins and peptides in PMMA microdevices has been evaluated in this chapter. The results indicate that ATRP grafting of PEG offers superior results to dynamic coating for biological separations in PMMA microdevices. I believe that PMMA microdevices should be broadly applicable in biomolecular analysis.

3.5 References

[1] Hebestreit, H. F., *Curr. Opin. Pharmacol.* 2001, *1*, 513-520.

[2] Twyman, R. M., *Principles of Proteomics*, BIOS Scientific Publishers, New York 2004.

[3] Liebler, D. C., *Introduction to Proteomics: Tools for the New Biology*, Humana Press, Totowa, NJ 2002.

[4] Weaver, R. F., *Molecular Biology*, The McGraw-Hill Companies Inc., New York 2005.

[5] Klose, J., *Electrophoresis* 1999, *20*, 643-652.

[6] O'Farrell, P. H., *J. Biol. Chem.* 1975, *250*, 4007-4021.

[7] Jorgenson, J. W., Lukacs, K. D., *Anal. Chem.* 1981, *53*, 1298-1302.

[8] Jorgenson, J. W., Lukacs, K. D., *Science* 1983, *222*, 266-272.

[9] Xiao, D., Le, T. V., Wirth, M. J., *Anal. Chem.* 2004, *76*, 2055-2061.

[10] Armenta, J. M., Gu, B., Humble, P. H., Thulin, C. D., Lee, M. L., *J. Chromatogr. A* 2005, *1097*, 171-178.

[11] Youssouf, B. M., Wong, M., Chiem, N., Salimi-Moosavi, H., Harrison, D. J., *J. Chromatogr. A* 2002, *947*, 277-286.

[12] Wiktorowicz, J. E., Colburn, J. C., *Electrophoresis* 1990, *11*, 769-773.

[13] Kinter, M., Sherman, N. E., *Protein Sequencing and Identification Using Tandem Mass Spectrometry*, Wiley-Interscience, New York 2000.

[14] Kelly, R. T., Woolley, A. T., *Anal. Chem.* 2003, *75*, 1941-1945.

[15] Liu, J., Pan, T., Woolley, A. T., Lee, M. L., *Anal. Chem.* 2004, *76*, 6948-6955.

[16] Kelly, R. T., Pan, T., Woolley, A. T., *Anal. Chem.* 2005, *77*, 3536-3541.

[17] Kelly, R. T., Li, Y., Woolley, A. T., *Anal. Chem.* 2006, *78*, 2565-2570.

[18] Carter, M. D., Southwick, K., Lukov, G., Willardson, B. M., Thulin, C. D., *J. Biomol. Tech.* 2004, *15*, 257-264.

[19] Thibault, C., Sganga, M. W., Miles, M. F., *J. Biol. Chem.* 1997, *272*, 12253-12256.

Chapter 4. In-Channel Atom-Transfer Radical Polymerization of Thermoset Polyester Microfluidic Devices for Bioanalytical Applications*

4.1 Introduction

Polymeric materials have become a common choice in the field of microfluidics [1], with an increasing number of microdevices being fabricated using polymers instead of glass [2, 3], as in earlier research. In addition to the general advantages of microfluidic devices for chemical analyses – reduced sample consumption, potential for integration of various operations, fast analysis times, multiplexing for high throughput, and portability – polymer microchips can reduce costs, making disposable devices more practical. Also, the polymers available for use offer a variety of inherent material properties to choose from (e.g., reversible sealing, resistance to selected solvents, etc.), and the associated fabrication techniques tend to be more flexible, in terms of making multilayer fluidic designs, and limiting the need for highly specialized equipment.

Common hard polymers used for the fabrication of microfluidic devices – including poly(methyl methacrylate) (PMMA) [4, 5], poly(carbonate) [6], cyclic olefin copolymer [7] and poly(ethylene terephthalate) [1] – are fabricated via the plastic machining techniques of embossing, injection molding, or laser ablation. The popular poly(dimethylsiloxane) (PDMS) [8, 9], a silicone elastomer that is microfabricated via replica molding, has been used widely in microfluidics research due to the speed and ease with which new fluidic designs can be created and then formed into devices, as well as

the capability of fabricating complex three-dimensional assemblies and multilayer channel networks [10-12].

While the use of PDMS remains popular for certain applications, some undesirable characteristics, such as surface instability [9] and incompatibility with most nonpolar solvents [13], have established a need for analogous materials that address these issues. One such polymer is thermoset polyester (TPE), which has been introduced previously for the fabrication of microfluidic devices [14, 15]. Importantly, TPE microchips combine the benefits of rapid and easy fabrication along with several desirable characteristics in common with glass. Indeed, TPE can be shaped by a replica molding process similar to PDMS, allowing for rapid prototyping of fluidic designs, but TPE also exhibits surface stability and solvent resistance similar to glass. Also of note, TPE is not elastomeric like PDMS; it is a rigid material.

For bioanalysis applications, the surfaces of materials, whether glass or polymeric, are often modified to increase separation efficiency and reproducibility, since biological molecules often interact with surfaces, causing sample loss and peak broadening. Surface modification in both capillary electrophoresis (CE) and microchip CE is common, and a variety of techniques are available, including dynamic surface coating [16] and many forms of chemical modification [17, 18]. Atom-transfer radical polymerization (ATRP) [19-21] has been used for chemical derivatization of PDMS [22, 23] and PMMA [5] microchannels. ATRP modification of plastics involves activation of the surface via plasma oxidation, immobilization of the initiator, and subsequent grafting of the chosen polymer to the surface. In ATRP, the length of polymer tethered to the surface can be controlled readily. ATRP has been used to attach various polymers, including

polyacrylamide [24], hydroxypropyl cellulose [25], methacrylate [26], poly(ethylene glycol) (PEG) [5], and peptidoglycans [27]. Typically, neutral polymers are used to eliminate the possibility of electrostatic interactions with analytes. PEG-modified PMMA devices have shown increased separation performance relative to unmodified microchips [5], so I was interested in applying this surface derivatization approach to different polymers.

Here, I present a new approach for in-channel ATRP grafting of a thin film of PEG on the surface of TPE microchannels. These modified TPE microdevices had reduced nonspecific analyte adsorption, and lower and more pH-stable electroosmotic flow (EOF). I have tested these PEG-grafted TPE microchips in CE analysis of amino acids and peptides. I have further demonstrated their utility in probing the phosphorylation efficiency for a model protein.

4.2 Experimental Section

4.2.1 Materials

2-Bromoisobutyryl bromide (98%), poly(ethylene glycol) methyl ether methacrylate (PEGMEMA, MW ~475), 2,2'-dipyridyl (99+%), copper(I) chloride (98+%), and copper(II) bromide (99%) were purchased from Aldrich (Milwaukee, WI) and used without further purification. Heptane, tetrahydrofuran, absolute methanol, and pyridine (all reagent grade) were obtained from Fisher Scientific (Fair Lawn, NJ). Fluorescein isothiocyanate (FITC), aspartic acid, glycine, asparagine, Phe-Ala (FA), Phe-Gly-Gly-Phe (FGGF) and angiotensin 1 were purchased from Sigma (St. Louis, MO). Phosducin-like protein (PhLP) and phosphorylated PhLP (p-PhLP) were gifts from Dr. Craig Thulin

in the Department of Chemistry and Biochemistry at Brigham Young University. PhLP has a molecular weight of ~33 kDa and pI of ~4.7 [28, 29]. Deionized water was from an EasyPURE UV/UF purification system (Barnstead, Dubuque, IA), and the buffer solution for CE experiments was 10 mM Trizma hydrochloride (Tris) at pH 8.7, which was filtered using 0.2-μm syringe filters (Pall Gelman Laboratory, Ann Arbor, MI).

4.2.2 Microfluidic Device Fabrication

Figure 4.1 is a schematic of the TPE microdevice fabrication procedure. TPE microchips were constructed similarly to the protocol described previously [15], with a modified pretreatment of the masters. SU-8 patterned silicon masters were prepared using photolithography as described elsewhere [1]. In short, SU-8 50 (Microchem, Newton, MA) negative photoresist was spin-coated onto 3-in. silicon wafers (Montco Silicon Technologies, Royersford, PA) to a thickness of 50 μm. A phototransparency with a printed design of a double-T microchannel with a pattern width of 50 μm was used as the lithography mask. Following exposure, the wafers were baked and developed with propylene glycol methyl ether acetate (Sigma-Aldrich, Milwaukee, WI), yielding a SU-8 patterned silicon master (Figure 4.1a). Instead of sputter coating the master with SnO_2 as before [1], in this work the SU-8 patterned silicon masters were treated by reaction with hexamethyldisilazane (HMDS, Sigma-Aldrich) prior to replica molding with TPE; masters and a minimal amount of HMDS were placed in a loosely covered container in a 60 ºC oven overnight. The microchannels were designed to be 50 μm wide by ~50 μm tall, and the offset spacing of the injection arms was 50 μm. Each arm of the double-T

section was 0.5 cm long, and the separation channel was 3 cm long. Circular areas for reservoirs were 5 mm in diameter (Figure 4.1).

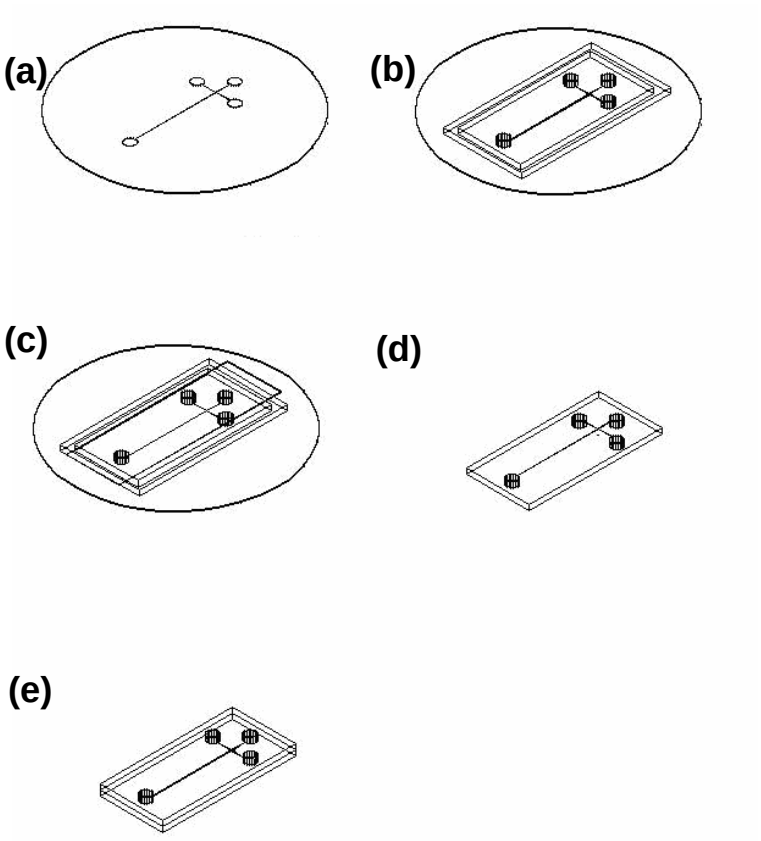

Figure 4.1 Schematic of the procedure for the fabrication of TPE microfluidic devices. (a) A SU-8 patterned silicon master is treated with HMDS vapor. (b) A PDMS mold enclosure and posts are placed on the master. (c) TPE resin containing UV photoinitiator and catalyst is poured into the master assembly; transparency film is used on the top. (d) Following exposure to UV radiation, the semicured TPE replicas are removed from the master, and (e) brought into contact. Additional UV exposure and heat are used to completely cure the TPE chip.

TPE was prepared by mixing the resin (Polylite 32030-10, Reichhold, Research Triangle, NC) with additional cross-linker (styrene, Sigma-Aldrich), UV photoinitiator (2,2-dimethoxyphenylacetophenone, Irgacure 651, Sigma-Aldrich), and methyl ethyl ketone peroxide (MEKP) catalyst (Crompton, Greenwich, CT). Approximately 0.10 g of the photoinitiator were dissolved in 0.25 g of styrene monomer and then added to 10 g of resin. Three drops of MEKP catalyst (~0.09 g) were added to the resin/styrene mixture, which was stirred and degassed to remove air bubbles. After degassing, the TPE mix was poured onto the patterned master. Cylindrical PDMS (Sylgard 184, Dow Corning, Midland, MI) posts were placed on the master to define access holes. In addition, a piece of PDMS was cut to form a mold enclosure, which was conformally sealed to the master to contain the resin in the desired region (Figure 4.1b). A piece of transparency film (3M), cut to an appropriate size, was used as a top cover over the resin to ensure a flat surface (Figure 4.1c).

The cast TPE resin was exposed to radiation using a custom-built UV exposure box, which contained two long-wave UV bulbs with peak intensity at 365 nm (TLK 40W/10R, Philips). Samples were placed ~15 cm from the sources. TPE pieces (one patterned and one flat) were exposed for 3 min and peeled away from the masters (Figure 4.1d). The patterned substrate was brought into contact with the flat piece to form an enclosed chip (Figure 4.1e), which was then exposed to UV light for an additional 2 min using four periods of 30-s exposures with 1.5-min intervals between exposures. Following UV curing, the TPE pieces were heated to 60 ºC for 30 min and 120 ºC for 1.5 h before finally cooling to room temperature.

4.2.3 ATRP Surface Modification of TPE Microdevices

Immobilization of Initiator. The method of in-channel ATRP used here (Figure 4.2) is similar to previously reported work [5]. A typical ATRP initiator, 2-bromoisobutyryl bromide, was immobilized on the channel surfaces of the TPE microdevice under a water-free environment. The immobilization solution was prepared by dissolving 2-bromoisobutyryl bromide (5 mM) and pyridine (5.5 mM) in a heptane/THF solution. Then the solution was pumped through the TPE microchannels at 2 μL/min using a syringe pump. After 6 h, heptane was rinsed through the microchannels to stop the initiator immobilization reaction. Lastly, vacuum was applied to dry the microchannels.

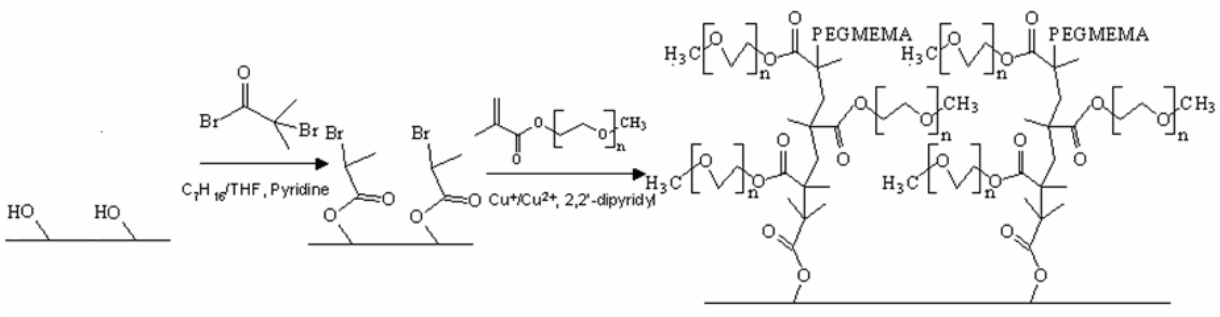

Figure 4.2 Scheme for in-channel ATRP surface modification.

In-channel Grafting of PEG on TPE surfaces. The preparation of the PEG grafting solution and the assembly of the syringe and TPE microdevice were carried out in a glove box. First, CuCl (0.0424 g), $CuBr_2$ (0.0287 g), 2,2'-dipyridyl (0.174 g), 4 mL of PEGMEMA, and 6 mL of DI water were mixed in the glove box for 15 min. 1 mL of this solution was transferred to a new container, and 9 mL of DI water was added to make the final diluted grafting solution. The syringe was filled with diluted grafting solution, and the fittings and TPE microdevice were assembled in the glove box and taken out. The

grafting solution was pumped through the TPE microchannels at 2 μL/min for 6 h to accomplish ATRP grafting, and then DI water was used to flush the microchannels.

4.2.4 X-ray Photoelectron Spectroscopy (XPS) and Contact Angle Measurements

A SSX-100 X-ray photoelectron spectrometer (Service Physics, Bend, OR) with a monochromatic Al K_α source and a hemispherical analyzer was used to investigate the TPE surfaces before and after ATRP modification. The investigations were carried out similar to previous work [15]. For the contact angle measurements, a NRL-100 goniometer (Ramé-Hart, Mountain Lakes, NJ) was used after 4 μL of DI water was placed on the surface with a syringe.

4.2.5 EOF Measurements

EOF measurements in TPE microdevices were done as I have reported previously [5], using the current monitoring method [30]. The EOF rates in TPE microdevices were measured at five different pH values. The buffers (all 30 mM) included 4-morpholineethanesulfonic acid (pH 6), N-[Tris(hydroxymethyl)methyl]-2-aminoethanesulfonic acid (pH 7), Tris (pH 8), phosphate buffered saline (pH 9) and 3-(cyclohexylamino)-1-propane sulfonic acid (pH 10); the ionic strength of these buffers was adjusted to 30 mM with NaCl. For a typical EOF measurement, the TPE microchannels were rinsed with DI water thoroughly, followed by buffer. Before measurement, one reservoir was emptied, and a lower concentration (1.5 mM) of the same buffer was introduced into that reservoir. The high voltage used in EOF measurements was provided by a PS-350 high voltage supply unit (Stanford Research

Systems, Sunnyvale, CA). The channel current signal was transferred to a computer through a PCI-1200 data acquisition board (National Instruments, Austin, TX), and was recorded using LabView 8i (National Instruments). For each pH point, three measurements were performed, and error bars represent ±1 standard deviation.

4.2.6 FITC Labeling of Amino Acids, Peptides and Proteins

The protocols for labeling amino acids, peptides and proteins with FITC were adapted from previous work [5, 31, 32]. Briefly, each analyte was dissolved individually in filtered 10 mM carbonate buffer (pH 9.2). FITC was dissolved in absolute dimethyl sulfoxide to make a 6 mM solution. For amino acids, 600 μL of each 3 mM amino acid solution was mixed thoroughly with 200 μL of 6 mM FITC solution. For peptides, 50 μL of 6 mM FITC solution was added to 200 μL of a 2 mM solution of each individual peptide. The FITC labeling reaction was run for at least 24 h in the dark at room temperature; longer reaction times (up to 5 days) led to more complete labeling and elimination of the unreacted FITC peak.

For FITC labeling of PhLP and p-PhLP, the proteins were desalted and concentrated individually using Microsep 3K Omega centrifuge tubes (Pall, East Hills, NY), which have a molecular weight cutoff of 3000. The solution in the upper chamber of the tube was diluted with carbonate buffer (pH 9.2) to make a ~2 mg/mL protein solution. An appropriate volume of 6 mM FITC solution was added to this protein solution to make a 5:2 molar ratio of FITC to protein. The reaction time was the same as for FITC labeling of amino acids and peptides.

4.2.7 Protein Adsorption Tests

To study the protein adsorption in both untreated and PEG-grafted TPE channels, I flushed FITC-labeled bovine serum albumin (BSA) through TPE microdevices at 2 μL/min [5]. After 30 min, 20 mM Tris buffer was used to wash out unbound protein for 1 h at 10 μL/min. Then, the microchip was placed on the microscope stage and a ~400-μm-diameter region of the channel was illuminated with 488 nm laser light. Fluorescence images were recorded with a Nikon Coolpix digital camera and analyzed using Digital V++ software (Digital Optics Limited, Auckland, New Zealand) as in earlier work [33].

4.2.8 Separation and Detection of Amino Acids, Peptides and Proteins

The microchip CE and laser-induced fluorescence detection methods have been described previously [5, 32]. For these experiments, the injection voltage was 0.8 kV, the separation voltage was 2.0 kV, and the data sampling frequency was 100 Hz.

4.3 Results and Discussion

4.3.1 Surface Modification

The cross-linkage bonding of TPE devices is one of the advantages of this fabrication method. However, the previous ATRP procedures for unbonded PMMA surfaces [5] would interfere with the cross-linking process. Thus, I developed an in-channel ATRP modification approach. The ATRP process is typically carried in still (i.e., not flowing) solution, particularly for PEG grafting, which could cause problems for microchannel surface modification [22, 34]. I hypothesized that if the reaction solution was flushed through microchannels at a sufficiently slow flow rate, the reaction conditions would be

close enough to “still” to allow ATRP functionalization. The method I report here, in-channel ATRP, uses slow flow of low-concentration reactant to carry out ATRP reactions inside the TPE channels. Importantly, since in-channel ATRP is done after the TPE microdevices have been bonded together, it does not interfere with device fabrication.

In the ATRP grafting of PMMA microdevices, the first step is plasma activation to form surface hydroxyl groups [5]. I expected TPE to have sufficient surface hydroxyl groups that I could omit the plasma oxidation step. Indeed, I obtained similar results with ATRP reactions on both plasma-activated and native TPE surfaces, so I skipped the plasma oxidation procedure in subsequent experiments. The second step for in-channel ATRP is the immobilization of initiator (2-bromoisobutyryl bromide) on the TPE channel surface. In this work, I used heptane/THF (v/v 4:1) as the solvent, since this mixture does not dissolve or swell TPE at room temperature. It was critical to optimize the concentrations of 2-bromoisobutyryl bromide and pyridine, because I found under some conditions that this reaction produced precipitates that could block the channels. The best results were obtained with 5 mM 2-bromoisobutyryl bromide and 5.5 mM pyridine in a heptane/THF solution. This mixture provided a uniform layer of initiator grafted on the TPE surface without blocking the channels. I also adjusted the PEG grafting solution composition and settled on a mixture that contained ten-fold lower PEG and catalyst concentrations compared to the earlier PMMA studies [5].

4.3.2 XPS and Contact Angle Measurements

XPS was used to determine the elemental composition of the TPE surfaces before and after modification, and the results are shown in Table 4.1. The XPS data indicate that the native TPE surface was composed of 75% carbon and 25% oxygen. After in-channel

ATRP, the elemental composition changed to 69% carbon and 31% oxygen, reflecting increased oxygen content due to PEG grafting. To obtain more detailed information about the elemental composition of the TPE surface, I took high-resolution scans of the C_{1s} binding energy, in a similar manner to prior studies [15]. After in-channel ATRP, the hydrocarbon (C-H) surface content decreased from 61% to 29%, the ester/acid (carboxyl) surface content decreased from 15% to 5%, and the ether/alcohol (C-O) surface content greatly increased from 24% to 66%.

Table 4.1 XPS investigation of in-channel ATRP surface modification of TPE.

	Intact TPE surface	TPE surface after plasma treatment	TPE surface after ATRP
C (%)	75	67	69
-carboxyl (%)	15	23	5
-C-O (%)	24	27	66
-C-H, C-C (%)	61	51	29
O (%)	25	33	31

Water contact angles for both PEG-grafted and native TPE were obtained. The contact angle for the PEG-grafted TPE surface was 43º, while native TPE had a contact angle of 61º. Both results agree well with previous reports of the contact angles of PEG-grafted PMMA [5] and native TPE [15]. The change in the contact angle before and after surface modification indicates that the chemistry and hydrophilicity of the TPE surface were altered through ATRP treatment, which is also consistent with the XPS investigation.

4.3.3 EOF Measurements

In PEG-grafted TPE microchips, the EOF goes from anode to cathode, which is similar to what I observed in untreated TPE devices. Figure 4.3 shows EOF measurements in both

PEG-grafted and untreated TPE microchannels for different pH values. Compared to the pH-variant EOF in untreated TPE microchannels, PEG-grafted TPE has very stable EOF (~1.0×10^{-5} $cm^2s^{-1}V^{-1}$) in a wide pH range (6 – 10), which should help in high-performance biomolecule analysis. Also, the EOF values in PEG-grafted TPE channels are 5-10 times lower than the corresponding measurements in untreated ones.

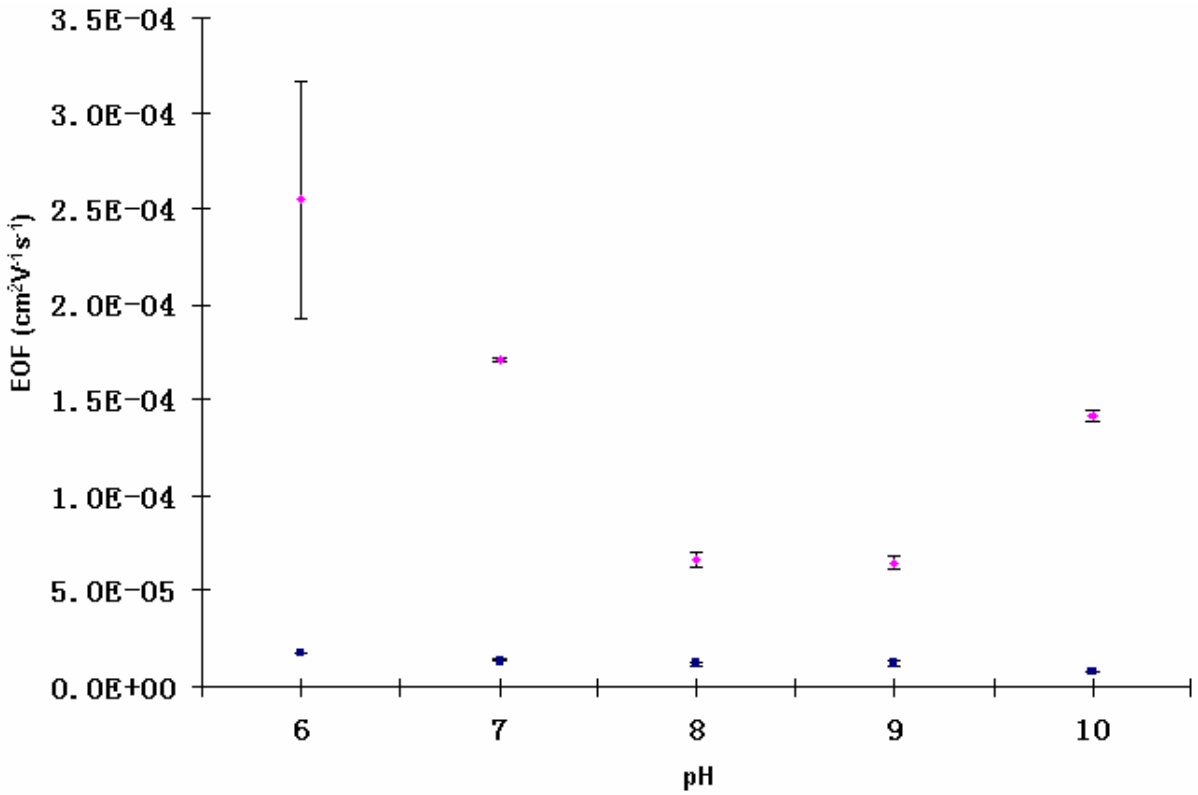

Figure 4.3 EOF measurements in untreated TPE microchannels (diamonds) and in-channel PEG-grafted TPE microchannels (squares). For some data points, error bars may be covered within the data points.

4.3.4 Protein Adsorption Studies

Although polymer microdevices are easy to fabricate and relatively cheap, they are not inherently the best choice for some bioanalytical applications. In untreated TPE devices,

protein adsorption and unstable EOF are two major barriers that would limit the use of these microdevices. However, after ATRP modification, the PEG-grafted TPE surface is expected to have reduced protein adsorption compared to untreated devices. To test this, I carried out BSA adsorption experiments, as shown in Figure 4.4. I noticed much greater BSA adsorption on the untreated TPE channel surfaces, compared to PEG-grafted TPE channels, indicating that the ATRP process significantly reduces protein adsorption on the surface.

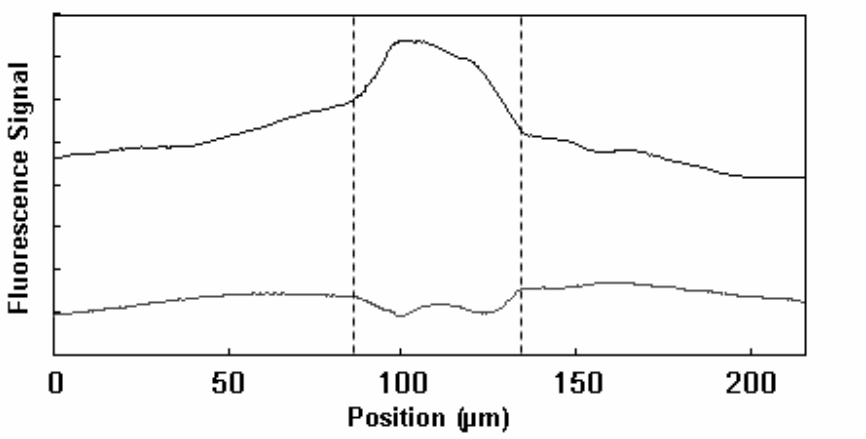

Figure 4.4 FITC-BSA adsorption tests on TPE chips before (upper, offset) and after (lower) in-channel ATRP PEG grafting. The dashed lines define the channel borders.

4.3.5 Electrophoresis of Amino Acids, Peptides and Proteins

Figure 4.5 shows CE results for the separation of amino acid and peptide mixtures. Both the amino acid and peptide mixtures were well resolved using PEG-grafted TPE microdevices. The glycine peak in Figure 4.5a was used to evaluate the CE performance of TPE microdevices, and 4.5×10^3 plates for a 3.0-cm-long separation channel were obtained. Moreover, the relative standard deviation for the glycine migration time over 4

runs was 2.1%. In addition to amino acid analysis, PEG-grafted TPE microdevices offer good performance in peptide separation. The number of theoretical plates for the FGGF peak in Figure 4.5b was 1.2×10^3, and the relative standard deviation for the FGGF migration time in 4 runs was 4.4%. The number of theoretical plates for amino acid separations in PEG-grafted TPE microdevices is similar to uncoated glass [3], TPE [15], PMMA [32] and PDMS [9] without buffer additives, but the PEG-grafted TPE microdevices could provide much more rapid amino acid separations. The performance of PEG-grafted microdevices may be worse than that of surface-derivatized glass microdevices, but glass chips are much harder to make. Moreover, CE separations in the PEG-grafted TPE microdevices were reproducible. The lifetime for good CE separations in a PEG-grafted TPE micrdevice is at least 50 runs, which indicates that the grafted PEG layer is very robust. These results indicate that in-channel ATRP is an effective surface modification method for TPE microdevices, leading to reduced EOF and reproducible separations.

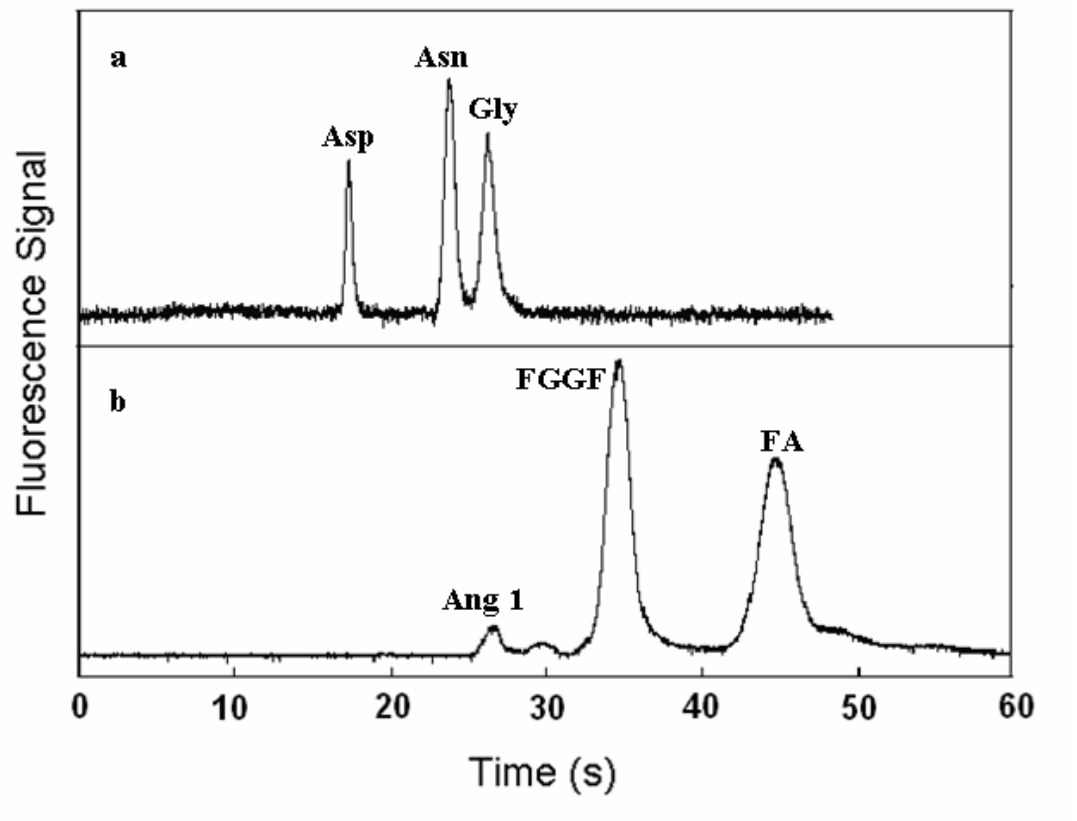

Figure 4.5 Microchip CE separation of FITC-tagged (a) amino acids and (b) peptides. The concentrations of peptides and amino acids tested in CE were all 50 μM.

To evaluate a biological application of PEG-grafted TPE microdevices, I developed a simple experiment to test the phosphorylation efficiency of PhLP. A widely expressed ethanol-responsive gene, PhLP, is a homologue of phosducin, a known major regulator of Gβγ signaling in the retina and pineal gland; however, as yet, the function of the PhLP remains unclear [35]. PhLP directly binds Gβγ in vitro, and phosphorylation of PhLP is important to its function, but the mechanism of phosphorylation is not yet known. In Chinese Hamster Ovary (CHO) cells, the concentration of PhLP is ~0.15 μM; but after angiotensin II treatment, the concentration of PhLP in CHO cells can be higher than 1

μM [36]. I have performed microchip CE of PhLP and p-PhLP mixtures, as shown in Figure 4.6. From these results, I see that the phosphorylation efficiency is high, but a small PhLP peak is still seen in the CE analysis of the PhLP phosphorylation mixture (Figure 4.6b). This result has also been verified by conventional gel electrophoresis of PhLP proteins (data not shown). The time variation between the two PhLP peaks in Figure 4.6a-b is due to small differences in the detection position selected during each CE experiment. The relative standard deviation for PhLP separation is 6.6% over 3 runs, while the deviation for p-PhLP separation is 4.1% over 4 runs. Importantly, this result indicates that PEG-grafted TPE microdevices are suitable for protein analysis work.

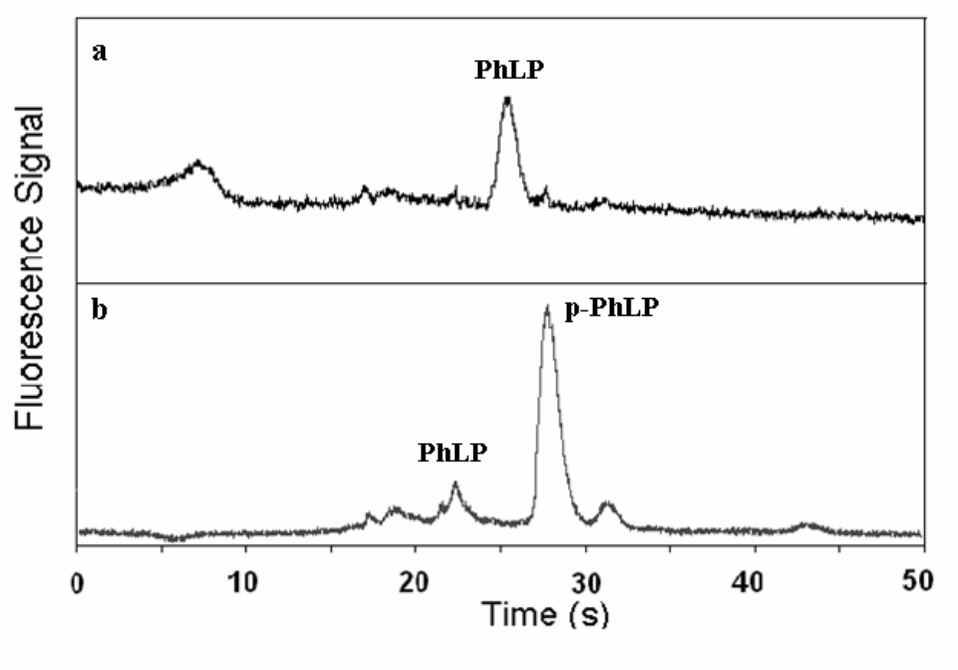

Figure 4.6 Microchip CE of (A) PhLP and (B) p-PhLP. The concentrations of both proteins were ~ 1.4 μM.

4.4 Conclusion

In-channel ATRP has been developed and applied in the surface modification of TPE microdevices. XPS and contact angle measurements confirm the grafting of PEG to the TPE surface. Significantly reduced EOF and nonspecific protein adsorption were observed in PEG-grafted TPE microchannels. Rapid CE separations of amino acids, peptides and proteins have been obtained, indicating that PEG-grafted TPE microdevices should be broadly applicable in biomolecular analysis.

4.5 References

[1] Fiorini, G. S., Chiu, D.T., *BioTechniques* 2005, *38*, 429-446.

[2] Manz, A., Harrison, D. J., Verpoorte, E. M. J., Fettinger, J. C., *et al.*, *J. Chromatogr.* 1992, *593*, 253-258.

[3] Harrison, D. J., Manz, A., Fan, Z., Luedi, H., Widmer, H. M., *Anal. Chem.* 1992, *64*, 1926-1932.

[4] Henry, A. C., Tutt, T. J., Galloway, M., Davidson, Y. Y., *et al.*, *Anal. Chem.* 2000, *72*, 5331-5337.

[5] Liu, J., Pan, T., Woolley, A. T., Lee, M. L., *Anal. Chem.* 2004, *76*, 6948-6955.

[6] Liu, Y., Ganser, D., Schneider, A., Liu, R., *et al.*, *Anal. Chem.* 2001, *73*, 4196-4201.

[7] Li, C., Yang, Y., Craighead, H. G., Lee, K. H., *Electrophoresis* 2005, *26*, 1800-1806.

[8] Effenhauser, C. S., Bruin, G. J. M., Paulus, A., Ehrat, M., *Anal. Chem.* 1997, *69*, 3451-3457.

[9] Duffy, D. C., McDonald, J. C., Schueller, O. J. A., Whitesides, G. M., *Anal. Chem.* 1998, *70*, 4974-4984.

[10] Unger, M. A., Chou, H.-P., Thorsen, T., Scherer, A., Quake, S. R., *Science* 2000, *288*, 113-116.

[11] Thorsen, T., Maerkl, S. J., Quake, S. R., *Science* 2002, *298*, 580-584.

[12] Anderson, J. R., Chiu, D. T., Jackman, R. J., Cherniavskaya, O., *et al.*, *Anal. Chem.* 2000, *72*, 3158-3164.

[13] Lee, J. N., Park, C., Whitesides, G. M., *Anal. Chem.* 2003, *75*, 6544-6554.

[14] Fiorini, G. S., Jeffries, G. D. M., Lim, D. S. W., Kuyper, C. L., Chiu, D. T., *Lab Chip* 2003, *3*, 158-163.

[15] Fiorini, G. S., Lorenz, R. M., Kuo, J. S., Chiu, D. T., *Anal. Chem.* 2004, *76*, 4697-4704.

[16] Liu, Y., Fanguy, J. C., Bledsoe, J. M., Henry, C. S., *Anal. Chem.* 2000, *72*, 5939-5944.

[17] Doherty, E. A. S., Meagher, R. J., Albarghouthi, M. N., Barron, A. E., *Electrophoresis* 2003, *24*, 34-54.

[18] Dolník, V., *Electrophoresis* 2004, *25*, 3589-3601.

[19] Wang, J.-S., Matyjaszewski, K., *J. Am. Chem. Soc.* 1995, *117*, 5614-5615.

[20] Kato, M., Kamigaito, M., Sawamoto, M., Higashimura, T., *Macromolecules* 1995, *28*, 1721-1723.

[21] Kamigaito, M., Ando, T., Sawamoto, M., *Chem. Rev.* 2001, *101*, 3689-3745.

[22] Xiao, D., Zhang, H., Wirth, M., *Langmuir* 2002, *18*, 9971-9976.

[23] Xiao, D., Le, T. V., Wirth, M. J., *Anal. Chem.* 2004, *76*, 2055-2061.

[24] Smith, E. A., Coym, J. W., Cowell, S. M., Tokimoto, T.*, et al.*, *Langmuir* 2005, *21*, 9644-9650.

[25] Shen, D., Yu, H., Huang, Y., *Celluose* 2006, *13*, 235-244.

[26] Zhai, G., Shi, Z. L., Kang, E. T., Neoh, K. G., *Macromol. Biosci.* 2005, *5*, 974-982.

[27] Velter, I., Ferla, B. L., Nicotra, F., *J. Carbohydrate Chem.* 2005, *25*, 97-138.

[28] Lazarov, M. E., Martin, M. M., Willardson, B. M., Elton, T. S., *Biochim. Biophys. Acta* 1999, *1446*, 253-264.

[29] Carter, M. D., Southwick, K., Lukov, G., Willardson, B. M., Thulin, C. D., *J. Biomol. Tech.* 2004, *15*, 257-264.

[30] Huang, X., Gordon, M. J., Zare, R. N., *Anal. Chem.* 1988, *60*, 1837-1838.

[31] Kelly, R. T., Pan, T., Woolley, A. T., *Anal. Chem.* 2005, *77*, 3536-3541.

[32] Kelly, R. T., Woolley, A. T., *Anal. Chem.* 2003, *75*, 1941-1945.

[33] Kelly, R. T., Li, Y., Woolley, A. T., *Anal. Chem.* 2006, *78*, 2565-2570.

[34] Matyjaszewski, K., Xia, J., *Chem. Rev.* 2001, *101*, 2921-2990.

[35] Thibault, C., Sganga, M. W., Miles, M. F., *J. Biol. Chem.* 1997, *272*, 12253-12256.

[36] McLaughlin, J. N., Thulin, C. D., Hart, S. J., Resing, K. A., *et al.*, *Proc. Natl. Acad. Sci. U.S.A.* 2002, *99*, 7962-7967.

Chapter 5. Design and Evaluation of a Coupled Monolithic Affinity Column−Capillary Zone Electrophoresis System for Cancer Marker Analysis

5.1 Introduction

As reviewed in Section 1.3.2, affinity methods can be useful in cancer marker analysis. As described in Section 1.3.3, several approaches have been developed to covalently attach antibodies on glycidyl methacrylate (GMA) monolith surfaces, but these techniques cannot effectively control the orientation of attached antibodies. In this chapter I report a method to attach appropriately oriented antibodies on GMA-based monoliths to ensure high bioactivity of the antibodies. In addition, I have applied this method to fabricate an affinity capillary electrophoresis (CE) column for human chorionic gonadotropin (hCG) analysis.

5.2 Experimental Section

5.2.1 Materials

Dextran sulfate sodium salt, dimethyl sulfoxide (DMSO), hexadimethrin bromide (polybrene), GMA 97%, trimethylolpropane trimethacrylate (TRIM), polyethylene glycol diacrylate (PEGDA), ethylene dimethacrylate (EDMA), 2,2-dimethoxy-2-phenylacetophenone (DMPA) 99%, glycine, ethylenediamine (EDA), fluorescein isothiocyanate (FITC), bovine serum albumin (BSA), trypsin, myoglobin and β-casein

were supplied by Sigma–Aldrich (Milwaukee, WI). Recombinant, enhanced green fluorescent protein (GFP) was purchased from Clontech (Palo Alto, CA). Sulfosuccinimidyl 4-N-maleimidomethyl cyclohexane-1-carboxylate (sulfo-SMCC), 2-mercaptoethylamine (2-MEA), and dextran desalting columns were obtained from Pierce (Rockford, IL). hCG, βhCG and anti-βhCG were acquired from Calbiochem (La Jolla, CA). Anhydrous methanol, acetone and hexanes were purchased from Mallinckrodt Chemicals (Phillipsburg, NJ). Cyclohexanol, ammonium formate and phosphate buffered saline (PBS) 10× solution (pH 7.4 ± 0.1) were from Fisher Scientific (Fair Lawn, NJ). Formic acid was from Anachemia Canada (Montréal, Canada). Sodium carbonate monohydrate and sodium bicarbonate were from EM Science (Darmstadt, Germany). Deionized water was from an EasyPURE UV/UF system (Barnstead, Dubuque, IA).

5.2.2 Fluorescent Labeling of Proteins

For the FITC labeling of proteins, each protein was diluted with carbonate buffer (pH 9.2) to make a ~2 mg/mL solution. An appropriate volume of 6 mM FITC in DMSO was added to each protein solution to make a 5:2 molar ratio of FITC to protein. The FITC labeling reaction was run for at least 24 h in the dark at room temperature.

5.2.3 Monolith Preparation in Capillaries

Fused silica capillaries with either UV-transparent or non-transparent coatings were obtained from Polymicro Technologies (Phoenix, AZ). Prior to monolith polymerization, capillary surfaces were treated by depositing alternating thin films of dextran and polybrene [1]. For UV transparent capillaries, a mask blocked the UV light so only

certain portions of the capillary had monolith polymerized. For polyimide-coated capillaries, a UV-transparent window was created 5-7 cm from one end of the capillary. Two kinds of monoliths were used in this project: GMA-EDMA and GMA-PEGDA. The GMA-EDMA monomer mixture was composed of 0.006 g DMPA (initiator); 0.24 g TRIM (cross-linker); 0.36 g GMA (monomer); and 0.72 g cyclohexanol, 0.44 g methanol and 0.19 g hexane (porogens). The GMA-PEGDA monolith prepolymer was composed of 0.008 g DMPA, 0.32 g PEGDA, 0.48 g GMA and 0.10 g cyclohexanol. For either monolith, the monomer mixture was sonicated for 5 min, and was loaded into the column by capillary action. Polymerization was performed using 320-390 nm UV radiation for 9-15 min. Unreacted monomer and porogens were removed by flowing methanol through the capillaries.

5.2.4 Immobilization of Antibodies on Polymer Monoliths

The mechanism of attaching antibodies to GMA-based monoliths is shown in Figure 5.1. The first step is to produce surface $–NH_2$ groups. EDA was dissolved in methanol to make a 50% solution, which was pumped through the monolith at 1 μL/min for 24 h (Figure 5.1a). Then, a mixture of 50 mM phosphate, 0.15 M NaCl, 10 mM EDTA, (pH 7.6, PBS-EDTA) was pumped through to flush the capillary. Anti-βhCG was partially reduced by 2-MEA to produce sulfhydryls for coupling (Figure 5.1b); 1 mg of antibody was dissolved in 125 μL PBS-EDTA, and 12.5 μL of 60 mg/mL 2-MEA solution in PBS-EDTA was added as the reducing agent. The reduction reaction was carried out at 37 ºC for 2 h, and then the antibody was purified using a desalting column equilibrated with PBS-EDTA buffer. Next, sulfo-SMCC was used as a crosslinker to couple partially reduced antibodies to the amine-treated monolith (Figure 5.1c). Briefly, the sulfo-SMCC

was dissolved in PBS-EDTA to make a 2 mg/mL solution, which was pumped through the amine-treated monolith at 1 μL/min for 2 h. Then, purified reduced antibody solution was pumped through the monolith for 4 h at 0.5 μL/min. Unbound antibodies were washed out using PBS-EDTA, and the capillaries were stored at 4 ºC until use.

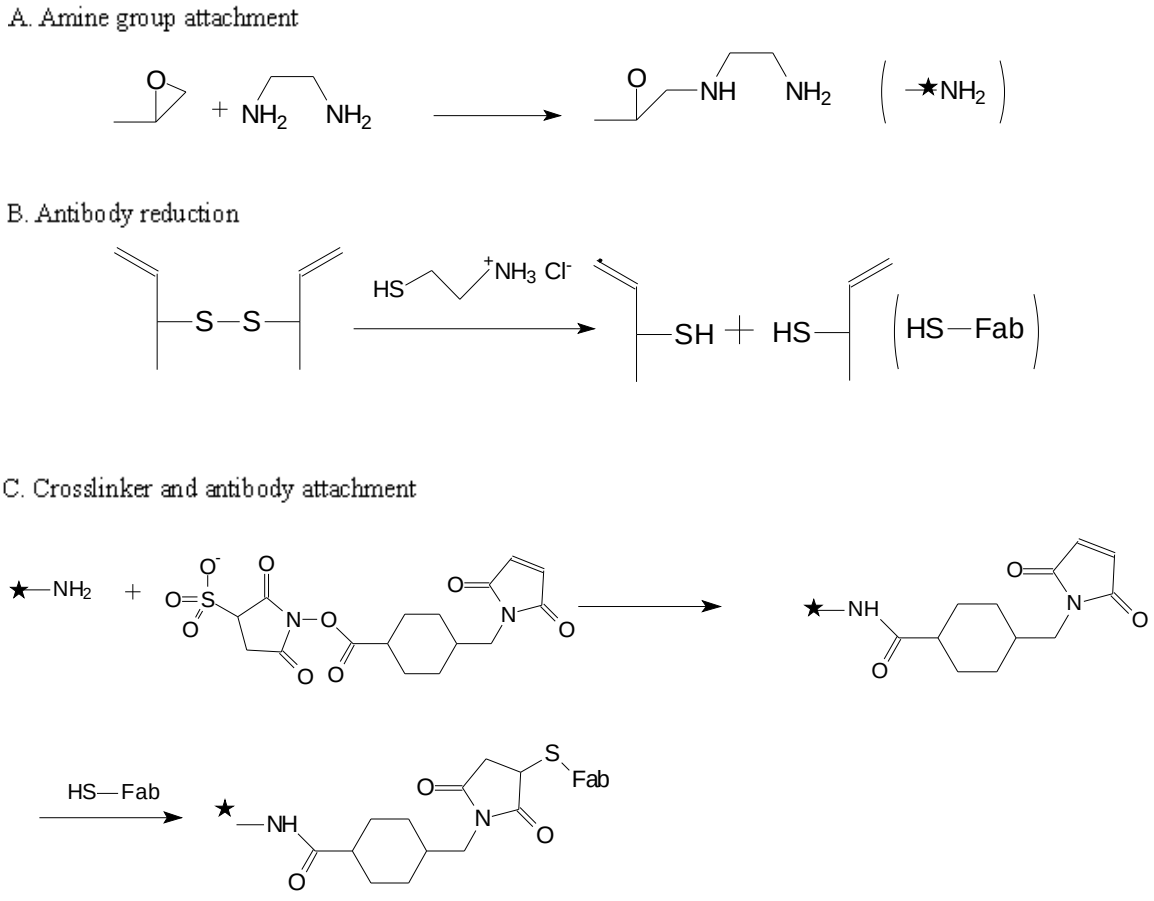

Figure 5.1 Scheme for attaching antibodies on a GMA monolith.

5.2.5 Blocking Nonspecific Adsorption on the Monolith

Nonspecific adsorption on the GMA-EDMA monolith was blocked using BSA. Briefly, 1% aqueous BSA solution was flushed through the monolith for 24 h at 0.2 μL/min, and then PBS was used to wash out unbound BSA. To study protein adsorption in both untreated and BSA-blocked GMA-based monoliths, I flushed each test protein (FITC-

BSA, FITC-trypsin, FITC-myoglobin, FITC-β-casein or GFP) through the monolith at 0.5 μL/min [2]. After 30 min, 20 mM Tris buffer was used to wash out unbound protein for 2 h at 1.0 μL/min. If Tris buffer could not wash out adsorbed protein effectively, 20 mM acetate buffer (pH 4.4) was flushed for 12 h at 1.0 μL/min. After washing, the monolithic capillary was placed on a microscope stage, and a ~400 μm length was illuminated with 488 nm laser light. Fluorescence images were recorded with a Nikon Coolpix digital camera and analyzed using Digital V++ software (Digital Optics Limited, Auckland, New Zealand) as in earlier work [3].

5.2.6 Adsorption-Desorption Test of hCG in Affinity Capillaries

For initial optimization of the adsorption-desorption tests, FITC-hCG in ammonium formate-formic acid buffer (AF-FA) was incubated on an affinity column for 1 h, followed by PBS washing to remove unbound analyte. Then, elution buffer (formic acid or glycine buffer) was injected into the affinity column using a syringe pump and incubated for 5-15 min, and any desorbed hCG was washed out. Finally, the affinity column was analyzed by fluorescence microscopy to observe protein adsorption as described in Section 5.2.5.

For quantitative adsorption-desorption testing of hCG in affinity capillaries, a 0.2 mg/mL hCG solution was prepared by dissolving hCG in 50 mM AF-FA buffer, pH 7.6. The hCG sample was introduced into the affinity capillary by pressure and incubated for 1 h, and then unbound sample was washed out of the column using PBS. The elution buffer (50 mM formic acid or glycine buffer, pH 2.4) was introduced into the affinity capillary and incubated for 15 min to desorb hCG. Finally, pressure was used to drive eluted hCG through the capillary for UV detection.

5.2.7 CE of hCG

I used a Crytstal CE 300 system (ATI, Madison, WI) with 50 mM AF-FA as the separation buffer for CE of hCG. UV-Vis absorbance detection at 214 nm was performed using an online Crystal 100 variable wavelength UV-Vis absorbance detector. Data were collected and analyzed using a ChromPerfect software workstation (Mountain View, CA). Following the preconditioning of the capillary, a small plug of 0.2 mg/mL hCG was injected into the capillary by pressure (1000 mbar) for 50 s, and 12 kV was used to separate the hCG sample. For preconcentration/CE experiments, preconcentration was performed as in the adsorption/desorption experiments in Section 5.2.6, and CE conditions were the same as above. Briefly, the hCG sample was introduced into the affinity capillary by pressure and incubated for 1 h, and then unbound sample was washed out of the column using PBS. The elution buffer (50 mM glycine buffer, pH 2.4) was introduced into the affinity capillary and incubated for 15 min to desorb adsorbed protein. Finally, CE was used to drive eluted hCG through the capillary for UV detection.

5.3 Results and Disscussion

5.3.1 Attachment of Antibodies on Monolith Surfaces

After polymerization, the GMA-based monolith surfaces have pendant epoxy groups, which are reactive under appropriate conditions [4]. As described in Section 1.3.3.1, these epoxy groups can react directly with protein amino groups to form a covalent linkage, but the reaction is slow, requires high protein concentrations, and cannot control the antibody orientation. Thus, I used a variant of Pierce protocols (see Section 1.3.3.5) [5] to attach oriented antibodies to GMA monoliths (Figure 5.1). In this method, an antibody is partially reduced to give reactive sulfhydryl groups at the end of the heavy chains, and

the sulfhydryls react with the monolith surface for covalent attachment. Since attachment only occurs through the heavy chains, the light chains are still free, which is advantageous, since in most cases the active sites of an antibody are on the light chains [6].

5.3.2 Blocking Nonspecific Adsorption on Monoliths

The epoxy groups of a native GMA monolith are prone to nonspecific protein adsorption, which could interfere with the antibody-antigen interaction. Also, the chemical treatments used to attach antibodies on the monolith (Figure 5.1) could provide adsorption sites. Thus, I used dynamic BSA coating to block nonspecific adsorption on native GMA-EDMA monoliths. After treatment with 1% BSA solution in PBS, myoglobin, GFP and trypsin did not adsorb to the monolith surface. Figure 5.2 shows fluorescence images of myoglobin adsorption on untreated and BSA-blocked GMA-EDMA monoliths. Nonspecific adsorption was not observed on BSA-blocked monoliths, while severe adsorption was found on untreated GMA-EDMA. Importantly, no detectable BSA bleed was found during CE experiments on these columns. These results indicate that BSA blocking might provide a good strategy to eliminate nonspecific protein adsorption in GMA monoliths.

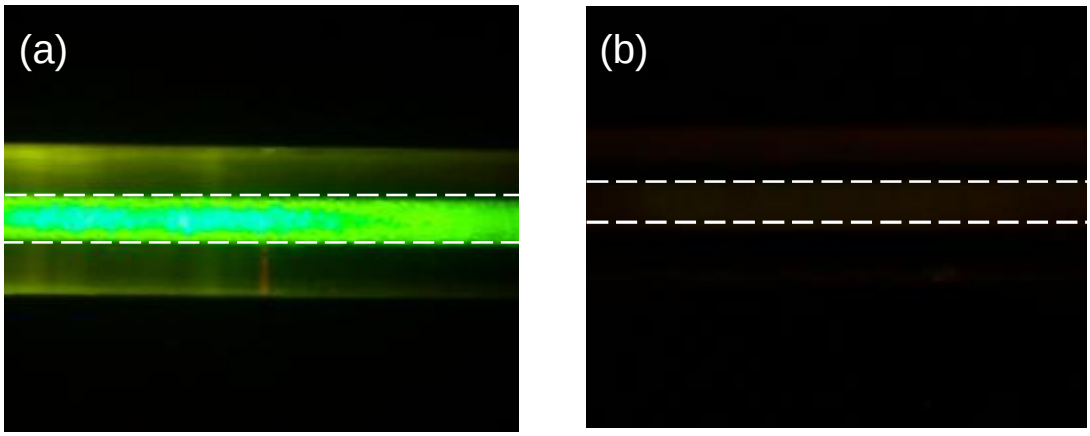

Figure 5.2 Fluorescence micrographs of adsorbed FITC-myoglobin in (a) untreated and (b) BSA-blocked GMA-EDMA monoliths. Dashed lines define the capillaries.

Another possible solution to nonspecific adsorption is to change the monolith recipe. As discussed in Chapters 3 and 4, a poly(ethylene glycol) (PEG) coating on a polymer surface can reduce nonspecific protein adsorption. Thus, I prepared a monolith that had PEGDA instead of EDMA as the crosslinking agent. FITC-BSA was used to test protein adsorption on GMA-PEGDA and GMA-EDMA monoliths, as described in Section 5.2.5. After 2 h Tris buffer washing, I observed severe protein adsorption on GMA-EDMA surfaces (Figure 5.3a), but no protein adsorption on the GMA-PEGDA surface (Figure 5.3c). After 12 h washing with acetic acid/acetate buffer (pH 4.4), most (~90%) of the FITC-BSA that had been adsorbed to the GMA-EDMA monolith was removed (Figure 5.3b). These results show that the GMA-PEGDA monolith should have better performance in dealing with nonspecific adsorption.

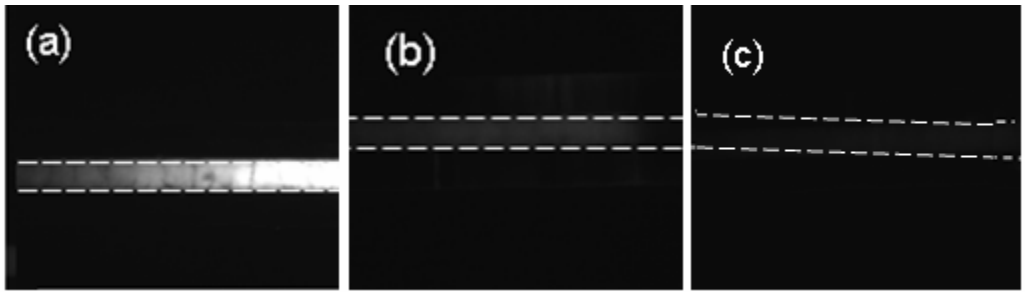

Figure 5.3 Fluorescence micrographs of adsorbed FITC-BSA on (a, b) GMA-EDMA and (c) GMA-PEGDA monoliths; (a) and (c) were taken after 2 h Tris buffer washing, while (b) was taken after 12 h acetate buffer washing.

5.3.3 Adsorption-Desorption Tests of hCG

To test the application of my monolith-based affinity columns in cancer marker detection, I used hCG as a model protein. As discussed in Section 1.3.1.2, hCG is important in cancer detection, and several variants exist in serum. Here, I tested preconcentration and CE of hCG and free βhCG on a GMA-EDMA-based affinity column. An adsorption/desorption test was used to determine optimum operation conditions for hCG preconcentration.

5.3.3.1 Incubation

I first determined the optimal incubation time for hCG/antibody interaction by testing times from 5-90 min. Longer incubation times gave greater hCG adsorption, but if the incubation time was too long, the column was not usable for affinity CE. Ultimately, I found 1 h to be the best incubation time.

5.3.3.2 Elution

The elution buffer is also critical for affinity interaction. To probe the elution, I designed a test using FITC-labeled hCG, as described in Section 5.2.6. The best elution condition was 15 min with glycine buffer. Although longer elution times could provide more

complete hCG removal, prolonged exposure of the monolith to acidic solution could cause damage to the affinity column. Figure 5.4 shows the elution of hCG from an affinity column. The adsorption/desorption tests were reproducible, as similar detector traces were found in 4 replicate experiments.

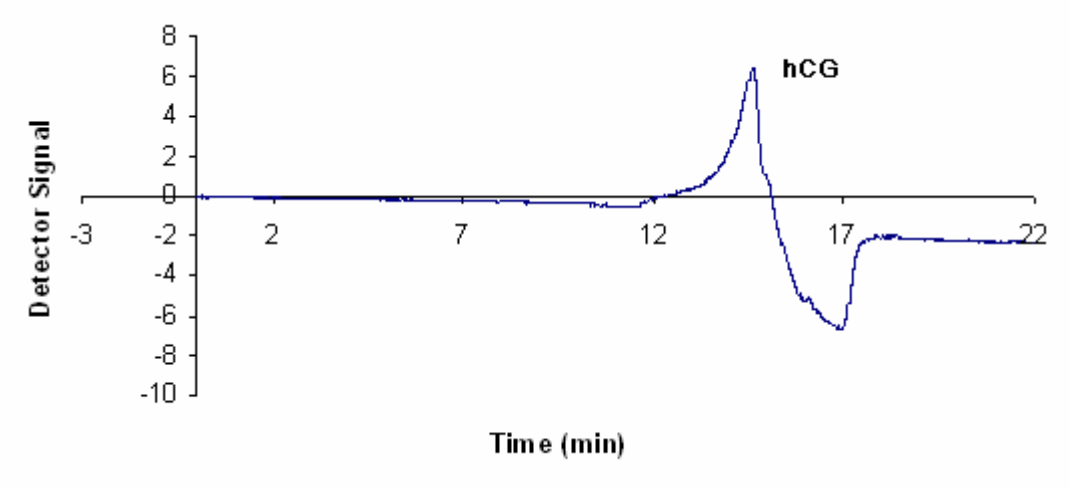

Figure 5.4 Elution of hCG from an affinity column.

5.3.4 CE of hCG

I carried out CE of hCG and βhCG in fused silica capillaries. The initial results indicate that βhCG and hCG have different mobilities (Figure 5.5). CE analysis of both hCG and βhCG was complete within 40 min, and the migration times for these two analytes differed by about 3 min, which indicates that CE could be used to separate hCG and βhCG after preconcentration.

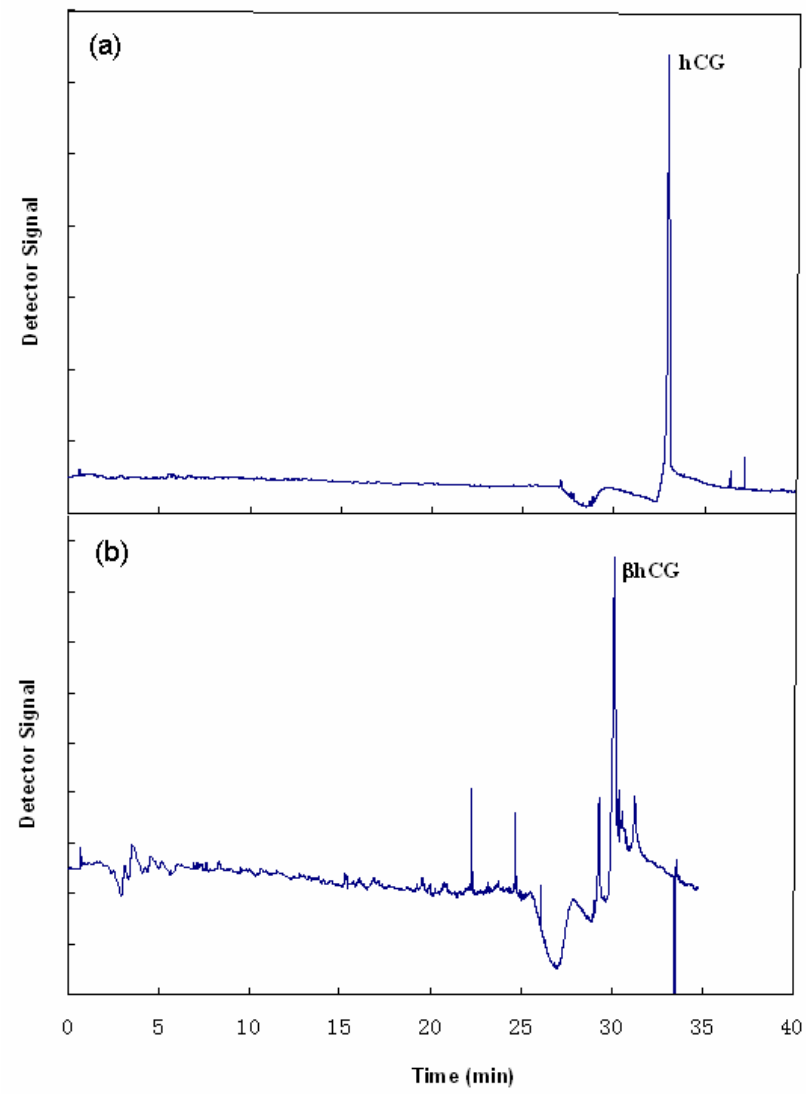

Figure 5.5 CE of (a) hCG and (b) bhCG. The narrow spikes in (b) are due to bubbles or instrumental instabilities.

5.3.5 Preconcentration and CE of hCG

Figure 5.6 shows CE of desorbed hCG after it was selectively enriched on a GMA-EDMA affinity column. Preconcentration and elution buffer incubation were carried out before the start of the electropherogram. This result indicates that my affinity column had the ability to selectively enrich hCG from a sample solution and separate it using CE.

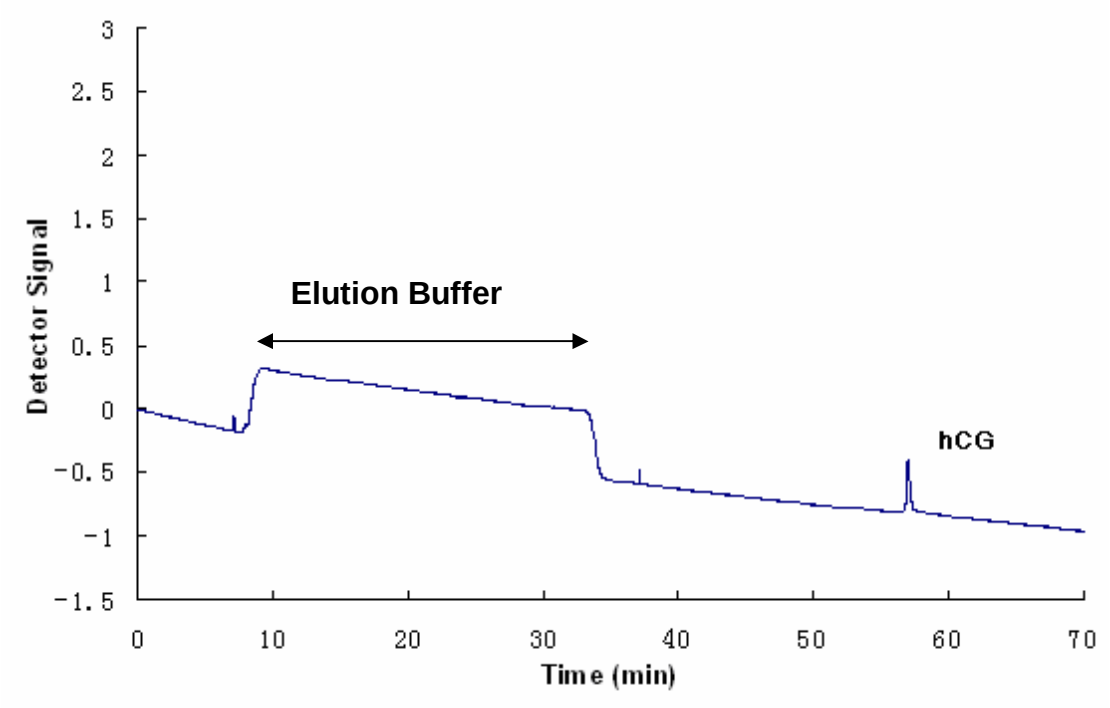

Figure 5.6 Preconcentration and CE of hCG in an affinity column.

5.4 Conclusion

A method (adapted from Pierce's published protocols) was developed to attach oriented antibodies on monoliths. To reduce nonspecific adsorption, BSA solution was used to block the monolith surface. Selective preconcentration and elution of hCG has been performed in these affinity columns, which indicates promise for application in cancer marker detection. Future work will involve preconcentration and CE separation of a mixture that contains both βhCG and hCG.

5.5 References

[1] Armenta, J. M., Gu, B., Humble, P. H., Thulin, C. D., Lee, M. L., *J. Chromatogr. A* 2005, *1097*, 171-178.

[2] Liu, J., Pan, T., Woolley, A. T., Lee, M. L., *Anal. Chem.* 2004, *76*, 6948-6955.

[3] Kelly, R. T., Li, Y., Woolley, A. T., *Anal. Chem.* 2006, *78*, 2565-2570.

[4] Svec, F., *Electrophoresis* 2006, *27*, 947-961.

[5] http://www.piercenet.com.

[6] Larijani, B., Woscholski, R., Rosser, C. A., *Chemical Biology: Applications and Techniques*, John Wiley and Sons Inc, Hoboken, NJ 2006.

Chapter 6 Conclusions and Future Directions

6.1 Conclusions

6.1.1 Fabrication of CaF_2 Capillary Electrophoresis Microdevices for on-chip IR Detection

In Chapter 2, I describe the fabrication and testing of microfluidic capillary electrophoresis (CE) devices made of CaF_2. These microchips open the door to optical detection in the ultraviolet, visible, and infrared spectral regions. I performed CE of fluorescently labeled amino acids in CaF_2 microdevices. Although the CE results in Chapter 2 are not optimal, they still indicate that CaF_2 microfluidic systems can provide a suitable platform for rapid biochemical separations. I also performed IR spectroscopy for qualitative analyte identification in CaF_2 microchannels, which was the first demonstration of on-chip IR detection in a μTAS device. My results show that CaF_2 microfluidic devices are suitable for online FT-IR identification of analytes in the channels. These CaF_2 microchips should enable both quantitative and qualitative optical analysis in lab-on-a-chip systems.

6.1.2 Surface Modification of Polymeric Microdevices

Chapters 3 and 4 show surface modification of polymer microdevices for bioanalytical applications. Two polymers, poly(methyl methacrylate) (PMMA, Chapter 3) and thermoset polyester (TPE, Chapter 4), were studied in this research. My results should further the application of polymer microdevices in biomolecular analysis.

In Chapter 3, microchip CE of proteins and protein digests was evaluated in PMMA

microdevices. To improve separation efficiency and reduce protein adsorption, two methods, dynamic coating and poly(ethylene glycol) (PEG) grafting using atom transfer radical polymerization (ATRP), were used for the surface modification of PMMA microdevices. Theoretical plate counts as high as 2.2×10^4 were achieved for protein separations in PEG-grafted PMMA microdevices. The relative standard deviation of migration time for BSA separations in PEG-modified PMMA microchips was 1.3% over 10 runs. My work indicates that ATRP grafting of PEG offers superior results to dynamic coating in PMMA microchip performance in protein separations. Moreover, my experiments show that PMMA microfluidic systems should be well suited for high-performance separations needed to characterize complex biological mixtures.

To apply surface modification more broadly in polymer microdevices, I developed in-channel ATRP and applied this approach in the surface derivatization of TPE microdevices with PEG. In-channel ATRP is performed after device bonding, so it is useful in polymer microchips that cannot be surface modified before enclosure. Moreover, my work showed that ATRP can be carried out in close-to-still (non-flowing) conditions, which had not been demonstrated previously. I have characterized PEG-grafted TPE microdevices with X-ray photoelectron spectroscopy, electroosmotic flow (EOF), and contact angle measurements. The results indicate that a thin PEG layer has been grafted in the TPE channels. Moreover, reduced nonspecific adsorption and lower, more pH-stable EOF was observed in PEG-grafted TPE microchannels. Amino acid and peptide mixtures were separated in PEG-modified TPE chips with good efficiency and reproducibility. CE of phosducin-like protein and phosphorylated phosducin-like protein was also done to measure the phosphorylation efficiency. Analysis of these mixtures

demonstrates the utility of surface-modified TPE microchips for the separation of complex biological samples.

6.1.3 Affinity Techniques for Cancer Marker Analysis

In Chapter 5, I show the development of a new affinity column−CE system for cancer marker analysis. I developed a method (adapted from Pierce's published protocols) to covalently attach appropriately oriented antibodies of interest on monolith surfaces such that antibody activity can be retained. This technique could also be applied to attach other proteins on monoliths, which could be useful in on-chip enzyme assays or protein digestion. Moreover, I developed an approach to reduce nonspecific protein adsorption on monoliths using bovine serum albumin (BSA). Selective preconcentration and elution of human chorionic gonadotropin (hCG) have been performed using these affinity columns, indicating promise for application in cancer marker detection. Importantly, my affinity techniques could be coupled with other analytical instruments to improve their performance.

6.2 Future Directions

6.2.1 CaF_2 CE Microdevices

6.2.1.1 Fabrication of CaF_2 Microdevices

In Chapter 2, I described the fabrication of CaF_2 CE microchips and their application in amino acid separation. However, the fabrication procedures need optimization. First, the etching speed for $FeNH_4(SO_4)_2$ is slow (less than 20 μm/day). Thus, new etchants are needed for making high-aspect-ratio CaF_2 microfeatures. Second, a new bonding method needs to be developed. In Chapter 2, I utilized photoresist as an adhesive to bond CaF_2

pieces together; this introduces some problems, such as non-uniform channel properties, EOF, nonspecific adsorption, etc. It would be valuable to develop a method to directly bond two CaF_2 substrates together. I propose that CaF_2 substrates can be bonded together at high temperature under an inert atmosphere. From my initial work on direct bonding, 900 °C should be sufficient to seal CaF_2 pieces together, but an inert atmosphere or vacuum is required, because trace water vapor in air can degrade CaF_2.

Figure 6.1 shows a proposed new scheme for CaF_2 microchannel fabrication. Briefly, after a CaF_2 substrate is cleaned with acetone (Figure 6.1a), a sacrificial layer that defines microdevice channel features is patterned photolithographically on the CaF_2 surface (Figure 6.1b). The sacrificial layer could be photoresist (e.g., SU-8), silicon dioxide, Si_3N_4, or a metal. Then, e-beam [1] or thermal evaporation [2] could be used to deposit a thin layer of CaF_2 on the patterned substrate (Figure 6.1c). Finally, the sacrificial layer could be etched, leaving channel features (Figure 6.1d), and high-temperature direct bonding will be used to enclose the microchannels. Compared to the approach in Chapter 2, this new method would provide more uniform surface properties for the bonded CaF_2 channels and greater device bond strength.

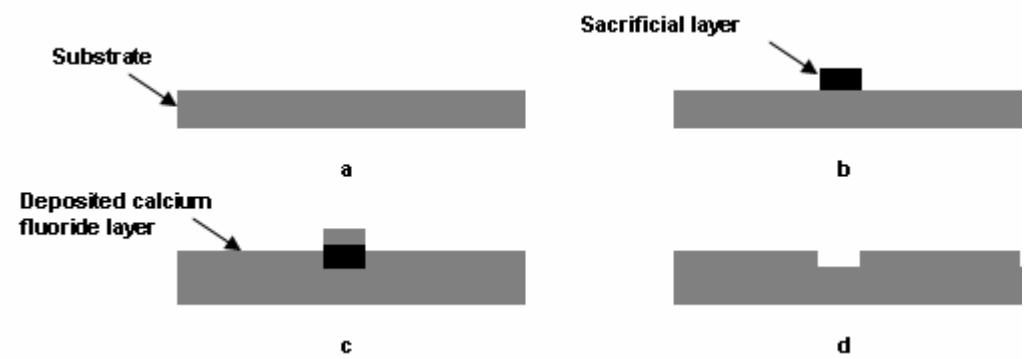

Figure 6.1 Fabrication of CaF_2 microdevices using sacrificial methods.

6.2.1.2 Separation and Detection in CaF_2 Microdevices

One unique feature of CaF_2 microdevices is that almost no EOF is present, which makes high-performance CE possible. Chapter 2 showed that amino acids could be separated in CaF_2 microdevices. In the future, it would be valuable to use these systems in the separation of peptides, proteins or nucleic acids. To achieve this goal, longer separation channels will be required and new fabrication methods, such as sacrificial techniques, thermal bonding, etc., will need to be developed.

In Chapter 2, I gave initial IR detection results in CaF_2 microchannels; however, on-chip IR detection of separations was not done. Thus, in the future, I propose to perform on-chip IR detection of protein or nucleic acid separations in CaF_2 microchannels. IR should be useful as a universal detection method for biomolecular analysis in CaF_2 microdevices.

6.2.2 Surface Modification of Polymeric Microdevices

6.2.2.1 ATRP Surface Modification

In Chapters 3-4 I showed that ATRP surface modification was an effective method to improve biomolecular analysis performance in polymeric microdevices. After ATRP, lower and pH-stable EOF, as well as reduced protein adsorption, were observed in PEG-grafted PMMA and TPE microchannels. The CE performance for PEG-grafted polymer microdevices was also improved. I propose that ATRP surface modification could be applied to other polymer microdevices to improve their biomolecular analysis performance. Moreover, new approaches need to be developed to graft other protein-resistant materials on polymer surfaces using ATRP.

6.2.2.2 New Bioanalytical Applications for Polymeric Microdevices

My research showed improved protein, peptide and amino acid separations in polymeric microdevices. Besides these biomolecules, nucleic acids, fatty acids, and hormones are other important species for separation. Since PEG grafting can reduce EOF and nonspecific adsorption, I am confident that such polymer microdevices should have broad potential in analysis of other biomolecules.

In Chapters 3 and 4, I only performed CE analyses in my polymer microdevices; however, there are many other analytical techniques that could be incorporated into polymer microchips. For example, affinity methods are important in biochemistry and medicine, because of selective and strong interaction toward targets. With the surface modification methods that I developed in Chapters 3 and 4, it should be possible to introduce affinity

columns into polymer microdevices. To achieve this goal, I propose to use anchor molecules (e.g., PEG-aldehyde derivatives, which can be obtained from Sigma) that can react with proteins or nucleotides and be grafted on surfaces through ATRP. Affinity-modified polymer microchips should be advantageous relative to the more costly and difficult to fabricate glass devices.

6.2.3 Affinity Techniques for Cancer Marker Analysis

6.2.3.1 New Methods to Attach Antibodies on Monoliths

Besides the methods discussed in Chapters 1 and 5, improved approaches should be developed to provide active and oriented antibodies attached to polymer surfaces. I propose an alternative method to attach antibodies on a monolith, based on DNA hybridization. This technique will include three steps: (1) attachment of oligonucleotides to the monolith, (2) linking of antibodies to nucleic acids, and (3) hybridization.

The first step is the attachment of oligonucleotides to monoliths. Methods have been developed to affix oligonucleotides to glass surfaces [3], and I will modify these approaches to attach oligonucleotides to monoliths. As shown in Figure 6.2a, epoxy groups can be reacted with ethylenediamine (EDA), leaving a pendant amine group. Two options are available to link oligonucleotides to amines. The first possibility is to link the oligonucletide 5'-phosphate group directly to surface amines under the catalysis of *N*-ethyl-*N*′-(3-dimethylaminopropyl) carbodiimide (EDC) imidazole (Figure 6.2b). The second option needs thiol-modified oligonucleotides [4-6]; sulfo-SMCC reacts with the monolith surface amine groups, and this is followed by attachment of thiol-labeled oligonucleotides (Figure 6.2c). Besides sulfo-SMCC, m-maleimidobenzoyl-N-

hydroxysulfosuccinimide ester; N-[g-maleimidobutyryloxy]sulfosuccinimide ester; sulfosuccinimidyl 4-[p-maleimidophenyl]butyrate, or N-sulfosuccinimidyl[4-iodoacetyl]aminobenzoate could also be used as the crosslinking agent [3].

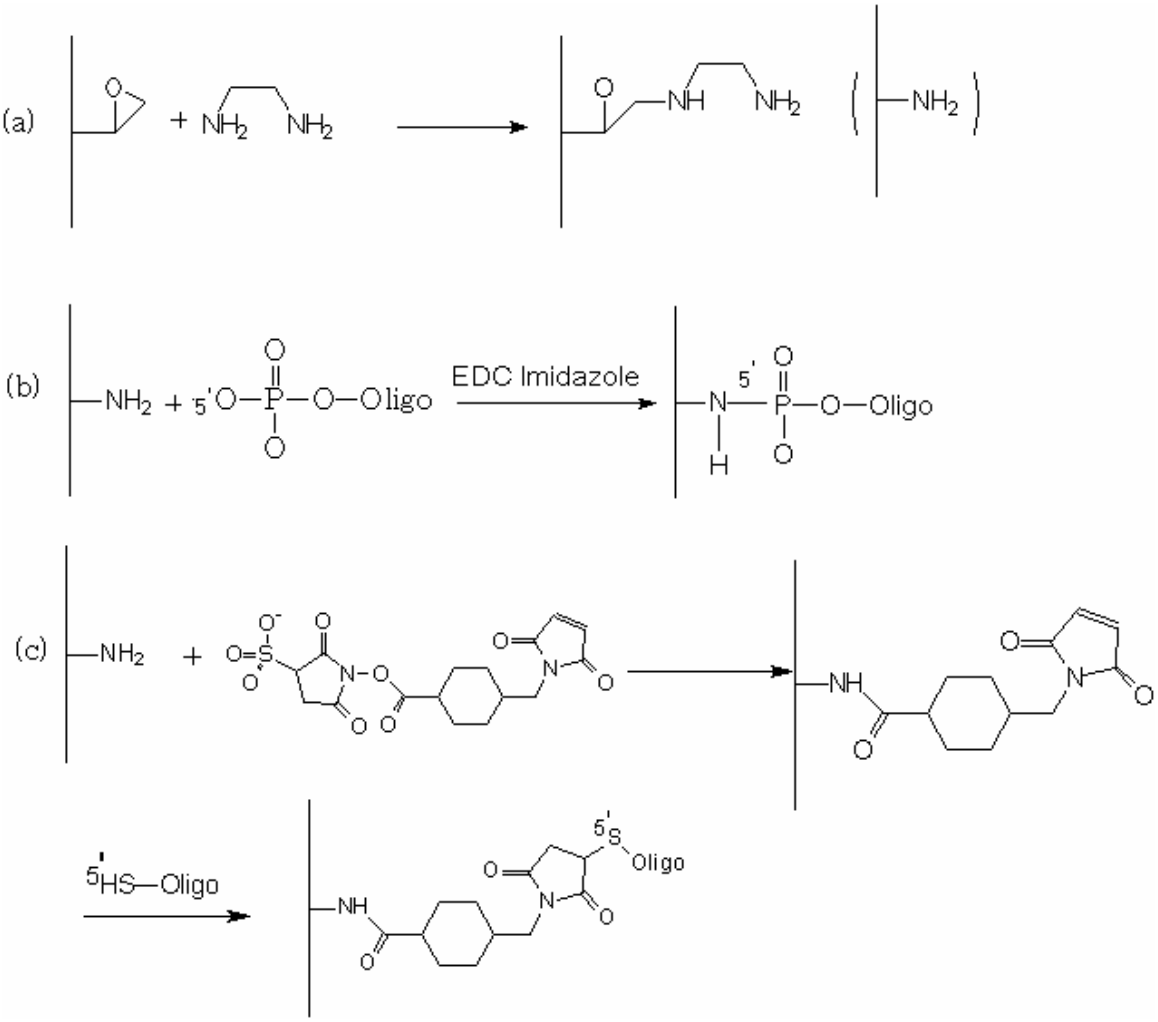

Figure 6.2 Antibody attachment to GMA monoliths using hybridization. Part 1: attaching oligonucleotides.

The second step is to attach the antibody to an oligonucleotide that is the perfect complement to the surface-affixed one. Two methods will be explored for this purpose. One option is to react partially reduced antibodies with thiol-labeled oligonucleotides

(Figure 6.3a). The other possibility is to use crosslinkers to attach antibodies to thiol-labeled oligonucleotides. For example, as shown in Figure 6.3b, sulfo-SMCC can link to antibodies through an antibody primary amine. Then the other side of SMCC can form a bond with a thiol-labeled oligonucleotide. The first of these methods is most promising, because the orientation of attached antibodies can be controlled best.

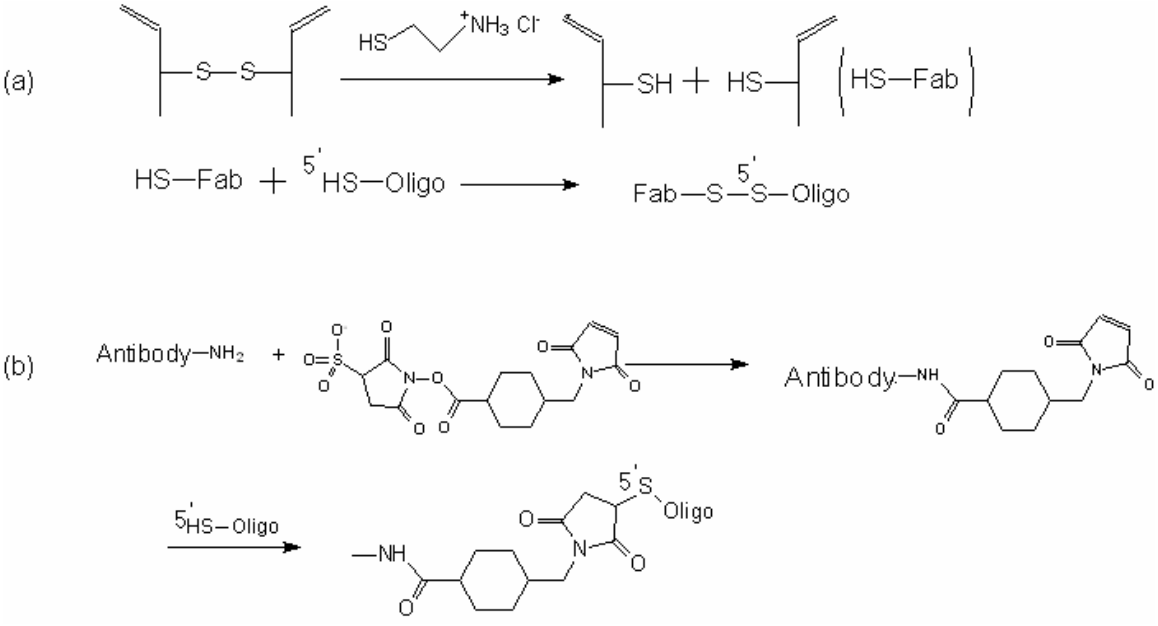

Figure 6.3 Antibody attachment to GMA monoliths using hybridization. Part 2: linking oligonucleotides to antibodies.

Once the first two steps are finished, the oligonucleotide-attached antibody solution will be flushed through the DNA-modified monolith, and specific hybridization will affix antibodies to the surface. This base-pairing attachment is strong, and normally only high temperature (>90 °C) or solvent can break it. Moreover, DNA denaturation can be used to detach antibodies from the monolith to allow changing or reconfiguration as desired.

6.2.3.2 Surface Modification to Eliminate Nonspecific Adsorption

As I have observed in Chapter 5.3.2, native GMA monoliths are prone to protein adsorption. I have tested hCG, β-casein, trypsin and green fluorescent protein, and all of them have some nonspecific adsorption on native GMA monoliths. Also, the attachment of antibodies on GMA monoliths includes three steps: amine group linkage, sulfo-SMCC reaction and antibody fragment attachment. Each step may introduce potential adsorption sites on the monolith surface. Some nonspecifically adsorbed proteins may be attaching to the monolith through the epoxy groups; these proteins are so strongly adsorbed that even acidic solution (pH 2.5) cannot elute them effectively. Some proteins are also adsorbed weakly on the monolith; these molecules may be eluted and washed out with the target protein, thus interfering with affinity experiments. One method used to eliminate nonspecific adsorption is to react the monolith with Tris, aspartic acid or hydrogen peroxide to remove residual active epoxy groups [7]. Although these reactions deactivate the epoxy groups, they introduce new functionalities on the monolith, which could also lead to nonspecific adsorption. One solution to nonspecific protein adsorption is to use a protein like bovine serum albumin (BSA) to block adsorption sites, as reported in Chapter 5. However, BSA blocking has several disadvantages: 1) it may interfere with the antibody/antigen interaction, 2) BSA bleeding from the monolith over time may increase nonspecific adsorption, and 3) BSA that bleeds from the monolith may co-elute with the target protein. Thus, new methods should be developed to solve the nonspecific adsorption problem.

In Chapters 3 and 4, I have attached PEG chains on polymer surfaces to reduce

nonspecific adsorption [8]. After PEG grafting, most proteins, including BSA and β-casein, do not adsorb. I propose that PEG could be used to block nonspecific adsorption on monoliths; however, there are two groups on the monolith that could cause nonspecific adsorption: unreacted epoxy groups and amine groups (unreacted sulfo-SMCC will be hydrolyzed so it should not cause problems). To block residual epoxy groups, I propose to flush a PEG derivative through the monolith (Figure 6.4a). To block unreacted amine groups, PEG aldehydes will be passed through the column (Figure 6.4b). Both these PEG derivatives can be purchased from Sigma. These surface blocking steps must be done after antibody attachment. Importantly, since the reaction between the PEG-aldehyde and antibody amine groups requires high antibody concentration (2 mg/mL) and long reaction time (4 h) [9], attachment of PEG to antibody amines should be limited.

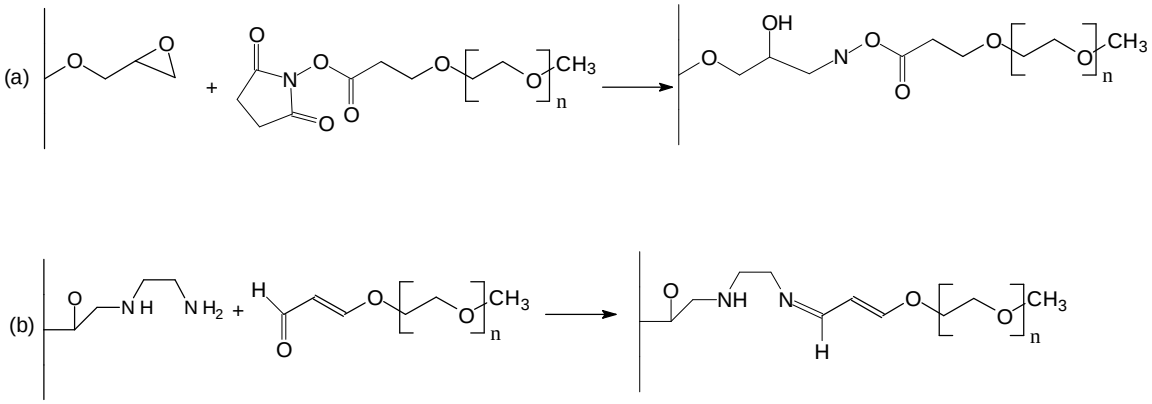

Figure 6.4 PEG grafting on GMA monoliths to reduce nonspecific adsorption. (a) Blocking epoxy groups with a PEG derivative and (b) blocking surface amine groups with a PEG-aldehyde reagent.

An alternative surface modification method for epoxy deactivation is PEG grafting using ATRP [10, 11] after EDA treatment of the monolith. ATRP [12-14] has been used for

chemical derivatization of PDMS [15, 16] and PMMA [8] microchannels. Surface GMA epoxy groups should react with the ATRP initiator under appropriate conditions, while the surface amine groups will be inert. Subsequently, the chosen polymer can be grafted to the surface, as shown in Figure 6.5. The grafted PEG layer should provide low and pH-stable EOF. Moreover, ATRP attachment of PEG chains should eliminate reactive GMA groups that could cause nonspecific adsorption. Last, the ATRP process has no interference with the immobilized amine groups, so subsequent antibody immobilization can be done.

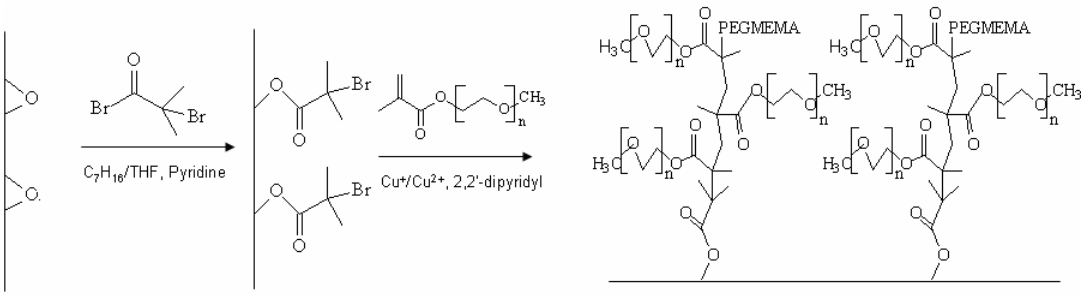

Figure 6.5 Schematic of ATRP modification of a GMA monolith.

A third option for surface modification is to grow a thin PEG layer using photoinitiation after antibody attachment. Photoinitiator-induced radical polymerization has been applied widely for polymerization of acrylate or styrene-based formulations, and a broad variety of radical photoinitiators have been developed, such as tetraalkylammonium salts, titanocene, and 2,2-dimethoxy-2-phenylacetophenone (DMPA) for initiation with 300-400 nm UV light [17]. The photo-induced polymerization includes two steps and would be performed after antibody attachment. First, I will convert unreacted epoxy groups to aldehydes by acid hydrolysis and $NaIO_4$ oxidation. After that, I propose to fill the monolith with PEG acrylate derivatives (monomers) and DMPA (initiator), and irradiate

UV light for polymerization. One concern for this approach is that attached antibodies could react with the surface aldehyde groups, which would reduce the performance of the affinity column.

6.2.3.3 Affinity-coupled Electric Field Gradient Focusing (EFGF) of hCG

As an extension of my work in Chapter 5, I suggest the coupling of affinity columns with EFGF devices, pursuing two approaches. The first method is to directly integrate an antibody column into an EFGF device, as shown in Figure 6.6a. This method is similar to my approach to connect an affinity column with CE in Chapter 5. After a capillary based-EFGF device is produced (as described in Section 1.4), an affinity column (1.5-2 cm long) can be made at one end, which can be connected to a syringe pump for sample introduction, preconcentration and elution. Then, EFGF can be used to separate and focus eluted proteins. This integration method is relatively simple and eliminates the problem of dead volume. However, a potential issue is that the integrated device will lose its function if either of its components (affinity or EFGF) fails. In addition, the integration will increase the device fabrication time and complexity.

The other solution is to utilize an injection valve to connect an affinity column to an EFGF device (Figure 6.6b). The affinity column could be fabricated separately from the EFGF device and connected through a valve. When protein preconcentration is performed, the valve would be adjusted to flow sample through the affinity column to sample waste, bypassing the EFGF device. After preconcentration is done, the valve would be switched to connect the affinity column to the EFGF section so the preconcentrated proteins could be eluted and transferred to the EFGF device for analysis. Once the sample is loaded from the affinity column, the valve would be switched to

connect the syringe pump (for EFGF flow control) to the EFGF device. Compared to the first method, the device fabrication for this design should be much easier. Moreover, the lifetime for this type of affinity-coupled EFGF device should be longer, because either the affinity column or the EFGF device could be easily changed to perform new tasks or replace non-functioning components. However, this method creates dead volume and other possible complications due to the usage of valves and/or fittings.

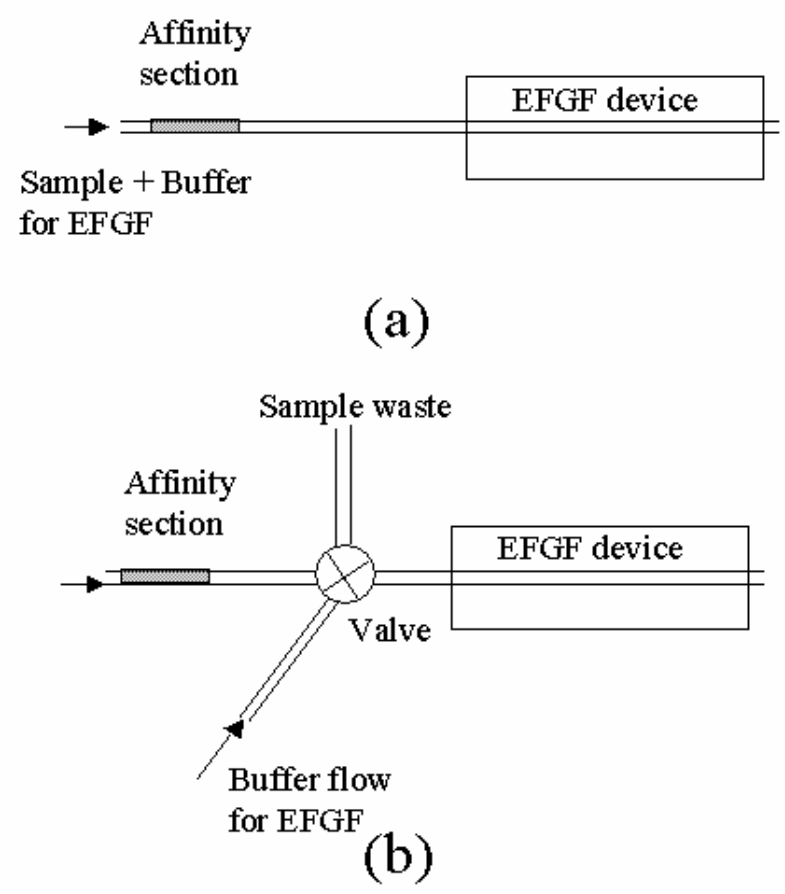

Figure 6.6 Coupling of an affinity column to an EFGF device.

The eventual objective of affinity-coupled EFGF is to analyze biological samples (such as blood or urine). In addition to proteins, real samples contain carbohydrates, fatty acids, nucleic acids and other small molecules, which need to be removed prior to loading on

the affinity column. I suggest that conventional protocols, which include centrifugation, acetonitrile extraction, aqueous methanol extraction and lyophilization, could be used to achieve this aim [18, 19]. For a real biological sample, IgG, albumin, hemoglobin and other abundant proteins are another concern. Commercially available abundant protein removal kits (e.g., Abundant Protein Removal Kit from Merck or ProteoSeek Albumin/IgG Removal Kits from Pierce) can remove these proteins. After these pretreatments, the sample can be introduced directly into the affinity column to extract target proteins. Once concentrated, the markers can be transferred to the EFGF device for focusing and separation.

6.2.3.4 Application of Affinity-Coupled EFGF to Cancer Marker Analysis

One of the advantages of antibody-coupled EFGF is that it should be able to enrich proteins of interest from a complex biological sample (e.g., blood or urine) Affinity-coupled monolith columns have good potential for analysis of several cancer markers: carcinoembryonic antigens, prostate-specific antigen, alpha-fetoprotein, cancer antigen 125, and cancer antigens 15-3 and 27.29. Antibodies to each type of marker need to be attached to the monolith column. It will also be necessary to optimize the sample, elution, and EFGF buffers, as well as voltage and flow parameters for EFGF. Each cancer marker can be tested in affinity-coupled EFGF individually to find the optimal conditions. Finally, multiple types of antibodies can be attached in one column to perform affinity preconcentration and EFGF of multiple markers at the same time.

6.3 Summary and Perspective

The ultimate aim of my research is to detect diseases at early stages using microdevices. My work has focused on the fabrication and testing of micro total analysis systems (μTAS) for bioanalytical applications. I developed microdevices made of CaF_2 and tested their application in CE separations and on-chip IR spectroscopy. I also worked on the surface modification of polymeric microdevices and applied them in protein, peptide and amino acid separations. Last, I developed a method for the attachment of appropriately oriented antibodies on GMA monoliths, and applied this setup in hCG preconcentration and separation. Importantly, there are many promising future directions for my work. My research on the fabrication and surface modification of microdevices should benefit the development of new μTAS applications, while my studies on protein, peptide, amino acid and cancer marker separations should be useful for biomarker analysis. I am optimistic that someday these techniques will be used clinically in routine analysis of real samples.

6.4 References

[1] Tsuge, H., Matsukura, N., *IEEE Trans. Appl. Supercond.* 1993, *3*, 2401-2404.

[2] dell'Orto, T., Terrasi, A., Marsi, M., Coluzza, C., *et al.*, *Phys. Rev. B* 1994, *50*, 18189-18193.

[3] Adessi, C., Matton, G., Ayala, G., Turcatti, G., *et al.*, *Nucleic Acids Res.* 2000, *28*, e87.

[4] Connolly, B. A., Rider, P., *Nucleic Acids Res.* 1985, *13*, 4485-4502.

[5] Zuckermann, R., Corey, D., Schultz, P., *Nucleic Acids Res.* 1987, *15*, 5305-5321.

[6] Sproat, B. S., Beijer, B., Rider, P., Neuner, P., *Nucleic Acids Res.* 1987, *15*, 4837-4848.

[7] Svec, F., *Electrophoresis* 2006, *27*, 947-961.

[8] Liu, J., Pan, T., Woolley, A. T., Lee, M. L., *Anal. Chem.* 2004, *76*, 6948-6955.

[9] Krcaronvenková, J., Bilková, Z., Foret, F., *J. Sep. Sci.* 2005, *28*, 1675-1684.

[10] Doherty, E. A. S., Meagher, R. J., Albarghouthi, M. N., Barron, A. E., *Electrophoresis* 2003, *24*, 34-54.

[11] Dolník, V., *Electrophoresis* 2004, *25*, 3589-3601.

[12] Kato, M., Kamigaito, M., Sawamoto, M., Higashimura, T., *Macromolecules* 1995, *28*, 1721-1723.

[13] Wang, J.-S., Matyjaszewski, K., *J. Am. Chem. Soc.* 1995, *117*, 5614-5615.

[14] Kamigaito, M., Ando, T., Sawamoto, M., *Chem. Rev.* 2001, *101*, 3689 -3746.

[15] Xiao, D., Zhang, H., Wirth, M., *Langmuir* 2002, *18*, 9971-9976.

[16] Xiao, D., Le, T. V., Wirth, M. J., *Anal. Chem.* 2004, *76*, 2055-2061.

[17] Davidenko, N., Garcia, O., Sastre, R., *J. Biomater. Sci. Polym. Ed.* 2003, *14*, 733-746.

[18] Brunzel, N. A., *Fundamentals of Urine & Body Fluid Analysis*, Elsevier Science

Health Science Division, Philadelphia, PA 2004.

[19] Bangert, S. K., Marshall, W. J., *Clinical Chemistry*, Elsevier Science Health Science Division, Philadelphia, PA 2004.